



# MASTERARBEIT / MASTER'S THESIS

Titel der Masterarbeit / Title of the Master's Thesis

## „The Implementation of the Full Configuration Interaction Method “

verfasst von / submitted by

Zoran Šukurma, BSc

angestrebter akademischer Grad / in partial fulfilment of the requirements for the degree of

Master of Science (MSc)

Wien, 2019 / Vienna, 2019

Studienkennzahl lt. Studienblatt /  
degree programme code as it appears on  
the student record sheet:

A 066 876

Studienrichtung lt. Studienblatt /  
degree programme as it appears on  
the student record sheet:

Masterstudium Physik

Betreut von / Supervisor:

Univ.-Prof. Dipl.-Ing. Dr. Georg Kresse



# Acknowledgments

I would first like to express great gratitude to my thesis advisor Georg Kresse. He was available for me, whenever I ran stuck into a problem or had a question about my thesis. The discussions with my advisor have often inspired me to do more and better than required. I would also like to thank him for introducing me to the CMS group. At this point, my thanks go to Merzuk Kaltak for providing the VASP output suitable for my code and for answering all my questions about research. I would also like to thank Doris Hecht-Aichholzer for helping me with all documentation problems. Finally, I want to thank all CMS group members for accepting me warmly in their group. I hope this is only the beginning of our cooperation.

My sincere thanks go to my friends, too. They were always with me, whenever I need any help. Especially, I want to thank Mirjana Jovanović for proofreading my thesis and Aljoša Vuković for taking the time and effort to read it and point out some mistakes. Last but not least, I would like to express my heartfelt thanks to my parents and my family for supporting me all the time. They did everything in their power to give me the opportunity to dedicate myself to the study.

# Abstract

In recent years, the investigation of impurities in solids and strong correlation effects that appear in such systems are of great interest in computational material science. Therefore, this work focuses on the full configuration interaction method (FCI) and its implementation. The full configuration interaction method is probably the most interesting correlation consistent method, because it is exact within a given basis set. Although conceptually a rather simple method, FCI scales exponentially with the number of orbitals and number of electrons. This limitation thwarted the further developments of full configuration interaction until the full configuration quantum Monte Carlo method appeared (FCIQMC). FCIQMC has enabled calculations of the CI wave function on substantially larger systems than it was possible with standard methods based on iterative diagonalization procedures. The implementation of both full configuration interaction methods will be the main focus of this work. The prerequisite for CI calculation is the implementation of one- and two-electron integrals over Gaussian basis and the Hartree-Fock method. In the end, the implemented methods will be adjusted to be used with VASP directly. The code will be applied for standard molecular systems and one application in solids will be presented. One hopes that in the future the code will be used as impurity solver in dynamical mean field theory (DMFT) or density matrix embedding theory (DMET).

# Zusammenfassung

In den letzten Jahren spielt die Untersuchung von Verunreinigungen in Feststoffen sowie das Studium von starken Korrelationseffekten, die in solchen Systemen auftreten, eine große Rolle in den rechnergestützten Materialwissenschaften. Diese Arbeit konzentriert sich auf die Methode der vollständigen Konfigurationsinteraktion (FCI) und deren Implementierung. Die Methode der vollständigen Konfigurationsinteraktion ist wahrscheinlich die interessanteste korrelationskonsistente Methode, da sie innerhalb eines gegebenen Basissatzes exakt ist. Obwohl konzeptionell eine eher einfache Methode, skaliert FCI exponentiell mit der Anzahl der Orbitale und der Anzahl der Elektronen. Diese Einschränkung verhinderte die Weiterentwicklung der vollständigen Konfigurationsinteraktion, bis die vollständige Konfigurationsinteraktions quantum Monte Carlo-Methode (FCIQMC) erschien. FCIQMC hat die Berechnungen der CI-Wellenfunktion für wesentlich größere Systeme ermöglicht, als es mit Standardmethoden auf Grundlage von iterativen Diagonalisierungsverfahren möglich war. Die Implementierung beider Methoden steht im Mittelpunkt dieser Arbeit. Voraussetzung für die CI-Berechnung ist die Implementierung von Ein- und Zweielektronenintegralen in der Gaußschen Basis sowie die Implementierung der Hartree-Fock Methode. Schließlich sollen die implementierten Methoden so angepasst werden, dass sie direkt in VASP verwendet werden können. Hier wird der Code für Molekularsysteme sowie auf einfache Feststoffe angewendet. Man hofft, dass der Code in Zukunft als Impurity solver in DMFT und DMET Methoden verwendet werden kann.

# Contents

<b>1</b>	<b>Introduction</b>	<b>1</b>
1.1	Organization of the Work . . . . .	2
<b>2</b>	<b>Many-Electron Wave Function and Second Quantization</b>	<b>3</b>
2.1	Non-Relativistic Time-Independent Schrödinger Equation . . . . .	3
2.2	The Born-Oppenheimer Approximation . . . . .	4
2.3	One-Electron Wave Function - Spatial and Spin Orbitals . . . . .	5
2.4	Many-Electron Wave Function - Slater Determinants . . . . .	6
2.5	One-Electron and Two-Electron Operators . . . . .	9
2.6	Slater-Condon Rules . . . . .	11
2.7	Second Quantization . . . . .	12
2.7.1	Creation, Annihilation and Excitation Operators . . . . .	13
2.7.2	Hamiltonian Operator in Second Quantization . . . . .	14
<b>3</b>	<b>Gaussian Basis Sets and Molecular Integral Evaluation</b>	<b>16</b>
3.1	Slater-Type Basis Functions . . . . .	17
3.2	Gaussian orbitals . . . . .	18
3.3	Gaussian Basis Sets . . . . .	19
3.3.1	Contracted Gaussians . . . . .	19
3.3.2	STO-LG Basis set . . . . .	19
3.3.3	Split-Valence Basis Sets . . . . .	20
3.3.4	Correlation Consistent Basis Sets . . . . .	21
3.4	Molecular Integral Evaluation . . . . .	22
3.4.1	Primitive Cartesian Gaussians . . . . .	22
3.4.2	Spherical-Harmonics Gaussians . . . . .	23
3.4.3	Gaussian Product Rule . . . . .	23
3.4.4	Hermite Gaussians . . . . .	24
3.4.5	McMurchie-Davidson Scheme . . . . .	25
3.5	The Boys Functions . . . . .	28
3.6	Wannier Basis Set . . . . .	30
3.7	Implementation Details - Calculation and Storing of Molecular Integrals	31
<b>4</b>	<b>Hartree-Fock Approximation</b>	<b>33</b>
4.1	Integro-Differential Hartree-Fock Equation . . . . .	33
4.2	Interpretation of Hartree-Fock Equations . . . . .	37
4.3	Roothaan Equations . . . . .	38
4.4	The Self-Consistent Field Procedure . . . . .	41

4.5	Open-Shell Hartree-Fock Calculations . . . . .	42
4.5.1	Unrestricted Open-Shell Hartree-Fock Model - UHF . . . . .	44
4.5.2	Restricted Open-Shell Hartree-Fock Model - ROHF . . . . .	45
4.6	Extrapolation of the Hartree-Fock Hamiltonian via Density Functional Theory . . . . .	46
4.7	Examples of Hartree-Fock Calculation . . . . .	47
<b>5</b>	<b>Møller-Plesset Perturbation Theory</b>	<b>52</b>
5.1	Rayleigh-Schrödinger Perturbation Theory . . . . .	53
5.2	Møller-Plesset Perturbation Theory . . . . .	54
5.3	Size-Extensivity of MP Energies . . . . .	55
5.4	Examples of MP2 Calculations . . . . .	57
<b>6</b>	<b>Direct Full Configuration Interaction Method - FCI</b>	<b>59</b>
6.1	Introduction to CI . . . . .	60
6.2	Size-Extensivity of the CI Wave Function . . . . .	61
6.3	Determinant-Based Direct CI Method . . . . .	63
6.4	Graphical Representation of Slater Determinants . . . . .	68
6.5	Iterative Diagonalization Procedures - Davidson Method . . . . .	70
6.6	Examples of CI Calculations . . . . .	73
<b>7</b>	<b>Full Configuration Interaction Quantum Monte Carlo - FCIQMC</b>	<b>77</b>
7.1	Algorithm Description . . . . .	77
7.2	Simulation Modes and Energy Estimators . . . . .	80
7.3	Stability Criteria . . . . .	83
7.4	Sampling Rules . . . . .	83
7.5	Initiator Quantum Monte Carlo Configuration Interaction - iFCIQMC	85
7.6	Technical Details of FCIQMC Algorithm . . . . .	86
7.7	Fermion Sign Problem in FCIQMC . . . . .	87
7.8	Statistical Error Analysis in FCIQMC Algorithm . . . . .	89
7.9	Calculations with FCIQMC Method . . . . .	91
<b>8</b>	<b>Conclusion</b>	<b>93</b>
<b>A</b>	<b>Variational Theorem</b>	<b>96</b>
<b>B</b>	<b>Density Functional Theory</b>	<b>98</b>
<b>C</b>	<b>Transformation of Molecular Integrals</b>	<b>103</b>
	<b>Bibliography</b>	<b>105</b>

# Chapter 1

## Introduction

The concurrent development of quantum physics and supercomputers in 20th century has enabled the appearance of computational methods that were capable to solve the Schrödinger equation for many-body problems. Two well-known methods were developed: on the one hand Hartree-Fock theory (Douglas Rayner Hartree and Vladimir Fock) [3], suitable for atoms and molecular systems and on the other hand Density Functional theory - DFT (Walter Kohn and Pierre Hohenberg) that was more suitable for periodic structures. Although DFT is in general computationally quite cheap, it uses appropriate approximations to include exchange and correlation contributions. On the other side, HF theory includes exact exchange effects, but it neglects electron correlation contributions. At the same time, Hartree-Fock calculations are much more expensive compared to DFT calculations.

The above mentioned methods are "standard" calculations in electronic structure theory, but for some materials, these calculations are simply not accurate enough. In such systems, the correlation effects can not be neglected and if the correlation energy is not included, the electronic structure calculations fail and they can not predict real properties in such strongly correlated systems. Therefore, more accurate methods, able to retrieve at least a fraction of exact correlation energy, are needed. The most famous methods, capable of doing that are: Møller-Plesset perturbation theory (MP), coupled-cluster approximation (CCA), configuration interaction (CI), random-phase approximation (RPA), etc. The first three methods are based on Hartree-Fock ground state calculations, while the latter three are more appropriate for density functional background calculations. In this work, the Møller-Plesset perturbation theory will be briefly discussed (see chapter 5), but most attention will be given to CI calculations. While MP and CC theories are capable of retrieving only a fraction of the correlation energy, the configuration interaction method is exact within a given basis set. For this specific reason many scientists are interested in CI calculations. At the same time, CI is very expensive and it is applicable only for modest system sizes.

The main goal of this work is the implementation of standard CI calculation - direct full configuration interaction (see chapter 6) and stochastic CI method - full configuration interaction quantum Monte-Carlo (FCIQMC, see chapter 7) that is capable of calculating correlation effects in some solids, too. The purpose of this

thesis is to develop the code that can be used with VASP (Vienna ab initio simulation package). VASP is density functional theory based code, but it was mentioned that CI is a post Hartree-Fock method. The approach to overcome these difficulties will be discussed in chapters 3,4.

## 1.1 Organization of the Work

In order to make this thesis more readable, a brief organization of work is presented in this section. General background about the many-body Schrödinger equation is presented in the beginning of the text. It is followed by the second quantization and its application in occupation number basis. The Gaussian basis sets, used to obtain solutions of the many-body problem, will be briefly presented in chapter 3. When the basis sets have been introduced, the molecular integrals over Gaussian basis functions will be evaluated. Because it is well-known that VASP and all other density functional codes use plane waves instead of Gauss-like functions, the extrapolation of the Hamiltonian matrix elements from VASP will be briefly explained at the end of that chapter. Once all ingredients for the first electronic structure calculation have been introduced, the theoretical background and practical implementation of a closed-shell Hartree-Fock code will be presented in chapter 4. How to obtain Hartree-Fock ground state using hybrid functionals in density functional theory will be described at the end of the fourth chapter. The next step is to include correlation effects in the current electronic structure calculation. In chapter 5, probably the simplest way to do that is presented - Rayleigh-Schrödinger perturbation theory and its descendant, Møller-Plesset perturbation theory. After the MP theory is presented, the main chapters about configuration interaction will be introduced. The classical implementation of CI, with iterative diagonalization procedure, originally introduced by Roos and Siegbahn [29] and later developed by Handy and Knowles [30–33] in 1980's will be discussed in chapter 6. In 2009, the new stochastic Monte Carlo-like CI calculation in the manner of diffuse Monte Carlo method was proposed by Alavi and co-workers. The implementation of this quantum Monte Carlo configuration interaction method and its extensions, initiator quantum Monte Carlo configuration interaction method, will be explained in more details in chapter 7.

All implementations and corresponding results will be presented at the end of each section. For all implementations, the following calculations will be reported:

- Calculations on He atom for different basis sets;
- H<sub>2</sub> molecule to study dissociation effects on different approximation levels;
- BeH<sub>2</sub> as a multi nuclei system and H<sub>2</sub>O, if it is required. In the end, the correlation effects of the Helium in fcc lattice will be studied on the CI level as an extra example of the application to solids.

# Chapter 2

## Many-Electron Wave Function and Second Quantization

In this chapter, the basics of quantum physics needed for the understanding of underlying physics is introduced. The structure of the many-body wave function and corresponding Hamiltonian are considered. The concept of antisymmetry of the N-electron wave function and Slater determinants are explained. The chapter begins with a brief discussion of the many-body electronic problem and the most general time-independent Schrödinger equation. After that, the first approximation, used in all many-body electronic structure methods, known as Born-Oppenheimer approximation is discussed. In the section 2.3 one-electron wave function - spatial and spin orbitals are introduced and the way to construct N-electron wave function from them (Hartree product and Slater determinant). The standard form of one-electron and two-electron operators are given in section 2.5. A more elegant way to express these operators in the sense of the second quantization is introduced in section 2.7. The second quantization is one of the most important concepts that will be used in all chapters of this work. Therefore, the familiarity with the concept will be a prerequisite for understanding of this work.

### 2.1 Non-Relativistic Time-Independent Schrödinger Equation

In the 20th century, all physicists were striving to solve the Schrödinger equation. It was noticed very soon that only the smallest systems can be solved analytically (H atom or quantum oscillator). For all other complex systems, a set of good approximations is necessary to obtain solutions numerically. Let us begin with the most general time-dependent form of the Schrödinger equation:

$$i\hbar\frac{\partial\Psi}{\partial t} = \hat{H}\Psi, \quad (2.1)$$

where  $\Psi$  denotes the wave function of the system and  $\hat{H}$  is the corresponding Hamiltonian operator of the given system. In the cases where the Hamiltonian of the system depends only on spatial (and spin) coordinates, the whole wave function can be factorized in spatial- and time-dependent parts. After this factorization, the

time-dependent Schrödinger equation decouples to the time-independent eigenvalue problem

$$\hat{H}\Psi_0 = E\Psi_0 \quad (2.2)$$

and the time evolution of the previous stationary eigenvalue problem

$$\Psi(t) = e^{-i\hat{H}(t-0)}\Psi(t=0) = \hat{U}(t,0)\Psi_0. \quad (2.3)$$

For more detailed derivation of the time-independent Schrödinger equation, see [1].

Let us have a closer look at the Hamiltonian operator of the corresponding many-body problem. Consider  $M$  nuclei with coordinates  $\mathbf{R}_A$  and  $N$  electrons with coordinates  $\mathbf{r}_i$ . Denote further  $R_{AB} = |\mathbf{R}_A - \mathbf{R}_B|$  as the distance between two nuclei  $A$  and  $B$ ,  $r_{iA} = |\mathbf{r}_i - \mathbf{R}_A|$  the distance between electron  $i$  and nuclei  $A$  and lastly the distance between two electrons  $i$  and  $j$  as  $r_{ij} = |\mathbf{r}_i - \mathbf{r}_j|$ . After the notation has been introduced, the whole Hamiltonian of the system in atomic units is

$$\hat{H} = \sum_A^M -\frac{1}{2M_A}\nabla_A^2 + \sum_i^N -\frac{1}{2m_i}\nabla_i^2 + \sum_{A=1}^M \sum_{B>A}^M \frac{Z_A Z_B}{R_{AB}} + \sum_{i=1}^N \sum_{j>i}^N \frac{1}{r_{ij}} - \sum_{i=1}^N \sum_{A=1}^M \frac{Z_A}{r_{iA}}, \quad (2.4)$$

where  $\nabla_i^2$  are Laplace operators corresponding to  $i$ -th electron (same for ions),  $Z_A$  is the atomic number of the corresponding nucleus  $A$ , and  $M_A$  and  $m_i$  are nuclei and electron mass, respectively. The first two terms describe kinetic energy of ions and electrons, respectively. The next two terms correspond to the Coulomb repulsion between positively charged ions and electrons, respectively. The last term describes the attractive Coulomb interaction between ions and electrons. This can be represented succinctly as

$$\hat{H} = \hat{T}_N + \hat{T}_e + \hat{V}_{N-N} + \hat{V}_{e-e} + \hat{V}_{N-e}. \quad (2.5)$$

The summation limits in the third and the fourth term of the equation (2.4) are limited to  $B > A$  and  $j > i$  to avoid double counting because the order of the particles does not play a significant role. In other words, interaction between  $i$ -th and  $j$ -th electron is the same as interaction between  $j$ -th and  $i$ -th electron. Note that these restrictions in limits of summations do not appear in the last term of the equation, because it is not summed up by the same kind of particles.

## 2.2 The Born-Oppenheimer Approximation

After the total Hamiltonian operator of the many-body problem has been introduced in the last section, the first approximation, used in all following electronic structure problems, will be introduced. Consider the motion of  $N$  electrons in the space of much more massive  $M$  positively charged ions. It is clear that electrons move much faster than nuclei. Therefore, the equation (2.2) can be further decoupled to the electronic part and nuclear part. It means that for each set of nuclear coordinates  $\mathbf{R}_A$  the electronic problem can be solved separately involving only the set of electronic coordinates  $\mathbf{r}_i$ . In other words, it can be said that electrons move in the fixed field of  $M$

nuclei. This decoupling in Born-Oppenheimer adiabatic approximation is presented by the following equations:

$$\begin{aligned}\Psi_0(\{\mathbf{r}_i, \mathbf{R}_A\}) &= \Psi_{\text{el}}(\{\mathbf{r}_i\}; \{\mathbf{R}_A\}) \times \Psi_{\text{N}}(\{\mathbf{R}_A\}) \\ \hat{H}_{\text{el}} &= \hat{T}_{\text{e}} + \hat{V}_{\text{e-e}} + \hat{V}_{\text{N-e}} \\ \hat{H}_{\text{N}} &= \hat{T}_{\text{N}} + \hat{V}_{\text{N-N}}.\end{aligned}\tag{2.6}$$

It has to be noted, before proceeding to the next step, that the electronic part of the wave function depends on electronic coordinates directly and on nuclear positions parametrically. It remains now to solve two Schrödinger equations of smaller size, one for electrons and one for nuclei:

$$\begin{aligned}\hat{H}_{\text{el}}\Psi_{\text{el}} &= \mathcal{E}_{\text{el}}(\{\mathbf{R}_A\})\Psi_{\text{el}} \\ (\hat{H}_{\text{N}} + \mathcal{E}_{\text{el}}(\{\mathbf{R}_A\}))\Psi_{\text{N}} &= \mathcal{E}_{\text{tot}}\Psi_{\text{N}},\end{aligned}\tag{2.7}$$

where  $\mathcal{E}_{\text{el}}$  denotes the energy of the electrons and  $\mathcal{E}_{\text{tot}}$  the total energy of the system. In most cases, one is interested only in the electronic part of the Schrödinger equation and the nuclear part is treated in the classical way by using Newton's laws of motion. In this picture, the exact total energy of a system (within the Born-Oppenheimer approximation) can be calculated as

$$\mathcal{E}_{\text{tot}} = \mathcal{E}_{\text{el}}(\{\mathbf{R}_A\}) + \sum_{A=1}^M \sum_{B>A}^M \frac{Z_A Z_B}{R_{AB}} + \sum_{A=1}^M \frac{M_A}{2} (\dot{\mathbf{R}}_A)^2 = \mathcal{E}_{\text{el}} + E_{\text{N}} + T_{\text{N}}.\tag{2.8}$$

In this section, the Born-Oppenheimer approximation, introduced by Max Born and J. Robert Oppenheimer is discussed only qualitatively. For its derivation and more details, see [2].

## 2.3 One-Electron Wave Function - Spatial and Spin Orbitals

The solutions of the one-electron Schrödinger equation are functions, known as orbitals. If it is assumed that an orbital depends only on spatial coordinates, then one calls it a spatial orbital, denoted as  $\psi(\mathbf{r})$ . For one-electron systems, these orbitals are defined as solutions of the corresponding Schrödinger equation (2.2) with a one-electron Hamiltonian operator that contains the kinetic energy of that electron and the potential energy. As a solution of the eigenvalue problem, the set of spatial orbitals  $\psi_i$  forms an orthonormal set, i.e.

$$\langle \psi_i | \psi_j \rangle = \int d^3r_1 d^3r_2 \psi_i^*(\mathbf{r}_1) \psi_j(\mathbf{r}_2) = \delta_{ij}.\tag{2.9}$$

This set is also complete, so that any function  $f(\mathbf{r})$  that depends only on spatial coordinates, can be expanded in this basis. The term  $|\psi_i(\mathbf{r})|^2$  represents the probability of finding an electron in the infinitesimally small volume element  $d\mathbf{r}$  about  $\mathbf{r}$ . Detailed analysis of spatial orbitals will be given in chapter 3.

To complete a description of an electronic wave function, the spin of the electron must be added to the wave function. It is well known that the electron is a fermion particle with a spin  $S = 1/2$ . That corresponds to two different spin states: spin up ( $M_s = 1/2$ ) and spin down ( $M_s = -1/2$ ). These states are eigenstates of the spin operators  $\hat{S}^2$  and  $\hat{S}_z$ . Therefore, two orthogonal functions  $\alpha(\omega)$  and  $\beta(\omega)$  depend on a new variable, the spin variable  $\omega$ , are added with the following properties:

$$\begin{aligned}\langle\alpha|\alpha\rangle &= \langle\beta|\beta\rangle = 1 \\ \langle\alpha|\beta\rangle &= \langle\beta|\alpha\rangle = 0.\end{aligned}\tag{2.10}$$

Having spin functions defined, one can add this additional degree of freedom to the description of the one-electron wave function to build the so-called spin orbitals. Consider a system of  $P$  orthonormal spatial orbitals  $\{\psi_i|i = 1, 2, \dots, P\}$ . One builds the set of  $2P$  spin orbitals from them in the following way:

$$\left. \begin{aligned}\chi_{2i-1}(\mathbf{x}) &= \psi_i(\mathbf{r})\alpha(\omega) \\ \chi_{2i}(\mathbf{x}) &= \psi_i(\mathbf{r})\beta(\omega)\end{aligned}\right\} \text{for } i = 1, 2, \dots, P.\tag{2.11}$$

Such a set of spin orbitals, where two electrons always share the same spatial orbital and differ only by a spin function, is called restricted spin orbitals (more about this in section 4.3). In the previous equation, a new variable  $\mathbf{x}$  was introduced, which unifies spatial coordinates and the spin variable:

$$\mathbf{x} = (\mathbf{r}, \omega).\tag{2.12}$$

It is important to note that if the set of spatial orbitals is orthonormal, then the set of spin orbitals built from them is orthonormal, too. To avoid misunderstanding, the notation  $|i\rangle$  is completely identical to  $|\chi_i\rangle \equiv \chi_i$ .

## 2.4 Many-Electron Wave Function - Slater Determinants

Once the orbitals are introduced, an appropriate machinery is needed to describe a system of  $N$  electrons. In general, a one-electron wave function can be chosen as a linear combination of spatial orbitals. Analogously, the  $N$ -electron wave function could be represented in the most general way as:

$$\Psi(\mathbf{x}_1, \mathbf{x}_2, \dots, \mathbf{x}_N) = \sum_i^N \sum_j^N \dots c_{i,j,\dots} \chi_i(\mathbf{x}_1) \chi_j(\mathbf{x}_2) \dots,\tag{2.13}$$

where  $c_{i,j,\dots}$  denotes the  $N$ -dimensional array of expansion coefficients. However, well intuitive, but very approximate solution to represent an  $N$ -electron wave function would be to build a product of one-electron spin orbitals. This form of the wave function is called the Hartree product. For a system of  $N$  electrons, the Hartree product is

$$\Psi^{\text{HP}}(\mathbf{x}_1, \mathbf{x}_2, \dots, \mathbf{x}_N) = \chi_i(\mathbf{x}_1) \chi_j(\mathbf{x}_2) \dots \chi_k(\mathbf{x}_N).\tag{2.14}$$

It can also be shown that a wave function is not only intuitive, but if the total Hamiltonian is defined as the sum of one-electron Hamiltonians  $\hat{h}(i)$ , whose eigenstates are spatial orbitals  $\chi_i(\mathbf{x})$  (formal definition of the one-electron Hamiltonian in section 2.5), then the Hartree product is the eigenstate of the total Hamiltonian operator with an eigenvalue that corresponds to the sum of one-electron Hamiltonian eigenvalues (for the derivation, see [3]):

$$\hat{H} = \sum_{i=1}^N \hat{h}(i) \implies \hat{H}\Psi^{\text{HP}} = \left( \sum_{i=1}^N \varepsilon_i \right) \Psi^{\text{HP}}. \quad (2.15)$$

Although the Hartree product seems to be a natural way to express the  $N$ -electron wave function, it suffers from two drawbacks, that can not be ignored. The first one is related to the probability of finding electron one in  $d\mathbf{x}_1$  around  $\mathbf{x}_1$ . It follows from the definition of the Hartree product (2.14) that this probability is independent of the positions of the other electrons in the system, although it is well known that these electrons repel each other, avoiding the space regions occupied by other electrons. Expressed in a formula:

$$|\Psi^{\text{HP}}|^2 = |\chi_i(\mathbf{x}_1)|^2 |\chi_j(\mathbf{x}_2)|^2 \cdots |\chi_k(\mathbf{x}_N)|^2. \quad (2.16)$$

In other words, this wave function is said to be uncorrelated. The second drawback is the fact, that the Hartree product wave function  $\Psi^{\text{HP}}$  does not fulfill the Pauli exclusion principle. Pauli principle tells that two identical Fermions can not occupy the same quantum state within a system. For the wave function that means it must be antisymmetric with respect to interchange of two particle coordinates. From the definition of the Hartree product wave function (2.14), it is clear it is not antisymmetric. In order to overcome this problem, a new form of the wave function, namely the Slater determinant, is introduced. The Slater determinants lift up listed drawbacks of the Hartree product wave function and they also fulfill the eigenvalue problem, given in equation (2.15). The formal definition of the Slater determinant wave function is

$$\Psi^{\text{SD}}(\mathbf{x}_1, \mathbf{x}_2 \cdots \mathbf{x}_N) = (N!)^{-1/2} \begin{vmatrix} \chi_i(\mathbf{x}_1) & \chi_j(\mathbf{x}_1) & \cdots & \chi_k(\mathbf{x}_1) \\ \chi_i(\mathbf{x}_2) & \chi_j(\mathbf{x}_2) & \cdots & \chi_k(\mathbf{x}_2) \\ \vdots & \vdots & \vdots & \vdots \\ \chi_i(\mathbf{x}_N) & \chi_j(\mathbf{x}_N) & \cdots & \chi_k(\mathbf{x}_N) \end{vmatrix}, \quad (2.17)$$

where the pre-factor  $(N!)^{-1/2}$  is a normalization factor. This wave function denotes  $N$  electrons in  $N$  spin orbitals but without specification which electron in which spin orbital. It has to be noted that each column of Slater determinant labels one specific spin orbital and each row labels one electron. Note that the interchange of two electrons means the interchange of two rows of a Slater determinant, which leads to the sign change. This property automatically includes the fulfillment of the Pauli exclusion principle. Summarized in the equation, it can be written as

$$\Psi^{\text{SD}}(\cdots \mathbf{x}_i \cdots \mathbf{x}_j \cdots) = -\Psi^{\text{SD}}(\cdots \mathbf{x}_j \cdots \mathbf{x}_i \cdots). \quad (2.18)$$

In the case when two electron coordinates  $\mathbf{x}_i$  are identical, the determinant would contain two identical rows and would be zero. This is also the consequence of the

Pauli principle (two Fermions in the same quantum state are not allowed). The notation for the Slater determinant given in equation (2.17) is not very legible, so the new shorthand notation will be used in the rest of the work (the superscript "SD" for Slater determinants will be dropped out, because the many-electron wave function will be always expressed in terms of Slater determinants, unless otherwise indicated)

$$\Psi(\mathbf{x}_1, \mathbf{x}_2 \cdots \mathbf{x}_N) = |\chi_i(\mathbf{x}_1)\chi_j(\mathbf{x}_2) \cdots \chi_k(\mathbf{x}_N)\rangle. \quad (2.19)$$

This shorthand notation includes the normalization factor implicitly. The last advantage of the Slater determinant mentioned in this section is the inclusion of exchange effects. It means that the motion of electrons with parallel spin is correlated, but the motion of electrons with different spin remains uncorrelated. For more details, see [3].

For a given set of  $2P$  spin orbitals, the simplest wave function describing an  $N$ -electron system would be the single Slater determinant with  $N$  occupied spin orbitals  $\chi_i$  (with the lowest energies  $\varepsilon_i$ ). The remaining  $2P - N$  spin orbitals are called unoccupied or virtual orbitals. Such a wave function will be denoted as  $|\Psi_0\rangle$  and can be represented as

$$|\Psi_0\rangle = |\chi_1\chi_2 \cdots \chi_a\chi_b \cdots \chi_N\rangle. \quad (2.20)$$

Additionally, the Hartree-Fock ground state wave function is depicted in figure 2.1-a. This method is called Hartree-Fock approximation and the corresponding energy value is the Hartree-Fock ground state energy  $E_0 = \langle\Psi_0|\hat{H}|\Psi_0\rangle$ . More details about the Hartree-Fock method will be presented in chapter 4. Clearly,  $\Psi_0$  is only one of many possible Slater determinants that can be constructed from the set of  $2P$  spin orbitals. Adding more Slater Determinants to the description of the wave function will make the approximation more accurate. A convenient way to introduce other Slater determinants is to take one determinant as the reference state (Hartree-Fock determinant for example) and the others can be described by how they differ from this reference state. Therefore, they are marked as excited determinants. The most interesting excitations are singly excited and doubly excited Slater determinants. In a singly excited determinant, one occupied electron from spin orbital  $\chi_a$  is promoted to an unoccupied orbital  $\chi_r$ . This excitation is depicted in figure 2.1-b and it can be written as follows:

$$|\Psi_a^r\rangle = |\chi_1\chi_2 \cdots \chi_r\chi_b \cdots \chi_N\rangle. \quad (2.21)$$

In a double excitation, an additional electron from  $\chi_b$  is promoted to the virtual orbital  $\chi_s$ . This situation is shown in figure 2.1-c. A double excitation can be represented as

$$|\Psi_{ab}^{rs}\rangle = |\chi_1\chi_2 \cdots \chi_r\chi_s \cdots \chi_N\rangle. \quad (2.22)$$

In conclusion, let us make the following convention: the Hartree-Fock ground state wave function will be denoted as  $|\Psi_0\rangle$  and the exact wave function of the system as  $|\Phi_0\rangle$ . This distinction will be very important for the next chapters.

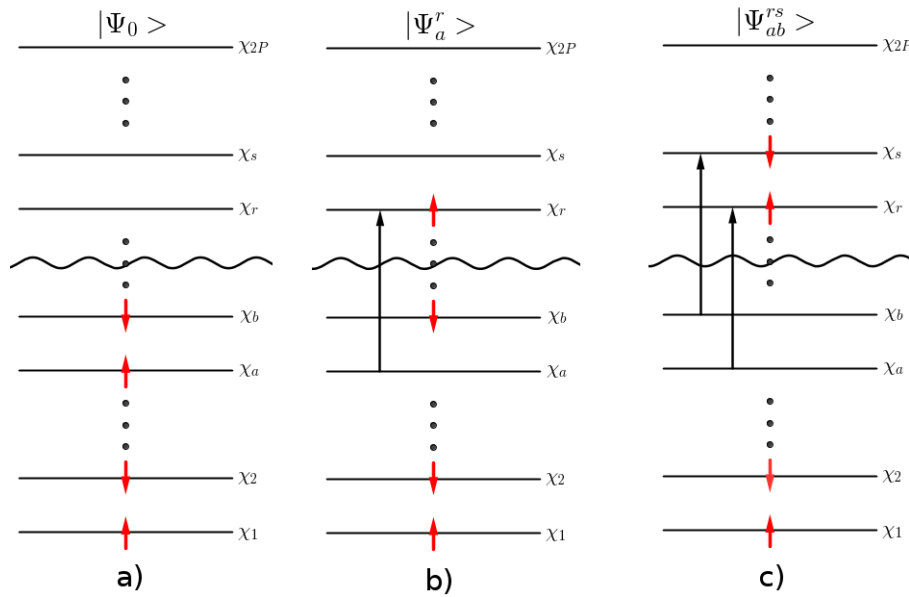


Figure 2.1: Three wave functions represented as single Slater determinants; a) Hartree-Fock ground state wave function  $\Psi_0$ ; b) Singly excited Slater determinant  $\Psi_a^r$  - an electron from spin orbital  $\chi_a$  is promoted to  $\chi_r$ ; c) doubly excited Slater determinant  $\Psi_{ab}^{rs}$  - additionally the second electron from spin orbital  $\chi_b$  is promoted to the spin orbital  $\chi_s$ .

## 2.5 One-Electron and Two-Electron Operators

Let us return to the electronic Hamiltonian operator defined in equation (2.6). It is a convention to separate this Hamiltonian in one-electron and two-electron parts. The first term contains contributions where only one electron arises, and the second term contributions where two electrons appear explicitly. It can be concluded that two-electron operator contains the interaction term between electrons ( $\hat{V}_{e-e}$  from equation (2.5)). The one-electron operator  $\hat{O}_1$  is simply the sum of one-electron Hamiltonians  $\hat{h}(i)$ , known as core Hamiltonian. This core Hamiltonian includes the kinetic energy of the corresponding electron and the potential energy with respect to fixed nuclei (see section 2.2). Thus, it can be written as

$$\hat{O}_1 = \sum_{i=1}^N \hat{h}(i) \quad ; \quad \hat{h}(i) = -\frac{1}{2} \nabla_i^2 - \sum_{A=1}^M r_{iA}^{-1}. \quad (2.23)$$

On the other hand, the two-electron operator contains only the repulsion between electrons

$$\hat{O}_2 = \sum_{i=1}^N \sum_{j>i}^N r_{ij}^{-1} = \frac{1}{2} \sum_{i \neq j}^N r_{ij}^{-1}. \quad (2.24)$$

Quantum chemists are interested in the evaluation of the matrix elements of one- and two-electron operators in the basis of Slater determinants. These values can be represented as  $\langle \Psi_1 | \hat{O} | \Psi_2 \rangle$ , where  $\hat{O}$  denote one- or two-electron operator.

## One-Electron Integrals

The matrix elements of the core Hamiltonian  $\hat{h}$  in the basis of spin orbitals are called one-electron integrals. These values are denoted as  $\langle i|\hat{h}|j\rangle$ . The formal definition of these integrals is

$$\langle i|\hat{h}|j\rangle = \langle \chi_i|\hat{h}|\chi_j\rangle = h_{ij} = \int d\mathbf{x}_1 \chi_i^*(\mathbf{x}_1)\hat{h}(\mathbf{r}_1)\chi_j(\mathbf{x}_1), \quad (2.25)$$

where the condition  $\langle i|\hat{h}|j\rangle = \langle j|\hat{h}|i\rangle^*$  follows immediately. The total number of one-electron integrals is equal to  $P^2$ , where  $P$  denotes the number of spatial orbitals (in the case of the restricted set of spin orbitals). If the spin orbitals are additionally real, all one-electron integrals are also real. In this case, the expression in the previous equation becomes symmetrical, so that the following symmetry relation is valid

$$\langle i|\hat{h}|j\rangle = \langle j|\hat{h}|i\rangle \quad (2.26)$$

and the number of one-electron integrals that need to be calculated is halved. In the case where the orbitals are complex, the complex conjugation appears in the previous relation, but the number of integrals that should be calculated and stored in memory is still halved (compared to the total number of one-electron integrals  $P^2$ ). The notation used here  $\langle i|\hat{h}|j\rangle$  is denoted as Dirac bra-ket (physicist's) notation. Very often, the other notation, chemist's notation, is used. For one-electron integrals, it looks the same as the bra-ket notation, except that the square brackets are used instead of angles:  $\langle i|\hat{h}|j\rangle = [i|\hat{h}|j]$ .

The reason why the other notation is introduced will be clear after the two-electron integrals are defined. In the end, let us find expressions for one-electron integrals over spatial orbitals. To do that the spin variable within a spin orbital must be integrated out. This discussion will focus on the restricted spin orbitals defined in (2.11). Recall the definition of the restricted spin orbitals and extend it to:

$$\left. \begin{aligned} \chi_{2i-1}(\mathbf{x}) &\equiv \psi_i(\mathbf{x}) = \psi_i(\mathbf{r})\alpha(\omega) \\ \chi_{2i}(\mathbf{x}) &\equiv \bar{\psi}_i(\mathbf{x}) = \psi_i(\mathbf{r})\beta(\omega) \end{aligned} \right\} i = 1, 2, \dots, P. \quad (2.27)$$

Because of the spin orthogonality (2.10) only the terms with the same spin (both with or without bar) survive. It can be summarized as

$$\begin{aligned} \langle i|\hat{h}|j\rangle &= \langle \bar{i}|\hat{h}|\bar{j}\rangle = (i|\hat{h}|j) \\ \langle i|\hat{h}|\bar{j}\rangle &= \langle \bar{i}|\hat{h}|j\rangle = 0. \end{aligned} \quad (2.28)$$

Note that the parentheses in previous equation involve the integration over spatial orbitals only.

## Two-Electron Integrals

Similar as for one-electron integrals, two-electron integrals are matrix elements of the Coulomb operator  $r_{ij}^{-1}$  in the basis of spin orbitals. The formal definition in bra-ket notation looks like

$$\langle ij|kl\rangle = \int d\mathbf{x}_1 d\mathbf{x}_2 \chi_i^*(\mathbf{x}_1)\chi_j^*(\mathbf{x}_2)r_{12}^{-1}\chi_k(\mathbf{x}_1)\chi_l(\mathbf{x}_2). \quad (2.29)$$

From the last equation, it is clear that the following relation holds

$$\langle ij|kl\rangle = \langle kl|ij\rangle^* . \quad (2.30)$$

In the previous subsection it was mentioned that the chemist's notation is of particular importance for two-electron integrals. Using this notation, the two-electron integral is defined as follows:

$$[ij|kl] = \int d\mathbf{x}_1 d\mathbf{x}_2 \chi_i^*(\mathbf{x}_1) \chi_j(\mathbf{x}_1) r_{12}^{-1} \chi_k^*(\mathbf{x}_2) \chi_l(\mathbf{x}_2) = \langle ik|jl\rangle . \quad (2.31)$$

Because it occurs very often in the evaluation of matrix elements over Slater determinants, the antisymmetric Coulomb integral is introduced:

$$\langle ij||kl\rangle = \langle ij|kl\rangle - \langle ij|lk\rangle = [ik|jl] - [il|jk] . \quad (2.32)$$

The meaning of this expression will be clear after the Hartree-Fock approximation is introduced. Until now, one can notice that this term satisfies identical conditions as (2.30), i.e. :

$$\langle ij||kl\rangle = \langle kl||ij\rangle^* . \quad (2.33)$$

Assuming all spin orbitals are real functions, it can be concluded that the following symmetry relations are fulfilled:

$$\begin{aligned} [ij|kl] &= [kl|ij] \\ [ij|kl] &= [ij|lk] = [ji|kl] = [ji|lk], \end{aligned} \quad (2.34)$$

so that the number of two-electron integrals is reduced by factor 8. Additionally, if the spin variable is integrated out, all terms with different spin on the same side of the rectangular brackets will disappear. The remaining non-zero two-electron integrals are

$$[ij|kl] = [\bar{i}\bar{j}|kl] = [ij|\bar{k}\bar{l}] = [\bar{i}\bar{j}|\bar{k}\bar{l}] = (ij|kl) . \quad (2.35)$$

The practical evaluation of one- and two-electron integrals in a given set of orbitals will be discussed in the next chapter.

## 2.6 Slater-Condon Rules

Once the one- and two-electron integrals have been introduced, it remains to establish the rules for the evaluation of the Hamiltonian matrix elements in a Slater space. They are named Slater-Condon rules after Slater and Condon, respectively. In this section, only the results will be shown. For the complete derivation, see [4, 5]. For the corresponding Slater determinants, the notation defined in equations (2.20-2.22) will be used. The reference determinant will be  $|\Psi_0\rangle$ , determinant that differs by one spin orbital from the reference state, i.e. single excitation  $|\Psi_a^r\rangle$  and the determinant that differs by two electrons, i.e. double excitation  $|\Psi_{ab}^{rs}\rangle$ .

- Let us begin with the identity operator - scalar product between two Slater determinants:

$$\boxed{\begin{aligned} \langle \Psi_0 | \Psi_0 \rangle &= 1 \\ \langle \Psi_0 | \Psi_a^r \rangle &= 0 \\ \langle \Psi_0 | \Psi_{ab}^{rs} \rangle &= 0 \end{aligned}} \quad (2.36)$$

- Operator  $\hat{O}_1$  (2.23):

$$\begin{aligned}
 \langle \Psi_0 | \hat{O}_1 | \Psi_0 \rangle &= \sum_i^N \langle i | \hat{h} | i \rangle = 2 \sum_i^{N/2} \langle i | \hat{h} | i \rangle \\
 \langle \Psi_0 | \hat{O}_1 | \Psi_a^r \rangle &= \langle a | \hat{h} | r \rangle = (a | \hat{h} | r) \\
 \langle \Psi_0 | \hat{O}_1 | \Psi_{ab}^{rs} \rangle &= 0
 \end{aligned}
 \tag{2.37}$$

- Operator  $\hat{O}_2$  (2.24):

$$\begin{aligned}
 \langle \Psi_0 | \hat{O}_2 | \Psi_0 \rangle &= \frac{1}{2} \sum_{ij}^N \langle ij || ij \rangle = \sum_{i,j}^{N/2} 2(ii|jj) - (ij|ji) \\
 \langle \Psi_0 | \hat{O}_2 | \Psi_a^r \rangle &= \sum_i^N \langle ai || ri \rangle = \sum_i^{N/2} 2(ar|ii) - (ai|ir) \\
 \langle \Psi_0 | \hat{O}_2 | \Psi_{ab}^{rs} \rangle &= \langle ab || rs \rangle = (ar|bs) - \delta_{\sigma_a, \sigma_b} (as|br)
 \end{aligned}
 \tag{2.38}$$

Notice, by the transition from spin orbitals to the spatial orbitals, the sum over spin orbitals is symbolically split into

$$\sum_{i=1}^N \chi_i = \sum_{i=1}^{N/2} \psi_i + \sum_{i=1}^{N/2} \bar{\psi}_i.
 \tag{2.39}$$

If the Slater determinants differ by more than two spin orbitals, all matrix elements are zero. To apply Slater-Condon rules, the two determinants must be in the state of maximum coincidence. That means, the spin orbitals that differ in two determinants must have the same place in a Slater determinant. When the ascending order is used for the Slater space, the total number of electron interchanges  $P$ , that have to be done to get the state of the maximum coincidence, must be counted in the process of the evaluation of the matrix elements. After the Slater-Condon rules are applied, this matrix element is additionally multiplied by the factor  $-1^P$ . This factor ensures the maximum coincidence between two Slater determinants and it was mentioned that the factor -1 arises each time when two spin orbitals within a determinant are interchanged. In the second quantization formalism, this factor will be automatically counted by anticommutation relation of creation and annihilation operators. Therefore, let us discuss the second quantization in more details.

## 2.7 Second Quantization

Second quantization is a powerful formalism in which not only the observables are represented by linear operators, but also the wave function itself. From the algebra of those operators, the wave function fulfills the antisymmetry principle automatically. For a strict mathematical derivation of the second quantization, see [6, 7]. In this chapter the application of the second quantization in the many-body problem will be

presented [8,9]. A Slater determinant can be represented in the spirit of the equation (2.19) as

$$|\Psi\rangle = |n_1, n_2, \dots, n_i, \dots, n_{2P}\rangle, \begin{cases} n_i = 1, & \text{if } \chi_i \text{ occupied} \\ n_i = 0, & \text{if } \chi_i \text{ unoccupied} \end{cases} \quad (2.40)$$

where in comparison with (2.19) not only the occupied orbitals are labeled, but also the unoccupied ones. The numbers  $n_i$  are called occupation numbers and this representation refers to occupation number representation. Note that this representation allows states with a variable number of electrons. A very special case is the state without any electrons, the so-called true vacuum state, denoted as:

$$|0\rangle = |\text{vac}\rangle = |0_1, 0_2, \dots, 0_{2P}\rangle, \text{ with } \langle 0|0\rangle = 1. \quad (2.41)$$

It raises the question, what kind of machinery is responsible for this variation of the number of electrons in a wave function. The answer is creation and annihilation operators.

### 2.7.1 Creation, Annihilation and Excitation Operators

The creation and annihilation operators play the central role in second quantization. The wave function and all quantum mechanical operators can be represented in terms of those operators. The creation operator  $\hat{a}_i^\dagger$ , as its name already implies, creates an electron in spin orbital  $\chi_i$ . The formal definition can be written as

$$\hat{a}_i^\dagger |n_1, n_2, \dots, n_i, \dots, n_{2P}\rangle = \delta_{n_i 0} \Gamma_i |n_1, n_2, \dots, 1_i, \dots, n_{2P}\rangle. \quad (2.42)$$

From this definition it follows, the wave function survives only if the occupation number  $n_i$  satisfies  $n_i = 0$  before the creation operator acts on the wave function. The factor  $\Gamma_i$  is defined as

$$\Gamma_i = \prod_{j=1}^{i-1} (-1)^{n_j} = (-1)^{\sum_{j=1}^{i-1} n_j}. \quad (2.43)$$

and it is equal to 1 if the number of electrons in spin orbitals with  $j < i$  is even, and -1 if the number of electrons in these orbitals is odd. From this definition, it is clear that each Slater determinant can be expressed as the pure product of the creation operators:

$$|\Psi\rangle = \left( \prod_{i=1}^{2P} (\hat{a}_i^\dagger)^{n_i} \right) |0\rangle = (\hat{a}_1^\dagger)^{n_1} (\hat{a}_2^\dagger)^{n_2} \dots (\hat{a}_{2P}^\dagger)^{n_{2P}} |0\rangle. \quad (2.44)$$

Similarly, the annihilation operator  $\hat{a}_i$  destroys an electron in the orbital  $\chi_i$ :

$$\hat{a}_i |n_1, n_2, \dots, n_i, \dots, n_{2P}\rangle = \delta_{n_i 1} \Gamma_i |n_1, n_2, \dots, 0_i, \dots, n_{2P}\rangle. \quad (2.45)$$

Opposite to the creation operator, the annihilation operator  $\hat{a}_i$  destroys the state if  $n_i = 0$ , before the action of the operator. It is actually only the adjoint of the creation operator

$$(\hat{a}_i^\dagger)^\dagger = \hat{a}_i. \quad (2.46)$$

Additionally, the set of Fermion-anticommutation relations, that these operators satisfy is

$$\begin{aligned}\{\hat{a}_i^\dagger, \hat{a}_j^\dagger\} &= \{\hat{a}_i, \hat{a}_j\} = 0 \\ \{\hat{a}_i^\dagger, \hat{a}_j\} &= \delta_{ij}.\end{aligned}\tag{2.47}$$

In the end of this subsection, one particularly important operator should be mentioned. That operator is the excitation operator  $\hat{E}_{ij}$  defined as

$$\hat{E}_{ij} = \hat{a}_i^\dagger \hat{a}_j, \quad \text{with} \quad [\hat{E}_{ij}, \hat{E}_{kl}] = \delta_{kj} \hat{E}_{il} - \delta_{il} \hat{E}_{kj}.\tag{2.48}$$

The excitation operator is the number-conserving operator and in the case  $i = j$ , it reduces to the occupation-number operator [8,9]. The meaning of this operator is the promotion of the electron from the spin orbital  $\chi_j$  to the spin orbital  $\chi_i$ . According to (2.48) the commutation relation disappears if all four indices differ.

## 2.7.2 Hamiltonian Operator in Second Quantization

Recall the definitions of one- and two-electron operators (2.23, 2.24) and rewrite them in the spirit of second quantization in both notations (physicist's and chemist's one):

$$\begin{aligned}\hat{O}_1 &= \sum_{ij}^{2P} \langle i|\hat{h}|j\rangle \hat{a}_i^\dagger \hat{a}_j = \sum_{ij}^{2P} [i|\hat{h}|j] \hat{a}_i^\dagger \hat{a}_j \\ \hat{O}_2 &= \frac{1}{2} \sum_{ijkl}^{2P} \langle ij|kl\rangle \hat{a}_i^\dagger \hat{a}_j^\dagger \hat{a}_l \hat{a}_k = \frac{1}{2} \sum_{ijkl}^{2P} [ij|kl] \hat{a}_i^\dagger \hat{a}_k^\dagger \hat{a}_l \hat{a}_j,\end{aligned}\tag{2.49}$$

where the sum runs over  $2P$  spin orbitals. Of particular interest is to rewrite the previous equations, so that the sum runs only over  $P$  spatial orbitals. In other words, the equations must be integrated over spin variable. To achieve that, one uses the sum splitting (2.39) and the fact that the creation and annihilation operators split in two irreducible representations: one for spin up  $|\alpha\rangle$  and one for spin down  $|\beta\rangle$ . According to this, the excitation operator (2.48) must be rewritten as

$$\hat{E}_{ij} = \hat{E}_{ij}^\alpha + \hat{E}_{ij}^\beta = \hat{a}_{i\alpha}^\dagger \hat{a}_{j\alpha} + \hat{a}_{i\beta}^\dagger \hat{a}_{j\beta}.\tag{2.50}$$

Although derivations of equations will be avoided in this work, this particular case will be written out step by step, because the resulting Hamiltonian operator will be the central concept for all CI calculations carried out in this thesis. With these considerations, the one-electron operator (2.49) becomes:

$$\hat{O}_1 = \sum_{ij}^{2P} [i|\hat{h}|j] \hat{a}_i^\dagger \hat{a}_j = \sum_{ij}^P [i|\hat{h}|j] \hat{a}_{i\alpha}^\dagger \hat{a}_{j\alpha} + \sum_{ij}^P [i|\hat{h}|j] \hat{a}_{i\alpha}^\dagger \hat{a}_{j\beta} + \sum_{ij}^P [\bar{i}|\hat{h}|j] \hat{a}_{i\beta}^\dagger \hat{a}_{j\alpha} + \sum_{ij}^P [\bar{i}|\hat{h}|j] \hat{a}_{i\beta}^\dagger \hat{a}_{j\beta}.\tag{2.51}$$

Applying spin orthogonalization rules for one-electron integrals listed in (2.28):

$$\hat{O}_1 = \sum_{ij}^P (i|\hat{h}|j) \left[ \hat{a}_{i\alpha}^\dagger \hat{a}_{j\alpha} + \hat{a}_{i\beta}^\dagger \hat{a}_{j\beta} \right] = \sum_{ij}^P (i|\hat{h}|j) \hat{E}_{ij}.\tag{2.52}$$

Analogously, the two-electron operator can be rewritten in the same way. After spin integration, only 4 of 16 two-electron integrals survive (2.35), and the two-electron operator looks like:

$$\hat{O}_2 = \frac{1}{2} \sum_{ijkl}^P [ij|kl] \left[ \hat{a}_{i\alpha}^\dagger \hat{a}_{k\alpha}^\dagger \hat{a}_{l\alpha} \hat{a}_{j\alpha} + \hat{a}_{i\alpha}^\dagger \hat{a}_{k\beta}^\dagger \hat{a}_{l\beta} \hat{a}_{j\alpha} + \hat{a}_{i\beta}^\dagger \hat{a}_{k\alpha}^\dagger \hat{a}_{l\alpha} \hat{a}_{j\beta} + \hat{a}_{i\beta}^\dagger \hat{a}_{k\beta}^\dagger \hat{a}_{l\beta} \hat{a}_{j\beta} \right]. \quad (2.53)$$

Using anticommutation relations (2.47) to transfer annihilation operator labeled with  $s$  to the second place, yields:

$$\begin{aligned} \hat{O}_2 = \frac{1}{2} \sum_{ijkl}^P (ij|kl) \{ & \hat{a}_{i\alpha}^\dagger \hat{a}_{j\alpha} \hat{a}_{k\alpha}^\dagger \hat{a}_{l\alpha} + \hat{a}_{i\alpha}^\dagger \hat{a}_{j\alpha} \hat{a}_{k\beta}^\dagger \hat{a}_{l\beta} + \hat{a}_{i\beta}^\dagger \hat{a}_{j\beta} \hat{a}_{k\alpha}^\dagger \hat{a}_{l\alpha} + \hat{a}_{i\beta}^\dagger \hat{a}_{j\beta} \hat{a}_{k\beta}^\dagger \hat{a}_{l\beta} \\ & - \delta_{j\alpha, k\alpha} \hat{a}_{i\alpha}^\dagger \hat{a}_{l\alpha} - \delta_{j\alpha, k\beta} \hat{a}_{i\alpha}^\dagger \hat{a}_{l\beta} - \delta_{j\beta, k\alpha} \hat{a}_{i\beta}^\dagger \hat{a}_{l\alpha} - \delta_{j\beta, k\beta} \hat{a}_{i\beta}^\dagger \hat{a}_{l\beta} \}. \end{aligned} \quad (2.54)$$

Note that the first four terms from the previous equation are the product of two excitation operators (2.50). Additionally the delta-Kronecker symbols with different spins reduce to 0, while  $\delta_{j\alpha, k\alpha}$  and  $\delta_{j\beta, k\beta}$  reduce to  $\delta_{jk}$ . With these results, the two-electron operator in the end becomes:

$$\hat{O}_2 = \frac{1}{2} \sum_{ijkl}^P (ij|kl) \left[ \hat{E}_{ij} \hat{E}_{kl} - \delta_{jk} \hat{E}_{il} \right]. \quad (2.55)$$

For the full derivation of the previous equations, see [10]. In the end of this chapter, the entire Hamiltonian for spatial orbitals in second quantization looks like:

$$\hat{H} = \sum_{ij}^P (i|\hat{h}|j) \hat{E}_{ij} + \frac{1}{2} \sum_{ijkl}^P (ij|kl) \left[ \hat{E}_{ij} \hat{E}_{kl} - \delta_{jk} \hat{E}_{il} \right]. \quad (2.56)$$

# Chapter 3

## Gaussian Basis Sets and Molecular Integral Evaluation

In the previous chapter, the basic quantum physics needed to solve the many-body Schrödinger equation was presented. In the section 2.3, the properties of spatial and spin orbitals were discussed. They are needed for the construction of the many-electron wave function. The main goal of this chapter is to introduce the initial set of orbitals - the basis set. These are simple mathematical functions that satisfy basic conditions proposed by abstract orbitals defined in quantum physics. In other words, the basis functions must have large amplitudes in regions where the probability of finding an electron is high and they have to be normalized. Although the exact solution of the Schrödinger equation requires an infinite basis set, in reality, one is limited by computational resources to a rather small and finite, but complete basis sets. Therefore, the basis set has to be chosen carefully, because the basis set will determine the quality of the solution. The goal is to get the best possible results with as few basis functions as possible.

The Slater-type orbitals (section 3.1) seem to be the most natural choice of the atomic orbitals, because of their convergence behavior for  $r \rightarrow \infty$ , that corresponds to the exact solution of the Schrödinger equation for the hydrogen atom. However, the evaluation of the molecular integrals (one- and two-electron integrals, see section 2.5) is a rather complex task, especially for Slater-type orbitals. The molecular integrals for Slater orbitals can not be determined analytically and various numerical methods must be applied. Francis S. Boys recommended the use of Gaussian basis sets (Gaussian like functions, see section 3.3). The evaluation of molecular integrals in this basis set is still tedious, but rather straightforward, as it will be seen in section 3.4. The various types of Gaussian basis sets will be discussed here: STO-LG basis sets - known as minimal basis sets, split-valence basis sets (X-YZG) and the largest, but also the most important correlation-consistent basis sets with notation (aug-)cc-PVXZ. At the end of the chapter, additionally, the delocalized plane waves basis set, together with its localized counterpart - localized Wannier functions are introduced. They are important for the extrapolation of Hartree-Fock Hamiltonian from density-functional theory via hybrid functionals, implemented in VASP.

Before the discussion of various basis functions begins, it should be noted that each

Table 3.1: The names of the most used shells in electronic structure theory calculations. The shell is entirely determined by the quantum numbers  $n$  and  $l$ . The number of members within a shell is  $2l + 1$ .

$n$	$l$	$2l + 1$	Name
1	0	1	1s
2	0	1	2s
2	1	3	2p
3	2	5	3d
4	3	7	4f

basis function  $\chi_{nlm}(r, \theta, \varphi)$  can be split in a radial and angular part as

$$\chi_{nlm}(r, \theta, \varphi) = R_{nl}(r)Y_{lm}(\theta, \varphi), \quad (3.1)$$

where  $n, l, m$  are main quantum number, angular momentum quantum number and magnetic quantum number, respectively. The term  $R_{nl}(r)$  denotes the radial part of the function and  $Y_{lm}(\theta, \varphi)$  its angular part. The angular part has an identical form for all basis functions and it is given by the spherical harmonics:

$$Y_{lm}(\theta, \varphi) = \sqrt{\frac{2l+1}{4\pi} \frac{(l-m)!}{(l+m)!}} P_l^m(\cos\theta) e^{im\varphi}, \quad (3.2)$$

where  $P_l^m(x)$  are associated Legendre polynomials. The spherical harmonics are the eigenfunctions of the angular momentum operators  $\hat{L}^2$  and  $\hat{L}_z$  and they are described by two quantum numbers -  $l$  and  $m$ . The restrictions obeyed by all three quantum numbers are:

$$\begin{aligned} n &> 0 \\ 0 &\leq l < n \\ |m| &\leq l. \end{aligned} \quad (3.3)$$

From these restrictions, it can be concluded that for a particular  $l$  one can build  $2l + 1$  different spherical harmonics and for each  $n$  one has  $n^2$  different orthogonal spherical harmonics. All orbitals that have the same main and angular momentum quantum number belong to one shell. The usual names of specific shells are given in table 3.1. Note that the number of orbitals within a shell is  $2l + 1$ .

### 3.1 Slater-Type Basis Functions

Slater-type functions (STOs) were introduced by Slater [12]. As it was mentioned at the beginning of this chapter, the angular part of the Slater-type orbitals is given by spherical harmonics  $Y_{lm}(\theta, \varphi)$ , while the radial part is given by

$$\phi_{nlm}^{\text{STO}}(r, \theta, \varphi) = S_{nlm}(\zeta) = \frac{(2\zeta)^{3/2}}{\sqrt{\Gamma(2n+1)}} (2\zeta r)^{n-1} e^{-\zeta r} Y_{lm}(\theta, \varphi), \quad (3.4)$$

where  $\zeta$  denotes a Slater exponent and  $\Gamma(n)$  is the gamma function, the extension of the factorial. For a fixed  $\zeta$  value, the set of Slater orbitals with different quantum numbers builds a complete set of functions. The advantage of Slater orbitals lies in the

fact that their radial part decays the same as the exact solutions of the Schrödinger equation for the hydrogen atom. On the other side, the evaluation of molecular integrals with Slater-type orbitals can not be done analytically. Therefore, various numerical methods have been developed to solve this problem. Those numerical methods are out of scope of this work. They are considered in more details in [13]. Because of these difficulties in evaluating the molecular integrals, Francis S. Boys suggested the Gaussian orbitals. In the next section, they will be introduced, together with a method for molecular integral evaluation.

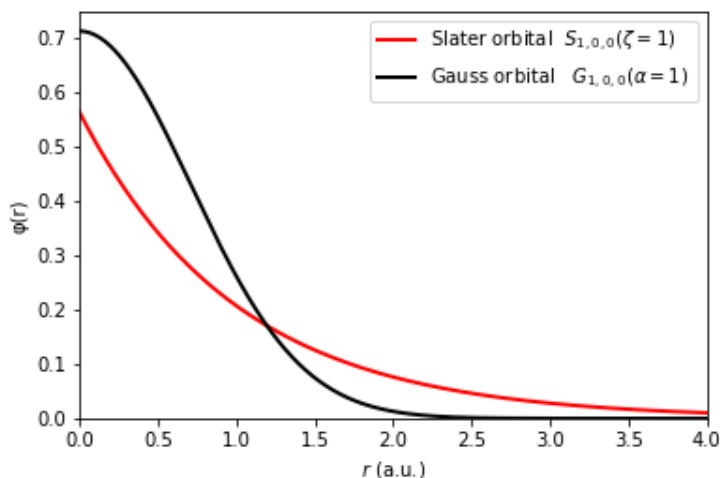


Figure 3.1: The radial part of normalized 1s Slater (red) and Gaussian (black) orbitals.

## 3.2 Gaussian orbitals

Analogously to the the Slater-type orbitals, Gaussian orbitals (GTO-s) are defined as

$$\phi_{lm}^{\text{GTO}}(r, \theta, \varphi, \alpha) = G_{lm}(r, \theta, \varphi, \alpha) = \frac{2(2\alpha)^{3/4}}{\pi^{1/4}} \sqrt{\frac{2^l}{(2l+1)!!}} (\sqrt{2\alpha}r)^l \exp(-\alpha r^2) Y_{lm}(\theta, \varphi), \quad (3.5)$$

where  $\alpha$  is an orbital exponent and  $!!$  is a double factorial. However, for most applications real spherical harmonics  $S_{lm}$  are used instead of complex spherical harmonics, and they are related to the spherical harmonics as:

$$S_{l0} = \sqrt{\frac{4\pi}{2l+1}} Y_{l0} \quad (3.6)$$

$$S_{lm} + iS_{l,-m} = (-1)^m \sqrt{\frac{8\pi}{2l+1}} r^l Y_{lm}, \quad m > 0$$

so that the usual form of the Gaussian function is simply

$$\phi_{lm}^{\text{GTO}} = N_{\alpha lm}^{\text{GTO}} S_{lm}(x, y, z) \exp(-\alpha r^2), \quad (3.7)$$

with a normalization constant  $N_{\alpha l m}^{\text{GTO}}$ . Gaussian orbitals defined in such a way are called spherical-harmonic GTOs. For the purpose of the molecular integral evaluation, the Cartesian and the Hermite Gaussians will be introduced in the section 3.4. The radial shape of the Gaussian orbitals is not as good as one of the Slater orbitals. They have the wrong decay for  $r \rightarrow \infty$  ( $e^{-r^2}$  instead of  $e^{-r}$ ) and the wrong slope at  $r \rightarrow 0$  (zero slope instead of the finite one). In the figure 3.1 the radial shapes of  $\phi_{00}^{\text{GTO}}$  and  $\phi_{100}^{\text{STO}}$  for unity exponents are depicted. Therefore, to achieve the same accuracy, more Gaussians than Slater orbitals must be included in the calculation. But this will be compensated with much faster evaluation of molecular integrals. In order to recover the radial shape of the Slater-type orbitals, a linear combination of Gaussians are used to represent one basis function. This type of a basis function is called a contraction. Let us discuss the most common used Gaussian basis sets and the way how they are constructed in the next section.

### 3.3 Gaussian Basis Sets

Contracted Gaussian type orbitals are introduced in this section, followed by a short overview of Gaussian basis sets.

#### 3.3.1 Contracted Gaussians

In order to minimize the number of basis functions in a basis set, each basis function will contain more primitive Gaussians. Such a basis function is called simply the contraction. The contraction can be written as

$$\phi_{\mu}^{\text{CGF}} = \sum_{\nu=1}^L d_{\mu\nu} \phi_{\nu}^{\text{GTO}}, \quad (3.8)$$

where  $L$  is a contraction length and  $d_{\mu\nu}$  are contraction coefficients. The final basis function is denoted as the contracted Gaussian function - CGF. In calculations, the contraction of basis functions should be performed as soon as possible, to reduce the number of one- and two-electron integrals.

#### 3.3.2 STO-LG Basis set

The most commonly used basis set, whose functions are the contractions of a constant length  $L$  ( $L$  ranges from 1 to 6) is called minimal basis set and is denoted as STO-LG. These basis sets are often used for Hartree-Fock type calculations. The first row elements (H, He) are described only by one Gaussian contraction, while the second row elements (Li-Ne) are described by 1s shell and 2sp shells (5 basis functions in total). sp shell denotes one s and one p shell with the same main quantum number and it will be considered as one single shell. For atoms from the third and fourth row, new sp shells are added, but in the minimal basis set, the functions with  $l > 1$  do not appear. Commonly used basis sets from this group are STO-3G and STO-6G.

Each function of the STO-LG basis set is a contraction of  $L$  spherical-harmonics Gaussian functions, that try to approximate a real STO function and its radial part.

This is achieved by the least square minimization of the following integral

$$\Delta_{\mu}^{\text{STO-LG}} = \|\phi_{\mu}^{\text{STO}}(\zeta = 1) - \sum_{\nu=1}^L d_{\mu\nu} \phi_{\nu}^{\text{GTO}}(\alpha_{\nu})\|^2. \quad (3.9)$$

Note that in the previous equation only a Slater orbital with unity exponent  $\zeta$  is approximated by optimized contraction coefficients  $d_{\mu\nu}$  and orbital exponents  $\alpha_{\nu}$ . In order to approximate Slater orbitals with different  $\zeta$  values, only the Gaussian orbital exponents  $\alpha_{\nu}$  have to be scaled, while the contraction coefficients remain unchanged:

$$\alpha_{\nu}(\zeta) = \zeta^2 \alpha_{\nu}(\zeta = 1). \quad (3.10)$$

It should be noted that all basis functions within a shell share the same exponent and contraction coefficients, because of computational efficiency. The best contraction coefficients and exponents, as well as the fact why the scaling factor  $\zeta^2$  arises and what are the scaling exponents  $\zeta$  for various atoms, can be found in a paper by Pople and Hehre [14], where *STO-LG* basis sets were originally introduced. The radial part of a  $1s$  basis function with a Slater exponent  $\zeta = 1$  in *STO-3G* and *STO-6G* basis sets are represented together with a normalized  $1s$  Slater-type orbital in the figure 3.2. One can notice that visible improvement is achieved with *STO-3G* and *STO-6G* basis sets in comparison with *STO-1G*. In the end, it should be mentioned, the *STO-LG* basis sets are used only for molecules in the first-row.

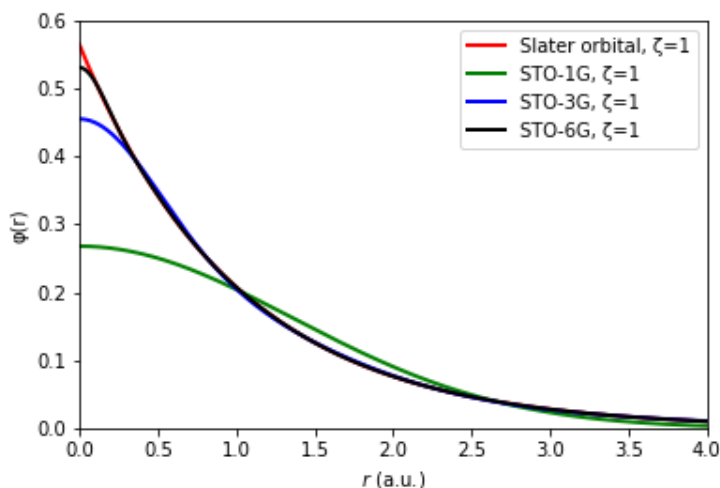


Figure 3.2: The approximation of a normalized  $1s$  Slater orbital with unity exponent  $\zeta = 1$  within *STO-LG* basis sets for  $L = 1, 3, 6$ . Obviously, the drastic improvement is achieved with increasing  $L$ .

### 3.3.3 Split-Valence Basis Sets

The split-valence basis set is the first improvement of the minimal basis set. It is recognized here that valence electrons are responsible for most properties of

molecules and therefore, one uses more basis functions to describe valence orbitals. The inner shells contribute very little to the ground state energy and even less to other chemical properties. Therefore, they are represented as a single contracted Gaussian. Let us introduce the notation for split-valence basis sets - X-YZG. X denotes the contraction length for the inner shell orbitals. The number of following letters determines how many Gaussian basis functions are used to describe valence orbitals. Each letter (Y,Z,...) is a contraction length of corresponding split valence orbital. In the split-valence basis sets, Gaussian exponents are obtained by the Hartree-Fock ground state solution of the corresponding atom, rather than by approximation with a Slater-type orbitals. The usually used split-valence basis sets were introduced by Pople and coworkers [15, 16]. The well-known members from this group of basis sets are: split-valence double-zeta basis sets (4-31G, 6-31G, 6-31G\*, 6-31+G\*) and split-valence triple-zeta basis sets (6-311G, 6-311G\*, 6-311+G\*). The sign \* (+) denotes additional polarization (diffuse) *d* or *f* valence orbitals on heavy atoms and the sign \*\*(++ ) adds also the polarization (diffuse) *p* orbitals on the hydrogen atom. The polarization functions are added when the polarization effects are present, for example the polarization of hydrogen electron density in the electric field. They have higher angular momentum than occupied atomic-like orbitals, for example *2p* orbitals for the H atom or *3d* orbitals for the second row elements. The same applies for the diffuse functions, which are added in cases where valence electrons play an important role for the ground state. As the name already implies, these diffuse functions are "wider" than normal Gaussians and they describe very well the electrons that are far away from the nucleus.

### 3.3.4 Correlation Consistent Basis Sets

In order to recover a significant part of the correlation energy, virtual-space orbitals have to be included in the description of the basis set to ensure more flexibility for the construction of a wave function. The most of attention is directed to the correlation of valence electrons, while the core electrons are treated as before with single or double contracted Gaussian functions. The widest used correlation-consistent basis sets were introduced by Dunning and coworkers [17–19], and they are the so-called cc-pVXZ basis sets, where cc stands for correlation-consistent, p for the polarized, V for valence and the number X is the cardinal number. If X=2 then the basis set is of the same quality as double-zeta basis set. For X=3, it is similar to the triple-zeta basis set and so on. The optimal contraction coefficients and exponents are obtained from very accurate Hartree-Fock calculations on atoms. The most commonly used basis sets in this group are: cc-pVDZ, cc-pVTZ, cc-pVQZ, cc-pV5Z basis sets. As it was mentioned previously, these basis sets are assigned to describe correlation effects in the valence shell. If a more accurate solution is desired, basis sets could be further extended with functions that describe core electron correlation effects. These are denoted as cc-pCVXZ basis sets, where CV represents core-valence. On the other hand, each of the previously mentioned basis sets can be further augmented with diffuse functions that try to improve the description of outer valence-electron regions. In this way, one obtains aug-cc-pVXZ and aug-cc-pCVXZ basis sets.

In the end of this section, the table with the most used Gaussian basis sets is presented (table 3.2). In this table, the name and the content of the basis set, as well as the total number of orbitals within a basis set, can be found. The content shows what are the primitive GTOs and how they are contracted. The simple example would be three  $s$  GTOs contracted in one CGF function, denoted as  $(3s)/[1s]$  contraction.

Table 3.2: The most commonly used Gaussian basis sets. In the table the number of uncontracted shells is given in parentheses, while the number of contracted shells is given in angle brackets. The last number denotes the total number of basis functions within a corresponding basis set.

Name	H-He	Li-Ne
STO-3G	$(3s)/[1s]; 1$	$(6s, 3p)/[2s, 1p]; 5$
STO-6G	$(6s)/[1s]; 1$	$(12s, 6p)/[2s, 1p]; 5$
6-31G	$(4s)/[2s]; 2$	$(10s, 4p)/[3s, 2p]; 9$
6-311G	$(5s)/[3s]; 3$	$(11s, 5p)/[4s, 3p]; 13$
cc-pVDZ	$(4s, 1p)/[2s, 1p]; 5$	$(9s, 4p, 1d)/[3s, 2p, 1d]; 14$
cc-pVTZ	$(5s, 2p, 1d)/[3s, 2p, 1d]; 14$	$(11s, 5p, 2d, 1f)/[4s, 3p, 2d, 1f]; 30$
cc-pvQZ	$(6s, 3p, 2d, 1f)/[4s, 3p, 2d, 1f]; 32$	$(12s, 6p, 3d, 2f, 1g)/[5s, 4p, 3d, 2f, 1g]; 55$
aug-cc-pVDZ	$(5s, 2p)/[3s, 2p]; 9$	$(10s, 5p, 2d)/[4s, 3p, 2d]; 23$
aug-cc-pVTZ	$(6s, 3p, 2d)/[4s, 3p, 2d]; 23$	$(12s, 6p, 3d, 2f)/[5s, 4p, 3d, 2f]; 46$
aug-cc-pVQZ	$(7s, 4p, 3d, 2f)/[5s, 4p, 3d, 2f]; 46$	$(13s, 7p, 4d, 3f, 2g)/[6s, 5p, 4d, 3f, 2g]; 80$

## 3.4 Molecular Integral Evaluation

The last piece of the electronic-structure mosaic needed to be able to perform the first calculations, is the evaluation of molecular integrals over a chosen basis set. As it was discussed in the last section, the Gaussian orbitals turn out to be the best choice for this problem. Short overview of Gaussian functions follows. Thereafter, the so-called McMurchie-Davidson scheme for the analytic evaluation of molecular integrals will be presented.

### 3.4.1 Primitive Cartesian Gaussians

The equation (3.7) rewritten in Cartesian coordinates gives the primitive Cartesian Gauss functions (PGFs). The primitive Cartesian Gaussian with an exponent  $\alpha$  centered on nucleus at position  $\mathbf{A} = (A_x, A_y, A_z)$  is defined relative to the site  $\mathbf{A}$  as

$$G_{ijk}(\mathbf{r}, \alpha, \mathbf{A}) = x_A^i y_A^j z_A^k \exp(-\alpha r_A^2), \quad (3.11)$$

where  $i, j, k$  are Cartesian quantum numbers. The total angular momentum is given as a sum of Cartesian quantum numbers  $l = i + j + k$ . The term  $r_A$  stands for

$$r_A = \|\mathbf{r}_A\| = \|\mathbf{r} - \mathbf{A}\| = \left\| \begin{pmatrix} x - A_x \\ y - A_y \\ z - A_z \end{pmatrix} \right\|. \quad (3.12)$$

$x_A, y_A$  and  $z_A$  are defined in the similar way. The number of primitive Gaussians within a shell (they all share the same quantum number  $l$  and exponent  $\alpha$ ) is given as

$$N_l^C = \frac{(l+1)(l+2)}{2}. \quad (3.13)$$

The main advantage of primitive Cartesian functions is the fact that they are separable in each coordinate:

$$G_{ijk}(\mathbf{r}, \alpha, \mathbf{A}) = G_i(x, \alpha, A_x) \cdot G_j(y, \alpha, A_y) \cdot G_k(z, \alpha, A_z), \quad \text{with} \quad (3.14)$$

$$G_i(x, \alpha, A_x) = (x - A_x)^i \exp(-\alpha(x - A_x)^2) = x_A^i \exp(-\alpha x_A^2).$$

The product of two Gaussian functions is often called overlap distribution function. If the Cartesian Gaussians are used, then one obtains Cartesian overlap distributions:

$$\Omega_{ij} = G_i(x, \alpha, A_x) \cdot G_j(x, \beta, B_x). \quad (3.15)$$

As it will later be seen, the possibility to factorize Cartesian Gaussian facilitates the evaluation of integrals. In the following text, primitive Gaussians will be referred as PGFs and denoted with  $G_{ijk}$ , while the spherical-harmonics Gaussians are usually labeled as GTOs (Gauss-type orbitals) and the notation  $G_{lm}$  or  $\phi_{lm}^{\text{GTO}}$  is used for them. Additionally, if a Gaussian is labeled with CGF, thus it means, it is a contraction of spherical-harmonics Gaussian functions.

### 3.4.2 Spherical-Harmonics Gaussians

The spherical-harmonics Gaussians are defined in (3.7). For their description, real solid-harmonics  $S_{lm}$  are used. Table 3.3 shows all solid-harmonics with  $l \leq 3$ . From the form of the real solid-harmonics, it is easy to conclude that they can be written as a sum of Cartesian Gaussian functions. In a shell of GTOs, they all share the same  $l$ . As it was mentioned at the beginning of this chapter, the shell described with quantum numbers  $l$  and  $m$  contains

$$N_l^S = 2l + 1 \quad (3.16)$$

functions. Comparing this number with the number of Cartesian Gaussians, one can notice that the condition  $N_l^S \leq N_l^C$  is true for all  $l$ . This difference becomes even more drastic with growing  $l$ . For that reason, the spherical-harmonics are always a better choice than the primitive Cartesian functions, because a smaller number of basis functions means a smaller number of molecular integrals, too. On the other side, the evaluation of molecular integrals is much easier in terms of Cartesian Gaussians. Therefore, the linear transformation from Cartesian to spherical-harmonics Gaussians should be done as early as possible, but at least before the integrals are calculated. To demonstrate this discrepancy, consider a single f shell. The number of different two-electron integrals evaluated over spherical-harmonics is roughly 300, while this number for the Cartesian Gaussians is 1250.

### 3.4.3 Gaussian Product Rule

The main advantage of Gaussians is the so-called Gaussian product rule, that applies for spherical Gaussians ( $l = 0$ ). It suggests that the product of two spherical Gaussians can be written as one single Gauss function. Consider two one-dimensional spherical Gaussians centered on sites  $\mathbf{A}$  and  $\mathbf{B}$  respectively. Using the Gaussian product rule, it becomes:

$$\exp(-\alpha x_A^2) \exp(-\beta x_B^2) = \exp(-\mu X_{AB}^2) \exp(-p x_P^2), \quad (3.17)$$

Table 3.3: The real-valued solid harmonics for  $l \leq 3$  and  $|m| \leq 3$ , where  $r^2 = x^2 + y^2 + z^2$ .

$\frac{l}{m}$	0	1	2	3
3				$\frac{1}{2}\sqrt{\frac{5}{2}}(x^2 - 3y^2)x$
2			$\frac{1}{2}\sqrt{3}(x^2 - y^2)$	$\frac{1}{2}\sqrt{15}(x^2 - y^2)z$
1		$x$	$\sqrt{3}xz$	$\frac{1}{2}\sqrt{\frac{3}{2}}(5z^2 - r^2)x$
0	1	$z$	$\frac{1}{2}(3z^2 - r^2)$	$\frac{1}{2}(5z^2 - 3r^2)y$
-1		$y$	$\sqrt{3}yz$	$\frac{1}{2}\sqrt{\frac{3}{2}}(5z^2 - r^2)y$
-2			$\sqrt{3}xy$	$\sqrt{15}xyz$
-3				$\frac{1}{2}\sqrt{\frac{5}{2}}(3x^2 - y^2)y$

where new exponents  $p$ ,  $\mu$  are introduced. They are defined as

$$\begin{aligned} p &= \alpha + \beta \\ \frac{1}{\mu} &= \frac{1}{\alpha} + \frac{1}{\beta}. \end{aligned} \quad (3.18)$$

The center  $\mathbf{P}$  of the new Gaussian can be found as

$$\mathbf{P} = \frac{\alpha\mathbf{A} + \beta\mathbf{B}}{p}. \quad (3.19)$$

The term  $X_{AB}$  in the first exponential factor on the right side is simply the  $x$  distance between the two centers  $\mathbf{A}$  and  $\mathbf{B}$ . Therefore, this first exponential factor is only a constant, because it does not depend on electronic coordinate  $x$ . It is usually called pre-exponential factor and it is denoted as  $K_{\alpha\beta}^x$ .

### 3.4.4 Hermite Gaussians

The last step, before the discussion of the McMurchie-Davidson scheme for the evaluation of integrals can begin, is to introduce the Hermite Gaussians. A Hermite Gaussian centered on the site  $\mathbf{P}$  with the orbital exponent  $p$  is given as

$$\Lambda_{tuv}(\mathbf{r}, p, \mathbf{P}) = \left(\frac{\partial}{\partial P_x}\right)^t \left(\frac{\partial}{\partial P_y}\right)^u \left(\frac{\partial}{\partial P_z}\right)^v \exp(-pr_{\mathbf{P}}^2). \quad (3.20)$$

Similarly as Cartesian Gaussians, the Hermite Gaussians are separable, too:

$$\begin{aligned} \Lambda_{tuv}(\mathbf{r}, p, \mathbf{P}) &= \Lambda_t(x, p, P_x)\Lambda_u(y, p, P_y)\Lambda_v(z, p, P_z), \quad \text{where} \\ \Lambda_t(x, p, P_x) &= \left(\frac{\partial}{\partial P_x}\right)^t \exp(-px_{\mathbf{P}}^2). \end{aligned} \quad (3.21)$$

The big advantage of Hermite Gaussian is the fact, that the integration over Hermite Gaussian is very simple and it is non-zero only for  $t = 0$

$$\int_{-\infty}^{\infty} dx \Lambda_t(x) = \delta_{t0} \sqrt{\frac{\pi}{p}}. \quad (3.22)$$

The Hermite Gaussians are used in McMurchie-Davidson scheme as expansion factors (see section 3.4.5). Although it is possible to use Hermite Gaussians as the basis function, they will be used only as intermediate states for the integral calculations over the Cartesian Gaussians.

### 3.4.5 McMurchie-Davidson Scheme

Introducing Hermite Gaussians, the McMurchie-Davidson scheme can be considered. In this scheme, the Cartesian overlap distribution (3.15) is expanded in terms of Hermite Gaussians. More details about this scheme can be found in [9, 20]. If one is interested only in the evaluation of integrals over spherical Gaussians ( $l = 0$ ), a good implementation is given in [21]. In order to keep the notation as simple as possible, three-dimensional Cartesian Gaussian will be denoted as  $G_\alpha$  or  $G_\beta$ , while one-dimensional Cartesian Gaussians are given as  $G_i$ ,  $G_j$  and so on. The following notation will be used in this section:

$$\begin{aligned} G_\alpha(\mathbf{r}, \alpha, \mathbf{A}) &= G_i(x, \alpha, A_x) \cdot G_k(y, \alpha, A_y) \cdot G_m(z, \alpha, A_z) \\ G_\beta(\mathbf{r}, \beta, \mathbf{B}) &= G_j(x, \beta, B_x) \cdot G_l(y, \beta, B_y) \cdot G_n(z, \beta, B_z) \\ \Omega_{\alpha\beta} &= G_\alpha \cdot G_\beta = \Omega_{ij} \cdot \Omega_{kl} \cdot \Omega_{mn}. \end{aligned} \quad (3.23)$$

For the evaluation of the electronic Hamiltonian (2.23, 2.24), the kinetic energy integrals  $T_{\alpha\beta}$ , one-electron attractive Coulomb integrals  $V_{\alpha\beta}$  and the two-electron repulsive Coulomb integrals  $[G_\alpha G_\beta | G_\gamma G_\delta] = [\alpha\beta | \gamma\delta]$  need to be calculated. The sum of the first two terms leads to the ordinary one-electron integrals  $\langle G_\alpha | \hat{h} | G_\beta \rangle$  defined in (2.25). Additionally, because the Gaussian orbitals do not form an orthonormal set, the overlap integrals  $S_{\alpha\beta} = \langle G_\alpha | G_\beta \rangle$  need to be calculated, too.

#### Overlap Integrals

Let us start with the simplest integrals. The overlap integral between two three-dimensional Cartesian Gaussians is:

$$S_{\alpha\beta} = \langle G_\alpha | G_\beta \rangle = \int_{\mathbb{R}^3} d^3r \Omega_{\alpha\beta}. \quad (3.24)$$

Using the separation rule for Cartesian Gaussians (3.14, 3.15), the previous equation can be rewritten as:

$$\begin{aligned} S_{\alpha\beta} &= S_{ij} \cdot S_{kl} \cdot S_{mn}, \quad \text{with} \\ S_{ij} &= \int_{-\infty}^{\infty} dx \Omega_{ij}. \end{aligned} \quad (3.25)$$

The Hermite Gaussians play the main role now, because the overlap distribution is simply a Gaussian of the exponent  $i + j$  and can be expanded as a linear combination of Hermite Gaussians

$$\Omega_{ij} = \sum_{t=0}^{i+j} E_t^{ij} \Lambda_t. \quad (3.26)$$

One obtains the expansion coefficients from McMurchie-Davidson recurrence relations, but they will not be derived here:

$$\begin{aligned} E_0^{00} &= K_{\alpha\beta}^x \\ E_t^{ij} &= 0 \quad \text{for} \quad t < 0 \quad \text{or} \quad t > i + j \\ E_t^{i+1,j} &= \frac{1}{2p} E_{t-1}^{ij} + X_{PA} E_t^{ij} + (t+1) E_{t+1}^{ij} \\ E_t^{i,j+1} &= \frac{1}{2p} E_{t-1}^{ij} + X_{PB} E_t^{ij} + (t+1) E_{t+1}^{ij}. \end{aligned} \quad (3.27)$$

Inserting (3.26) in (3.25) and using the equation (3.22) gives the simple relation for  $S_{ij}$

$$S_{ij} = \int dx \Omega_{ij} = \sum_{t=0}^{i+j} E_t^{ij} \int dx \Lambda_t = E_0^{ij} \sqrt{\frac{\pi}{p}}. \quad (3.28)$$

From the last equation, the total overlap between two three-dimensional Gaussians can be written as follows:

$$S_{\alpha\beta} = E_0^{ij} E_0^{kl} E_0^{mn} \left( \frac{\pi}{p} \right)^{3/2}, \quad (3.29)$$

where the coefficients  $E_0^{ij}$ ,  $E_0^{kl}$ ,  $E_0^{mn}$  can be calculated from McMurchie-Davidson recurrence relations (3.27). These three factors belong to two Cartesian Gaussians with exponents  $\alpha$  and  $\beta$ , so that the product of these factors can be written shortly as  $E_{000}^{\alpha\beta}$ , giving the final relation

$$S_{\alpha\beta} = E_{000}^{\alpha\beta} \left( \frac{\pi}{p} \right)^{3/2}. \quad (3.30)$$

### Kinetic Energy Integrals

Kinetic energy integrals are defined similarly to overlap integrals as follows:

$$T_{\alpha\beta} = \langle G_\alpha | -\frac{1}{2} \nabla^2 | G_\beta \rangle. \quad (3.31)$$

Using the fact that the Laplace operator can be written as a sum of second derivatives over the Cartesian directions, one gets the following relation for kinetic energy integrals

$$T_{\alpha\beta} = T_{ij} S_{kl} S_{mn} + S_{ij} T_{kl} S_{mn} + S_{ij} S_{kl} T_{mn}, \quad (3.32)$$

where  $S_{ij}$  are overlap integrals defined in (3.28) and the derivation of the term  $T_{ij}$  is given in [9]. The result can be written in terms of overlap integrals as follows:

$$T_{ij} = -2\beta^2 S_{i,j+2} + (2j+1)\beta S_{ij} - \frac{1}{2}j(j+1)S_{i,j-2}. \quad (3.33)$$

With these previous two equations, kinetic energy integrals can be very efficiently calculated from overlap integrals.

### One-Electron Coulomb Integrals

To describe electronic interaction with nuclei, one-electron Coulomb integrals are needed. They are formally defined as

$$V_{\alpha\beta}^C = \langle G_\alpha | \hat{r}_C^{-1} | G_\beta \rangle = \int_{\mathbb{R}^3} d^3r \Omega_{\alpha\beta}(\mathbf{r}) r_C^{-1}, \quad (3.34)$$

where  $\mathbf{C}$  is the center of the nucleus. Equivalently, one-electron Coulomb integrals could be defined over Hermite Gaussians and that leads to  $V_{tuv}$ :

$$V_{tuv}^C = \int_{\mathbb{R}^3} d^3r \Lambda_{tuv}(\mathbf{r}) r_C^{-1} = \frac{2\pi}{p} \left( \frac{\partial}{\partial P_x} \right)^t \left( \frac{\partial}{\partial P_y} \right)^u \left( \frac{\partial}{\partial P_z} \right)^v F_0(pR_{PC}^2) = \frac{2\pi}{p} R_{tuv}(p, \mathbf{R}_{PC}), \quad (3.35)$$

where the definition of Hermite Gaussians (3.20) is used. The function  $F_0(x)$  is the so-called Boys function of order 0, that will be discussed in next section 3.5. The term  $R_{PC}$  indicates the distance between nucleus site C and the center of the Hermite Gaussian given by (3.19).  $R_{tuv}$  defined in this way, are known as Hermite Coulomb integrals. Expanding the overlap distribution over the Hermite Gaussians in (3.34) and using the definition of Hermite Coulomb integrals (3.35), one obtains

$$V_{\alpha\beta}^C = \int_{\mathbb{R}^3} d^3r \sum_{tuv}^{i+j,k+l,m+n} E_{tuv}^{\alpha\beta} \Lambda_{tuv}(\mathbf{r}) r_C^{-1} = \frac{2\pi}{p} \sum_{tuv}^{i+j,k+l,m+n} E_{tuv}^{\alpha\beta} R_{tuv}(p, \mathbf{R}_{PC}). \quad (3.36)$$

While the expansion coefficients  $E_{tuv}^{\alpha\beta}$  can be calculated with recurrence relations (3.27), the Hermite Coulomb integrals  $R_{tuv}$  are still unknown. To be able to evaluate them, the auxiliary integrals  $R_{tuv}^n$  are introduced by McMurchie and Davidson [20]

$$R_{tuv}^n(p, \mathbf{R}_{PC}) = \left( \frac{\partial}{\partial P_x} \right)^t \left( \frac{\partial}{\partial P_y} \right)^u \left( \frac{\partial}{\partial P_z} \right)^v R_{000}^n(p, \mathbf{R}_{PC}), \quad \text{with} \quad (3.37)$$

$$R_{000}^n = (-2p)^n F_n(pR_{PC}^2).$$

In the previous equation, the term  $F_n(x)$  indicates the  $n$ -th Boys function (see section 3.5). They have also evaluated the recurrence relations for the calculations of Hermite Coulomb integrals  $R_{tuv}^0$  as a linear combination of the auxiliary integrals  $R_{000}^n$ . The derivation of these recurrence relations can be found in the work of McMurchie and Davidson [20] or the electronic structure book from Helgaker [9]. Here, only the final results will be listed:

$$\begin{aligned} R_{t+1,u,v}^n(p, \mathbf{R}_{PC}) &= tR_{t-1,u,v}^{n+1}(p, \mathbf{R}_{PC}) + X_{PC} R_{t,u,v}^{n+1}(p, \mathbf{R}_{PC}) \\ R_{t,u+1,v}^n(p, \mathbf{R}_{PC}) &= uR_{t,u-1,v}^{n+1}(p, \mathbf{R}_{PC}) + Y_{PC} R_{t,u,v}^{n+1}(p, \mathbf{R}_{PC}) \\ R_{t,u,v+1}^n(p, \mathbf{R}_{PC}) &= vR_{t,u,v-1}^{n+1}(p, \mathbf{R}_{PC}) + Z_{PC} R_{t,u,v}^{n+1}(p, \mathbf{R}_{PC}) \\ R_{000}^n(p, \mathbf{R}_{PC}) &= (-2p)^n F_n(pR_{PC}^2) \\ R_{tuv}^n(p, \mathbf{R}_{PC}) &= 0 \quad \text{if } t, u, v < 0. \end{aligned} \quad (3.38)$$

In order to get the total contribution to the one-electron Coulomb integrals, they must be summed up over all nuclei centers, so that the entire one-electron Coulomb integral is

$$V_{\alpha\beta} = \sum_{A=1}^M V_{\alpha\beta}^{C_A} = \frac{2\pi}{p} \sum_{i=1}^M \sum_{tuv}^{i+j,k+l,m+n} E_{tuv}^{\alpha\beta} R_{tuv}(p, \mathbf{R}_{PC_A}). \quad (3.39)$$

## Two-Electron Coulomb Integrals

In the end, it remains to explain the evaluation of two-electron Coulomb integrals. They are defined as follows:

$$[\alpha\beta|\gamma\delta] = \int_{\mathbb{R}^3} \int_{\mathbb{R}^3} d^3r_1 d^3r_2 \frac{\Omega_{\alpha\beta}(\mathbf{r}_1)\Omega_{\gamma\delta}(\mathbf{r}_2)}{r_{12}}. \quad (3.40)$$

Similarly as for one-electron Coulomb integrals, two-electron Coulomb integrals can also be expanded in terms of Hermite Gaussians, but in this case with two Hermite

Gaussians centered on two sites P and Q

$$V_{tuv,\tau\nu\phi} = \int_{\mathbb{R}^3} \int_{\mathbb{R}^3} d^3r_1 d^3r_2 \frac{\Lambda_{tuv}(\mathbf{r}_1)\Lambda_{\tau\nu\phi}(\mathbf{r}_2)}{r_{12}}. \quad (3.41)$$

Using the properties of the Boys functions and the definition of the Hermite Gaussians (3.20), the previous relation can be simplified and it leads to

$$V_{tuv,\tau\nu\phi} = (-1)^{\tau+\nu+\phi} \frac{2\pi^{5/2}}{pq\sqrt{p+q}} \left(\frac{\partial}{\partial P_x}\right)^{t+\tau} \left(\frac{\partial}{\partial P_y}\right)^{u+\nu} \left(\frac{\partial}{\partial P_z}\right)^{v+\phi} F_0(pR_{PQ}^2), \quad (3.42)$$

where  $R_{PQ}$  is the distance between the centers P and Q of Hermite Gaussians given by the relation (3.19). Recognizing the definition of Hermite Coulomb integrals (3.35) and using the expansion of Hermite Coulomb integrals, like in the equation (3.36) for one-electron Coulomb integrals, a similar relation for two-electron Coulomb integrals can be obtained:

$$[\alpha\beta|\gamma\delta] = \frac{2\pi^{5/2}}{pq\sqrt{p+q}} \sum_{tuv} E_{tuv}^{\alpha\beta} \sum_{\tau\nu\phi} (-1)^{\tau+\nu+\phi} E_{\tau\nu\phi}^{\gamma\delta} R_{t+\tau,u+\nu,v+\phi}(\alpha, \mathbf{R}_{PQ}). \quad (3.43)$$

From the last equation, it should be noted that two-electron Coulomb integrals (3.43) can be calculated in the same manner as one-electron Coulomb integrals (3.36). To be able to evaluate them, it is necessary to discuss how to obtain the set of Boys functions  $F_n(x)$  needed for the evaluation of Hermite Coulomb integrals. As a summary of this section, the whole McMurchie-Davidson procedure for the calculation of molecular integrals is depicted on figure 3.3.

## 3.5 The Boys Functions

The Boys functions were introduced by S. F. Boys [22]. The  $n$ -th order Boys function  $F_n(x)$  for  $x \geq 0$  is defined as

$$F_n(x) = \int_0^1 dt \exp(-xt^2)t^{2n}. \quad (3.44)$$

They are strictly decreasing positive functions with limits

$$0 < F_n(x) \leq \frac{1}{2n+1}. \quad (3.45)$$

Integrating the Boys functions by the part, one arrives to the following recurrence relations that can be very useful for their evaluation. The upward recursion is given as

$$F_{n+1}(x) = \frac{(2n+1)F_n(x) - \exp(-x)}{2x}, \quad (3.46)$$

and the downward recursion is

$$F_n(x) = \frac{2xF_{n+1}(x) + \exp(-x)}{2n+1}. \quad (3.47)$$

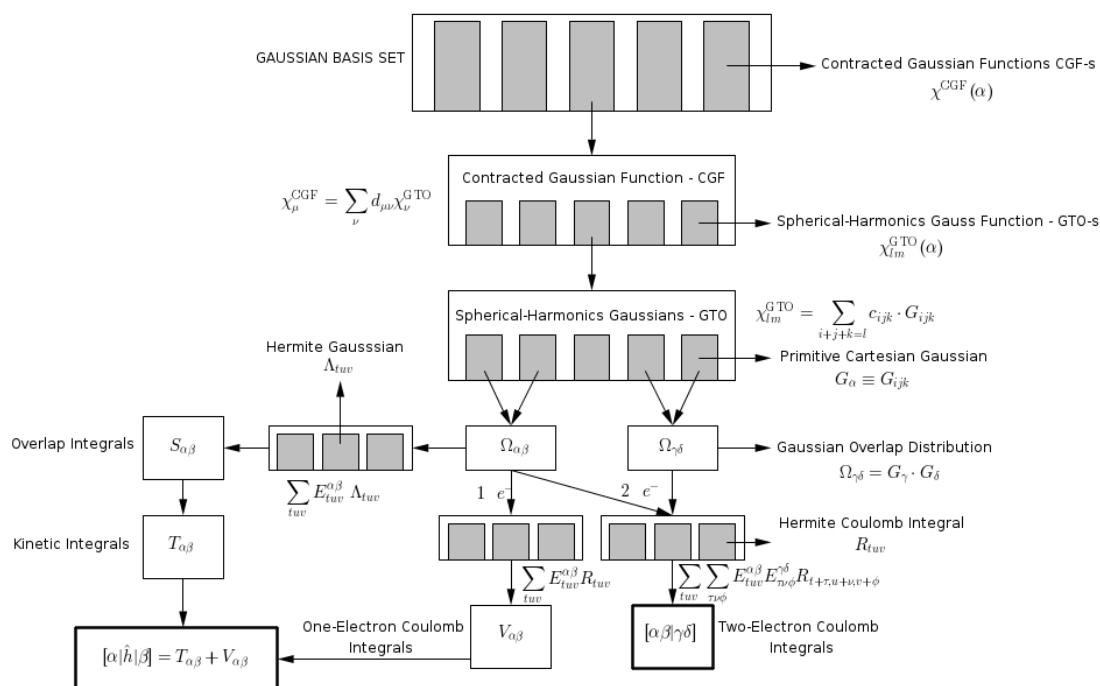


Figure 3.3: Representation of a Gaussian basis set and McMurchie-Davidson scheme for the calculation of molecular integrals over Gaussians.

The upward recursion (3.46) suffers from numerical instability, because the denominator can be very small, leading to singularities. On the other hand, the downward recursion (3.47) is numerically very stable, but it requires the knowledge of the Boys function of the highest order.

The zero-order Boys function can be related to the error function as:

$$F_0(x) = \sqrt{\frac{\pi}{4}} \frac{\text{erf}(\sqrt{x})}{\sqrt{x}} \quad (3.48)$$

and it can be evaluated for arbitrary large or small  $x$  values. The error function is the intrinsic FORTRAN function (ERF). Extremely useful is also the relation between the incomplete gamma function and the  $n$ -th order Boys function:

$$F_n(x) = \frac{\gamma(n + \frac{1}{2}, x)}{2x^{n+1/2}}, \quad \text{where} \quad (3.49)$$

$$\gamma(n, x) = \Gamma(n) \cdot \int_0^x dt \exp(-t) t^{n-1}.$$

Knowing the incomplete gamma function (there are various implementations of it in FORTRAN), each Boys function can be calculated. However, the problem remains for small or large  $x$  values, where the incomplete gamma function can not be calculated. Since these values are necessary for the precise evaluation of molecular integrals, additional approximations of the Boys functions for small and large  $x$  values are needed. Accuracy of roughly  $10^{-9}$  is needed to get the accuracy of  $10^{-6}$  in the calculation of molecular integrals. Especially the  $x$  values in the range

$x \in [10^{-9}, 10]$  with the resolution  $10^{-9}$  are needed to fulfill this accuracy condition. For large  $x$  values, the integrand goes to zero, because of the exponential decay (3.44). Thus, large value approximation is obtained by extending the integrals limits:

$$F_n(x) \approx \int_0^\infty dt \exp(-xt^2)t^{2n} = \frac{\Gamma(n + \frac{1}{2})}{2^{n+1}}, \quad \text{for large } x, \quad (3.50)$$

where  $\Gamma(n)$  is the ordinary Gamma function, also an intrinsic FORTRAN function (**GAMMA**). For small  $x$  values, on the other hand, the Boys function could be approximated by a Taylor expansion around  $x = 0$  as

$$F_n(x) = \sum_{p=0}^{\infty} \frac{(-x)^p}{(2(n+p)-1)p!} \quad \text{for small } x. \quad (3.51)$$

The sum is truncated at  $p = 10$  and with these two approximations, one obtains an accuracy of the order  $10^{-10}$  for regions  $x < 0.5$  and  $x > 20.0$  for the first 25 Boys functions. The incomplete Gamma function covers the remaining region for all  $n$  values between 0 and 24. Note that the highest order Boys function needed for the evaluation of molecular integrals over  $s, p, d, f, g$  shells is of the order 24, so that the desired accuracy of the molecular integrals is ensured.

## 3.6 Wannier Basis Set

Until now, only the basis sets for small systems like atoms and molecules were considered. However, as it was mentioned at the beginning, the goal of this thesis is to extend the CI calculation to the application in solids. For this purpose, a localized basis set is needed, obtained from a set of delocalized eigenfunctions of a crystalline Hamiltonian. From Bloch's theorem [23], it is known that the eigenfunctions of a Hamiltonian are the plane waves multiplied by the periodic function  $u(\mathbf{r})$ , with the same periodicity as a crystal lattice. These functions are called Bloch waves:

$$\psi_{\mathbf{k}}(\mathbf{r}) = u(\mathbf{r}) e^{i\mathbf{k}\cdot\mathbf{r}}. \quad (3.52)$$

Including the fact that there are many Bloch waves for the same wave vector  $\mathbf{k}$ , the new index  $n$ , the so-called band index, is introduced. In this way, one obtains a whole set of delocalized Bloch waves  $\psi_{n\mathbf{k}}$ . Wannier [24] has shown that the Fourier like linear transformation of Bloch waves leads to a complete set of orthogonal functions, called Wannier functions. One Wannier function [24–26] can be represented through a Fourier series as

$$\phi_{n\mathbf{R}}(\mathbf{r}) = \phi_n(\mathbf{r} - \mathbf{R}) = \frac{V}{(2\pi)^3} \int_{\text{BZ}} d^3k e^{-i\mathbf{k}\cdot\mathbf{R}} \psi_{n\mathbf{k}}(\mathbf{r}), \quad (3.53)$$

with a formal back transformation:

$$\psi_{n\mathbf{k}}(\mathbf{r}) = \sum_{\mathbf{R}} e^{i\mathbf{k}\cdot\mathbf{R}} \phi_{n\mathbf{k}}(\mathbf{r}), \quad (3.54)$$

where BZ denotes the first Brillouin zone. The set of Wannier functions is orthogonal, but it suffers from the fact that they are not uniquely defined. This arbitrariness

comes from a  $\mathbf{k}$ -dependent phase factor that in general can be written as a unitary transformation  $U_{mn}^{(\mathbf{k})}$ . Its role is to mix  $N$  Bloch bands at wave vector  $\mathbf{k}$ . Therefore, the set of general Wannier functions is given as follows:

$$\phi_{n\mathbf{R}}(\mathbf{r}) = \frac{V}{(2\pi)^3} \int_{\text{BZ}} d^3k \sum_{m=1}^N U_{mn}^{(\mathbf{k})} e^{-i\mathbf{k}\cdot\mathbf{R}} \psi_{m\mathbf{k}}(\mathbf{r}). \quad (3.55)$$

Choosing a quadratic spread as a localization criterion (see [25, 26]), a unique set of Wannier basis functions is obtained by minimizing this quadratic spread. Such a Wannier basis set is referred to as maximally localized Wannier functions. The standard implementation of MLWFs was developed by Marzari, Vanderbilt and coworkers. The program is called WANNIER90 and VASP provides an interface to WANNIER90.

### 3.7 Implementation Details - Calculation and Storing of Molecular Integrals

In this short section, it will be shown that not all integrals have to be calculated explicitly. Because of simplicity, all integrals are stored in arrays - one-electron integrals in a two-dimensional array and two-electron integrals in a four-dimensional arrays. Having  $2P$  spin orbitals, the calculation contains  $P^2$  one-electron and  $P^4$  two-electron integrals (for restricted set of orbitals). For real-valued orbitals (such as Gaussians or Hartree-Fock) the symmetry rules (2.26, 2.34) could be applied. With this rule, the calculation of one-electron integrals is reduced by factor 2, and the calculation of two-electron integrals is reduced by factor 8. All these integrals are calculated in nested loops, and to use symmetry rules, one needs only to keep track of the limits of the summations. In other words, if two summation indices  $i$  and  $j$  can interchange, then the restriction  $i < j$  can be applied. For two-electron integrals, the situation becomes more complicated, but still the same rules apply. For more details, see [21]. A short listing of the FORTRAN pseudocode for the efficient calculations of molecular integrals is shown in the listing 3.1.

```
1 DO j = 1, P
2   DO i = 1, j - 1
3     CALC(h(i,j))
4   ENDDO
5 ENDDO
6
7 !use symmetry [i|h|j] = [j|h|i]
8 h = h + TRANSPOSE(h)
9
10 !add diagonal elements, too
11 DO j = 1, P
12   CALC(h(j,j))
13 ENDDO
14
15
16 DO l = 1, P
17   DO k = 1, l
18     DO j = 1, l - 1
19       DO i = 1, j
20         CALC((ij|kl))
21         !apply symmetry
22         (ij|kl) = (kl|ij)
23         (ij|kl) = (ji|kl) = (ij|lk) = (ji|lk)
24       ENDDO
25     ENDDO
26
27     j = l
28     DO i = 1, k
29       CALC((ij|kl))
30       !apply symmetry
31       (ij|kl) = (kl|ij)
32       (ij|kl) = (ji|kl) = (ij|lk) = (ji|lk)
33     ENDDO
34   ENDDO
35 ENDDO
36
```

Listing 3.1: Fortran pseudocode for the efficient calculation of one- and two-electron integrals.

# Chapter 4

## Hartree-Fock Approximation

Hartree-Fock approximation is the first electronic structure calculation that will be introduced in this thesis. In the Hartree-Fock formalism, electrons occupy specific orbitals. This is a very natural description of reality, but still an approximation. Therefore, the Hartree-Fock wave function is simply a single Slater determinant, where electrons occupy the lowest-energy orbitals - the Hartree-Fock determinant. Beginning with an initial basis set, the orbitals will be optimized by iterative minimization of the total ground state energy. As it was shortly discussed in the introduction, Hartree-Fock includes exchange effects exactly (consequence of Slater determinants), and it neglects correlation effects completely. However, the Hartree-Fock approximation is still used often, because it is a good starting point for more accurate methods that will be discussed in the next chapters. Therefore, it can be understood that this chapter is the first stepping stone into the configuration interaction calculations.

At the beginning, the formal Hartree-Fock equations will be presented together with definitions of Coulomb, exchange and Fock operators (see section 4.1). After the Hartree-Fock equations are introduced, the general aspects and properties of these equations will be investigated in section 4.2. Thereafter, the Hartree-Fock equations will be applied for the set of restricted spin orbitals (2.27), leading to the famous Roothaan equations (section 4.3). The self-consistent field theory (SCF) will be further discussed as a way to solve Roothaan equations. UHF and ROHF methods will be briefly described in section 4.5, followed by results in section 4.7. As it has been the case so far, only the most important equations and results will be derived.

### 4.1 Integro-Differential Hartree-Fock Equation

Knowing only that the Hartree-Fock is a single determinant approximation and requiring that the set of Hartree-Fock orbitals remains orthonormal, the so-called integro-differential Hartree-Fock equation can be derived from variational theorem. Following the procedure of Appendix A and minimizing the single determinant energy, obtained via Slater-Condon rules (2.36-2.38), the Lagrange function looks like

$$\mathcal{L}[\{|i\rangle\}] = E_0[\{|i\rangle\}] - \sum_{ij} \varepsilon_{ji} (\langle i|j\rangle - \delta_{ij}), \quad (4.1)$$

where  $E_0$  is the determinantal energy and  $\varepsilon_{ji}$  are Lagrange multipliers. Because the energy is a real number and using the properties of scalar products, the following constraint on Lagrange multipliers is obtained:

$$\langle i|j\rangle = \langle j|i\rangle^* \implies \varepsilon_{ji} = \varepsilon_{ij}^*. \quad (4.2)$$

Splitting the energy term  $E_0$  in terms that come from one-electron and two-electron integrals as  $E_0 = E_0^{(1)} + E_0^{(2)}$ , the variation of the Lagrange function can be simply written as the sum of variations of all terms on the right side of (4.1). Let us look at the variation of the constraint term first:

$$\begin{aligned} \delta \sum_{ij} \varepsilon_{ji} (\langle i|j\rangle - \delta_{ij}) &= \sum_{ij} \varepsilon_{ji} \langle \delta i|j\rangle + \sum_{ij} \varepsilon_{ji} \langle i|\delta j\rangle \\ &= \sum_{ij} \varepsilon_{ji} \langle \delta i|j\rangle + \sum_{ij} \varepsilon_{ij} \langle j|\delta i\rangle \\ &= \sum_{ij} \varepsilon_{ji} \langle \delta i|j\rangle + \sum_{ij} \varepsilon_{ji}^* \langle \delta i|j\rangle^* \\ &= \sum_{ij} \varepsilon_{ji} \langle \delta i|j\rangle + \text{c.c.} \end{aligned} \quad (4.3)$$

In the previous derivation, the condition (4.2) was used and also the fact that the indices  $i$  and  $j$  can interchange. In the next step, one considers the variation of energy contribution from one-electron integrals:

$$\begin{aligned} \delta E_0^{(1)} &= \sum_i \langle \delta i|\hat{h}|i\rangle + \sum_i \langle i|\hat{h}|\delta i\rangle \\ &= \sum_i \langle \delta i|\hat{h}|i\rangle + \sum_i \langle \delta i|\hat{h}|i\rangle^* \\ &= \sum_i \langle \delta i|\hat{h}|i\rangle + \text{c.c.} \end{aligned} \quad (4.4)$$

The last and the most complicated term is a variation of two-electron contributions to the determinantal energy:

$$\delta E_0^{(2)} = \frac{1}{2} \sum_{ij} \langle \delta ij||ij\rangle + \langle i\delta j||ij\rangle + \langle ij||\delta ij\rangle + \langle ij||\delta ij\rangle. \quad (4.5)$$

Using the relation (2.33), one arrives at:

$$\begin{aligned} \delta E_0^{(2)} &= \frac{1}{2} \sum_{ij} \langle \delta ij||ij\rangle + \frac{1}{2} \sum_{ij} \langle i\delta j||ij\rangle + \text{c.c.} \\ &= \frac{1}{2} \sum_{ij} \langle \delta ij||ij\rangle + \frac{1}{2} \sum_{ij} \langle \delta ij||ij\rangle + \text{c.c.} \\ &= \sum_{ij} \langle \delta ij||ij\rangle + \text{c.c.}, \end{aligned} \quad (4.6)$$

where the fact was used that the summation indices can interchange, as well as dummy variables in two-electron integrals ( $\langle ij||kl\rangle = \langle ji||lk\rangle$ ). Summing up all variations of

Lagrange function, the following expression is obtained:

$$\sum_i^N \int d\mathbf{x}_1 \delta\chi_i^*(1) \left\{ \hat{h}(1)\chi_i(1) + \sum_j^N \int d\mathbf{x}_2 \frac{\|\chi_j(2)\|^2}{r_{12}} \chi_i(1) - \sum_j^N \int d\mathbf{x}_2 \frac{\chi_j^*(2)\chi_i(2)}{r_{12}} \chi_j(1) - \sum_j^N \varepsilon_{ji}\chi_j(1) \right\} = 0. \quad (4.7)$$

Because the variations  $\delta\chi_i$  are arbitrary functions, the sum in curly braces must be zero for each  $i$ . The first sum in braces represents a total Coulomb potential of all spin orbitals averaged over the whole space. Because of this interpretation, the Coulomb operator acting on the spin orbital  $\chi_j$  is defined as

$$\hat{J}_j(1)\chi_i(1) = \left[ \int d\mathbf{x}_2 \frac{\|\chi_j(2)\|^2}{r_{12}} \right] \chi_i(1). \quad (4.8)$$

Similarly, the second sum in the braces of (4.7) denotes the exchange effects and it does not have a simple classical physical interpretation, but it arises from the antisymmetric nature of the Slater determinant and it reduces the probability of finding two electrons with parallel spins at the same position in space. Therefore, the exchange operator, acting on the spin orbital  $\chi_i$  has a peculiar form:

$$\hat{K}_j(1)\chi_i(1) = \left[ \int d\mathbf{x}_2 \frac{\chi_j^*(2)\chi_i(2)}{r_{12}} \right] \chi_j(1). \quad (4.9)$$

From the definition (4.9), one can note that the action of the operator  $\hat{K}(1)$  on the spin orbital  $\chi_i$  requires the exchange of the electrons 1 and 2 among spin orbitals  $\chi_i$  and  $\chi_j$ . The expectation values of these two operators for an electron occupying the spin orbital  $\chi_i$  are:

$$\begin{aligned} \langle \chi_i(1) | \hat{J}_j(1) | \chi_i(1) \rangle &= \langle ij | ij \rangle = [ii | jj] = J_{ij} \\ \langle \chi_i(1) | \hat{K}_j(1) | \chi_i(1) \rangle &= \langle ij | ji \rangle = [ij | ji] = K_{ij}. \end{aligned} \quad (4.10)$$

The integrals appearing in the last equations are called Coulomb integrals and exchange integrals, respectively. After these considerations, the equation (4.7) can be rewritten as follows:

$$\begin{aligned} \left[ \hat{h}(1) + \sum_j^N \left( \hat{J}_j(1) - \hat{K}_j(1) \right) \right] \chi_i(1) &= \left[ \hat{h}(1) + \hat{J}(1) - \hat{K}(1) \right] \chi_i(1) \\ &= \hat{f}(1)\chi_i(1) = \sum_j^N \varepsilon_{ji}\chi_j(1), \end{aligned} \quad (4.11)$$

where the term in angle brackets is denoted as the Fock operator  $\hat{f}$ , and  $\hat{J}(1)$  and  $\hat{K}(1)$  represent the total Coulomb and exchange interaction acting on electron 1 respectively. The Fock operator is the sum of the core Hamiltonian (kinetic energy and attractive Coulomb potential) and the averaged electron-electron interaction, given as a sum of

the Coulomb and exchange operators over all spin orbitals. The last equation has still a certain degree of flexibility reflected in the fact that a mixing among spin orbitals  $\{\chi_i\}$  does not change the determinantal energy. To show that, consider that the mixing among spin orbitals in general can be described by a unitary transformation  $U$  ( $UU^\dagger = \mathbb{1}$ ). Let us write a set of spin orbitals as a vector  $\tilde{\chi}$ . The transformation to another set of spin orbitals  $\chi$  can be written as

$$\tilde{\chi} \rightarrow \chi = U\tilde{\chi}. \quad (4.12)$$

By a complex conjugation of the previous equation, the transformation behaviour of  $\tilde{\chi}^\dagger$  can be obtained:

$$\tilde{\chi}^\dagger \rightarrow \chi^\dagger = \tilde{\chi}^\dagger U^\dagger. \quad (4.13)$$

Further, from the requirement that the trace of the Fock operator is independent of the basis choice

$$\text{Tr}(\hat{f}) = \text{Tr}(\hat{\tilde{f}}) \rightarrow \tilde{\chi}^\dagger \hat{\tilde{f}} \tilde{\chi} = \tilde{\chi}^\dagger U^\dagger \hat{f} U \tilde{\chi}, \quad (4.14)$$

the transformation law for the Fock operator becomes

$$\hat{\tilde{f}} \rightarrow \hat{f} = U \hat{\tilde{f}} U^\dagger. \quad (4.15)$$

This transformation law can be explicitly proven by showing that the core Hamiltonian  $\hat{h}$  as well as the Coulomb operator  $\hat{J}$  and the exchange operator  $\hat{K}$  from the equation (4.11) transform like (4.15). Showing that for the core Hamiltonian is trivial, but to show the same for the Coulomb and exchange operators the additional invariance of the density matrix  $\chi\chi^\dagger$  under any unitary transformation must be used, which follows immediately from the fact that  $UU^\dagger = U^\dagger U = \mathbb{1}$ . Now, when transformation laws are known, the first form of Hartree-Fock equation (4.11) can be transformed using relations (4.12-4.15)

$$\hat{\tilde{f}} \tilde{\chi} = \varepsilon \tilde{\chi} \rightarrow U \hat{f} U^\dagger U \tilde{\chi} = \varepsilon U \tilde{\chi}. \quad (4.16)$$

Further, using the unitarity of the matrix  $U$ , one arrives at

$$\hat{f} \chi = U^\dagger \varepsilon U \chi. \quad (4.17)$$

On the right side of the last equation the term  $U^\dagger \varepsilon U$  appears and because  $\varepsilon$  is a Hermitian matrix,  $U$  can be chosen in such a way that diagonalizes the matrix of Lagrange coefficients  $\varepsilon$ . Choosing  $U$  in this way, the so-called canonical Hartree-Fock equations are obtained

$$\hat{f} \chi_i = \varepsilon_i \chi_i, \quad (4.18)$$

or in bra-ket notation rewritten as:

$$\hat{f} |i\rangle = \varepsilon_i |i\rangle, \quad (4.19)$$

where  $\varepsilon_i$  are eigenvalues of the Fock operator. It should be noted, that all sets of spin orbitals possess the same set of eigenvalues and there is no physical distinction between them. Some of them are more localized, some of them are completely delocalized, but none of them own superior physical meaning.

## 4.2 Interpretation of Hartree-Fock Equations

Before it is shown how to solve Hartree-Fock equations on a computer, i.e. how to translate the equation (4.19) into a matrix equation, the general aspects of Hartree-Fock theory should be discussed. Let us begin with a general matrix element of the Fock operator in a basis of spin orbitals  $\{\chi_i\}$ . It is defined as:

$$f_{ij} = \langle i|\hat{f}|j\rangle = \langle i|\hat{h}|j\rangle + \sum_k^N \langle ik||jk\rangle. \quad (4.20)$$

This result follows immediately from (4.11). Inspecting general Fock matrix elements, it is straightforward to show with the help of equations (2.26) and (2.30) that the Fock operator is Hermitian. The expectation value of the Fock operator is given by the same equation, with the additional condition  $j = i$ . In the basis of spin orbital eigenfunctions, the matrix representation of the Fock matrix is diagonal, with corresponding eigenvalues on the diagonal:

$$f_{ij} = \langle i|\hat{f}|j\rangle = \varepsilon_j \langle i|j\rangle = \varepsilon_j \delta_{ij}. \quad (4.21)$$

From the last result, it follows that the eigenvalue of the Fock matrix is given as

$$\varepsilon_i = \langle i|\hat{h}|i\rangle + \sum_k^N \langle ik||ik\rangle. \quad (4.22)$$

If the spin orbital  $\chi_a$  is already occupied, then the eigenvalue  $\varepsilon_a$  represents the "energy of an electron" in  $\chi_a$ . The self-interaction term will be automatically removed, because of the condition  $\langle aa||aa\rangle = 0$ . On the other side, if the spin orbital  $\chi_r$  is empty, then the eigenvalue  $\varepsilon_r$  denotes the interaction with all other  $N$  electrons from the system, so that the eigenvalue in that case can be interpreted as the energy of an additional electron added to the state  $\chi_r$ . Note that indices  $a, b, c, \dots$  will be used for occupied and  $r, s, t, \dots$  for unoccupied orbitals.

In this way, one can approximate the ionization potential, where the electron leaves the orbital  $\chi_a$  with a negative orbital energy  $-\varepsilon_a$ , by assumption that eigenstates do not change during the ionization. In a similar way, electron affinity to produce the state with an extra electron in the spin orbital  $\chi_r$  is equal to the negative orbital energy  $-\varepsilon_r$ . These results are known as Koopman's theorem. The derivation of Koopman's theorem is straightforward, but it will be skipped here. For more details, see [3]. Symbolically, the Koopman's theorem can be written as

$$\begin{aligned} |^N\Psi_0\rangle &\longrightarrow |^{N-1}\Psi_a\rangle \implies \text{IP} = -\varepsilon_a \\ |^N\Psi_0\rangle &\longrightarrow |^{N+1}\Psi_r\rangle \implies \text{EA} = -\varepsilon_r, \end{aligned} \quad (4.23)$$

where the state  $|^{N-1}\Psi_a\rangle$  ( $|^{N+1}\Psi_r\rangle$ ) is obtained by removing (adding) an electron in the spin orbital  $\chi_a$  ( $\chi_r$ ). Discarding the relaxation of orbitals in  $N \pm 1$  states leads to ionization potential values (IP) which are too positive and too negative values for the electron affinity (EA). In general, the Koopman's theorem can be used as the first approximation for the ionization potential, but the values for the electron affinity tend to be inaccurate.

Consider now that the solution of (4.18) gives an orthonormal set of spin orbitals  $\chi_i$ .  $N$  electrons fulfill the  $N$  lowest energy spin orbitals and make the Hartree-Fock determinant  $|\Psi_0\rangle$ . The rest of spin orbitals are virtual orbitals. The second important consequence of the Hartree-Fock equations is that there is no mixing between Hartree-Fock determinant and single excited determinants  $|\Psi_a^r\rangle = a_r^\dagger a_a |\Psi_0\rangle$ , i.e.

$$\langle \Psi_0 | \hat{H} | \Psi_a^r \rangle = 0. \quad (4.24)$$

This statement is called the Brillouin theorem. It will be extremely useful for beyond Hartree-Fock methods. Using Slater-Condon rules (2.37, 2.38) to write Hamiltonian matrix element  $\langle \Psi_0 | \hat{H} | \Psi_a^r \rangle$  and using (4.20), one obtains:

$$\langle \Psi_0 | \hat{H} | \Psi_a^r \rangle = \langle a | \hat{h} | r \rangle + \sum_i^N \langle ai || ri \rangle = f_{ar} = \varepsilon_r \delta_{ar} = 0. \quad (4.25)$$

Because  $a$  is one of the occupied orbitals and  $r$  is an unoccupied one, the term  $\delta_{ar}$  is 0 in any case.

### 4.3 Roothaan Equations

This section shows how to formulate the matrix equations from the Hartree-Fock equation (4.19). To do that, the form of the spin orbitals has to be specified. In this work, mainly restricted orbitals (2.27) will be considered. They are built in such a way that spin up and spin down electrons share the same spatial part of the orbital. Additionally, systems with doubly occupied orbitals will be handled, while open-shell systems will be shortly discussed in the section 4.5. This method is therefore referred to as closed-shell restricted Hartree-Fock (RHF). On the other side, there are open-shell unrestricted Hartree-Fock (UHF) or even more complicated open-shell restricted Hartree-Fock (ROHF) calculations (see section 4.5). In this work, restricted closed-shell Hartree-Fock will be discussed in more details with appropriate derivations of corresponding equations, while UHF and ROHF models will be briefly presented. In the RHF method, calculations will be constrained on systems with even number of electrons  $N$ , where  $N/2$  is the number of spatial orbitals. The ground state Hartree-Fock wave function is therefore given as

$$|\Psi_0\rangle = |\psi_1 \bar{\psi}_1 \psi_2 \bar{\psi}_2 \cdots \psi_{N/2} \bar{\psi}_{N/2}\rangle. \quad (4.26)$$

As the first step towards a matrix representation of RHF, the spin variable  $w$  in (4.19) must be integrated out. For this purpose, the splitting of a sum over spin orbitals will be used (2.39). The actual derivation is similar to the one performed in Slater-Condon rules by the transition from spin to spatial orbitals (2.37, 2.38). The Coulomb interaction will be doubled, because of the sum over parallel and antiparallel spins, but the exchange interaction will survive only for electrons with parallel spin. This behavior is a direct consequence of spin orthogonality (see equations 2.28 and 2.35). After these considerations, the restricted closed-shell Hartree-Fock equation looks like

$$\left[ \hat{h}(1) + \sum_{j=1}^{N/2} 2\hat{\mathcal{J}}_j(1) - \hat{\mathcal{K}}_j(1) \right] \psi_i(1) = \hat{f}(1)\psi_i(1) = \varepsilon_i \psi_i(1). \quad (4.27)$$

It should be noted that calligraphic letters are used to emphasize the closed-shell operators and that integration is done only over spatial orbitals. In other words, they can be written as

$$\begin{aligned}\hat{\mathcal{J}}_j(1)\psi_i(1) &= \left[ \int d^3r_2 \frac{\|\psi_j(2)\|^2}{r_{12}} \right] \psi_i(1) \\ \hat{\mathcal{K}}_j(1)\psi_i(1) &= \left[ \int d^3r_2 \frac{\psi_j^*(2)\psi_i(2)}{r_{12}} \right] \psi_j(1),\end{aligned}\tag{4.28}$$

with expectation values that correspond to two-electron integrals over spatial orbitals:

$$\begin{aligned}\langle \psi_i(1) | \hat{\mathcal{J}}_j(1) | \psi_i(1) \rangle &= (ii|jj) = \mathcal{J}_{ij} \\ \langle \psi_i(1) | \hat{\mathcal{K}}_j(1) | \psi_i(1) \rangle &= (ij|ji) = \mathcal{K}_{ij}.\end{aligned}\tag{4.29}$$

Before the introduction of the concrete set of basis functions, the results for the ground state energy and for the orbital energy will be emphasized within a RHF theory:

$$\begin{aligned}E_0 = \langle \Psi_0 | \hat{H} | \Psi_0 \rangle &= \sum_{i=1}^{N/2} 2(i|h|i) + \sum_{i,j}^{N/2} 2(ii|jj) - (ij|ji) \\ \varepsilon_i &= (i|h|i) + \sum_j^{N/2} 2(ii|jj) - (ij|ji).\end{aligned}\tag{4.30}$$

From the previous equation, it is clear that the simple sum of orbital energies does not give the ground state energy, because the electron-electron interaction is double-counted. Let us now introduce a basis set of  $P$  basis functions ( $P \geq N$ ):

$$\psi_\mu = \sum_{j=1}^P C_{j\mu} \phi_j ; \quad \mu = 1, 2, \dots, P,\tag{4.31}$$

so that each spatial orbital can be represented as a linear combination of those functions. In this way, one constructs  $P$  spatial orbitals ( $2P$  spin orbitals) and the Hartree-Fock problem simplifies to the finding of optimal coefficients  $C_{j\mu}$ . Note that the alphabet letters  $i, j, \dots$  will stand for the basis functions, while the Greek letters  $\mu, \nu, \dots$  will stand for actual spin orbitals. Because of technical limitations, one is always restricted to a finite and incomplete set of basis functions. The standard basis used for Hartree-Fock theory are Gaussian basis sets, discussed in the previous chapter 3. Integrating the restricted closed-shell integro-differential Hartree-Fock equation (4.27) over basis functions  $\phi_i^*$ , one obtains

$$\sum_{j=1}^P C_{j\mu} \int d^3r \phi_i^* \hat{f} \phi_j = \varepsilon_\mu \sum_{j=1}^P C_{j\mu} \int d^3r \phi_i^* \phi_j\tag{4.32}$$

The integral appearing on the right side of the previous equation was already introduced in the last chapter (see section 3.4.5). It is a general element of the overlap matrix  $S$

$$S_{ij} = \langle i|j \rangle = \int d^3r \phi_i^* \phi_j.\tag{4.33}$$

The overlap matrix is in general Hermitian, but because the Gaussian basis sets are always real, the overlap matrix is a real symmetric  $P \times P$  matrix in most cases. Diagonal elements always have the value of 1, because the basis functions are normalized. The off-diagonal elements are always less than 1. Because the overlap matrix is symmetric, there always exists a unitary matrix that diagonalizes overlap. On the other side of the equation (4.33) appears the integral that defines the Fock matrix  $F$

$$F_{ij} = \langle i | \hat{f} | j \rangle = \int d^3r \phi_i^* \hat{f} \phi_j. \quad (4.34)$$

This matrix is also Hermitian, because it was shown that the Fock operator is Hermitian. For the set of real basis functions, the Fock matrix is a real symmetric  $P \times P$  matrix. With these two matrices, the final version of the restricted closed shell Hartree-Fock equation is

$$FC = SC\varepsilon. \quad (4.35)$$

This equation is known as the Roothaan equation and it is actually generalized eigenvalue problem. There are many LAPACK routines, which could be used to solve this equation. The last step before the diagonalization can be performed is to find a formal expression of the Fock matrix. Using the definition of the Fock operator (4.27), one obtains

$$F_{ij} = \langle i | \hat{f} | j \rangle = \langle i | \hat{h} | j \rangle + \sum_{\mu=1}^{N/2} 2 \langle i | \hat{\mathcal{J}}_{\mu} | j \rangle - \langle i | \hat{\mathcal{K}}_{\mu} | j \rangle = (i | \hat{h} | j) + \sum_{\mu=1}^{N/2} 2(ij | \mu\mu) - (i\mu | \mu j). \quad (4.36)$$

The first term represents a matrix of one-electron integrals - core electron matrix  $H^{\text{core}}$ , which includes the kinetic energy integrals  $T$  and attractive Coulomb potential  $V$  (see section 3.4.5):

$$H_{ij}^{\text{core}} = T_{ij} + V_{ij} = (i | \hat{h} | j). \quad (4.37)$$

The second term of (4.36) is more complicated, because it contains the spin orbitals  $\chi_{\mu}$  that must be expanded in the basis with actual coefficients  $C$ :

$$\begin{aligned} F_{ij} &= (i | \hat{h} | j) + \sum_{\mu=1}^{N/2} 2 \left( i j \left| \sum_{k=1}^P C_{k\mu}^* \phi_k^* \sum_{l=1}^P C_{l\mu} \phi_l \right. \right) - \left( i \sum_{l=1}^P C_{l\mu} \phi_l \left| \sum_{k=1}^P C_{k\mu}^* \phi_k^* j \right. \right) \\ &= (i | \hat{h} | j) + \sum_{\mu=1}^{N/2} \sum_{k,l=1}^P C_{k\mu}^* C_{l\mu} [2(ij | kl) - (il | kj)] \\ &= H_{ij}^{\text{core}} + G_{ij}, \end{aligned} \quad (4.38)$$

where the matrix  $G$  is simply the part of Fock matrix that describes the two-electron interactions. From this equation, it can be concluded that the Fock matrix depends on an actual set of coefficients  $C$ , leading to a set of nonlinear equations

$$F(C)C = SC\varepsilon, \quad (4.39)$$

that must be solved in an iterative way. It should be mentioned that the matrices  $S$  and  $H^{\text{core}}$  depend only on the basis functions, while the Fock matrix  $F$ , specifically its part  $G$ , depends on the actual coefficients  $C$ . Therefore, the first two mentioned

matrices have to be calculated only once during the Hartree-Fock calculation. Before presenting the whole procedure of solving the Hartree-Fock equations, the final simplification of the Roothaan equations should be done. This simplification reflects in the orthogonalization of the basis. Because  $S$  is a symmetric matrix, it can be diagonalized by the unitary matrix  $U$ . The transformation matrix  $X = Us^{-1/2}$ , where  $s$  is a diagonal matrix whose elements are the square roots of the eigenvalues of the overlap matrix  $S$ , will orthogonalize the basis, because:

$$X^\dagger SX = s^{-1/2}U^\dagger SU s^{-1/2} = s^{-1/2} s s^{-1/2} = \mathbb{1}. \quad (4.40)$$

Defining the new set of coefficients  $\tilde{C}$  through

$$C = X\tilde{C} \quad (4.41)$$

and inserting it in Roothaan equation (4.35) and multiplying with  $X^\dagger$  from the left side, one obtains:

$$\begin{aligned} X^\dagger FX\tilde{C} &= X^\dagger SX\tilde{C}\varepsilon \\ X^\dagger FX\tilde{C} &= \tilde{C}\varepsilon \\ \tilde{F}\tilde{C} &= \tilde{C}\varepsilon, \end{aligned} \quad (4.42)$$

with transformed Fock matrix  $\tilde{F} = X^\dagger FX$ . In this way, the Roothaan equations become a simple eigenvalue problem.

## 4.4 The Self-Consistent Field Procedure

Self-consistent field, or SCF, is simply the second name for the Hartree-Fock procedure. This section provides a summary of all the facts and results discussed before, needed to obtain Hartree-Fock ground state wave function of a molecular system. As the first step, input data, coordinates of atoms and the basis set, should be defined. Gaussians are the most commonly used basis functions for self-consistent field calculations on molecular systems. The next step is the calculation of one- and two-electron integrals over Gaussian functions described in section 3.4.5. Overlap integrals also need to be calculated, because the Gaussian functions are normalized, but not orthogonalized. For this purpose, one orthogonalization method is used. There is a symmetric orthogonalization method, or even better canonical orthogonalization, discussed in section 4.3. Once the transformation matrix  $X$  is obtained, an initial guess is needed for the expansion of spin orbitals over the Gaussian basis set. There are many possibilities to choose the initial spin orbitals in a clever way, but in most cases a simple choice suffices. For example, a random number generator can be used for the initial guess, or even simpler, all coefficients could be taken as 0. That actually means that the whole Hartree-Fock Hamiltonian is approximated only by the one-electron Hamiltonian  $\hat{h}$ . Finally, the SCF loop can start. In this loop, the Fock matrix is updated with actual expansion coefficients, transformed according to equation (4.42) and diagonalized. From the diagonalization procedure, a new set of transformed coefficients has been obtained, and transformed back via equation (4.41). After the updated set of expansion coefficients is obtained, the SCF convergence criterion is checked. There are many

possibilities to choose one criterion, for example the absolute change of the total ground state energy is probably the most natural choice, but not the cheapest one. Therefore, in this implementation the absolute change of the lowest Hartree-Fock eigenvalue is used as convergence criterion. It is found that the eigenvalue accuracy of  $10^{-4}$  normally ensures the accuracy of  $10^{-6}$  in the ground state energy. Once the SCF loop converges, all other properties of the system can be investigated. With this SCF procedure, the solution of the electronic Hamiltonian (2.7), within a Born-Oppenheimer approximation, is obtained. The total energy of the molecule is then obtained by relation (2.8), that depends on nuclear positions, too. In this way, it is possible to calculate total energies of the system for different configuration of nuclei and to find out the optimal geometry of the system. The simple optimization of the molecular geometry will be discussed in section 4.7.

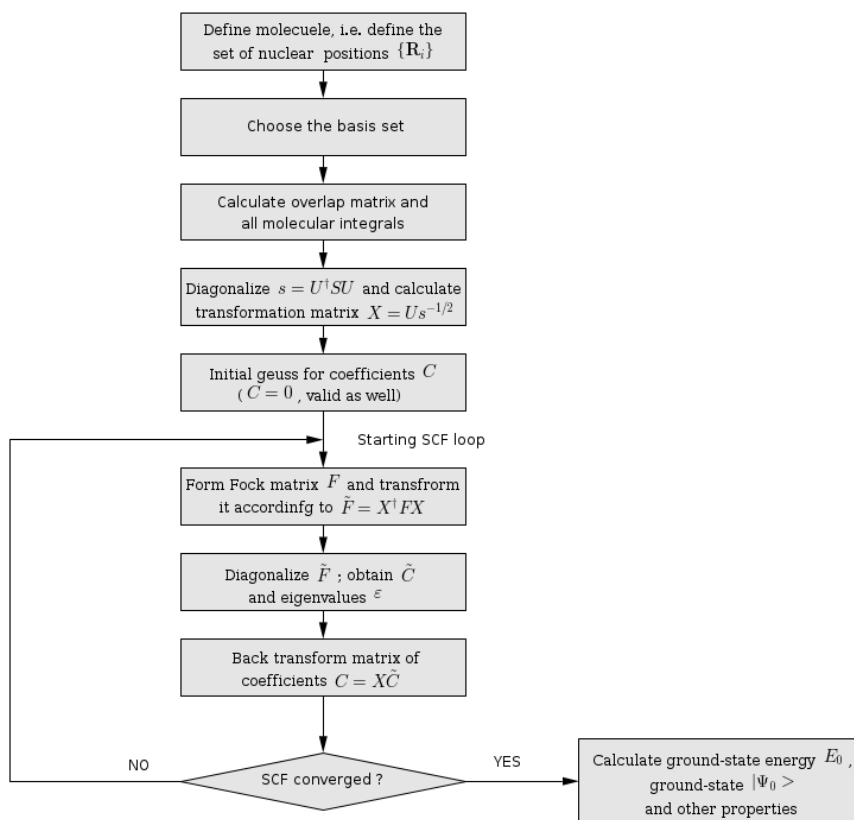


Figure 4.1: The SCF algorithm.

## 4.5 Open-Shell Hartree-Fock Calculations

As it was already discussed above, most attention is given to the description and derivation of the RHF model and the Roothan equations. However, problems arise for systems where the ground state is not a singlet spin state, i.e. for spin-polarized systems. Such situations appear often in solids where vacancies are considered. The

closed-shell calculations fail for those systems and the ground state can not be described correctly. More involved post Hartree-Fock calculations based on those closed-shell ground state calculations will also not be able to correct the already incorrect description of the system in the mean-field calculation. Therefore, the calculation will be extended to open-shell model, which is able to handle systems with an odd number of electrons, i.e. spin-polarized systems in general. The first and the most straightforward extension will be to introduce an unrestricted set of orbitals where different spatial orbitals are used for spin-up and spin-down channels. This model will relate to unrestricted Hartree-Fock theory, the so-called UHF model. On the other side, the restricted orbitals can also be used for open-shell calculations, but two different shells must be considered separately: doubly occupied closed-shell with occupation number  $f_D = 2$  and singly occupied open-shell with occupation number  $f_S = 1$ . In such systems intra-shell and inter-shell interaction must be treated separately. More details about this procedure are presented in the section 4.5.2. The main difference between those two systems is presented in the figure 4.2. Before proceeding to the actual implementation, the (dis)advantages of both methods will be presented. Although the UHF model is just a simple extension of the already proposed RHF method, the number of basis functions will be doubled and, as a result, two sets of one-electron integrals ( $h_{ij}^\alpha$  and  $h_{ij}^\beta$ ), and three sets of two-electron integrals ( $(ij|kl)^{\alpha\alpha}$ ,  $(ij|kl)^{\beta\beta}$  and  $(ij|kl)^{\alpha\beta}$ ) are obtained. Such a situation is highly undesirable, because of the large number of integrals and it should be avoided, if possible. The ROHF model provides a solution where only one set of one-electron and two-electron integrals is needed. Additionally, the many-electron wave functions (Slater determinants) obtained in ROHF model are eigenfunctions of the spin operator  $\hat{S}^2$ . The ROHF model is also computationally cheaper than UHF model. However, the actual implementation of ROHF model is methodically more involved, and the main disadvantage is the remaining set of degrees of freedom which results in a non-unique set of eigenvalues. However, the actual form of orbitals and the total energy of system stay invariant.

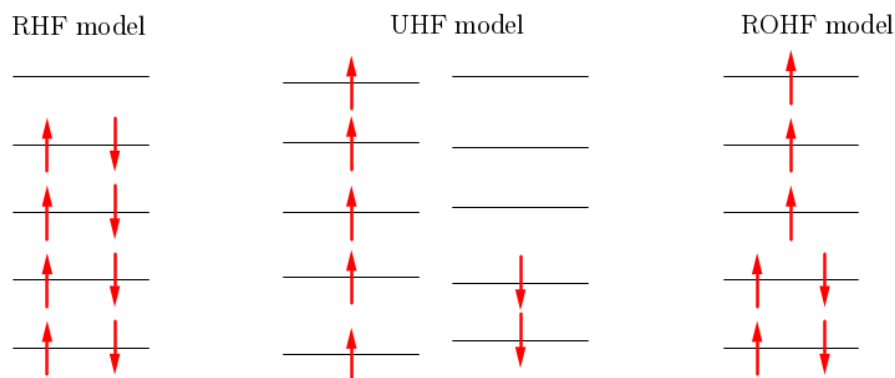


Figure 4.2: Orbital models of various Hartree-Fock methods: restricted closed-shell RHF method, unrestricted Hartree-Fock UHF method and restricted open-shell Hartree-Fock ROHF method.

### 4.5.1 Unrestricted Open-Shell Hartree-Fock Model - UHF

In this model, a set of unrestricted orbitals is introduced:

$$\begin{aligned}\psi_\mu^\alpha &= \sum_{j=1}^P C_{j\mu}^\alpha \phi_j, \quad j = 1, 2, \dots, P \\ \psi_\mu^\beta &= \sum_{j=1}^P C_{j\mu}^\beta \phi_j, \quad j = 1, 2, \dots, P.\end{aligned}\tag{4.43}$$

In this model the Hartree-Fock determinant becomes

$$|\Psi_{\text{UHF}}\rangle = |\psi_1^\alpha \bar{\psi}_1^\beta \cdots \psi_{N/2}^\alpha \bar{\psi}_{N/2}^\beta\rangle.\tag{4.44}$$

Applying Slater-Condon rules (2.37, 2.38) in this example gives the expression for the total energy:

$$E_0 = \sum_{i=1}^{N_\alpha} h_{ii}^\alpha + \sum_{i=1}^{N_\beta} h_{ii}^\beta + \frac{1}{2} \sum_{i,j=1}^{N_\alpha} (J_{ij}^{\alpha\alpha} - K_{ij}^{\alpha\alpha}) + \frac{1}{2} \sum_{i,j=1}^{N_\beta} (J_{ij}^{\beta\beta} - K_{ij}^{\beta\beta}) + \sum_{i=1}^{N_\alpha} \sum_{j=1}^{N_\beta} J_{ij}^{\alpha\beta},\tag{4.45}$$

where the definition of Coulomb and exchange matrix elements is taken from (4.10), but this time with explicit notation of spins. Note that the last term from the previous expression counts only the Coulomb interaction between antiparallel spins and the exchange contributions disappear. From this total energy expression, Fock matrices can be derived similarly as in RHF theory with the significant difference that two different Fock matrices are obtained in the UHF model:

$$\begin{aligned}F_{ij}^\alpha &= h_{ij} + \sum_{\mu=1}^{N_\alpha} \sum_{k,l=1}^P C_{k\mu}^\alpha C_{l\mu}^\alpha [(ij|kl) - (ik|lj)] + \sum_{\mu=1}^{N_\beta} \sum_{k,l=1}^P C_{k\mu}^\beta C_{l\mu}^\beta (ij|kl) \\ F_{ij}^\beta &= h_{ij} + \sum_{\mu=1}^{N_\beta} \sum_{k,l=1}^P C_{k\mu}^\beta C_{l\mu}^\beta [(ij|kl) - (ik|lj)] + \sum_{\mu=1}^{N_\alpha} \sum_{k,l=1}^P C_{k\mu}^\alpha C_{l\mu}^\alpha (ij|kl).\end{aligned}\tag{4.46}$$

The indices  $i, j, k$  and  $l$  refer to basis functions (Gaussian basis functions in this work) and the same basis set is used for both spin channels. Therefore, there are no indices in notation for one-electron integrals  $h_{ij}$  and two-electron integrals  $(ij|kl)$ . The actual distinction comes from coefficients  $C^\alpha$  and  $C^\beta$ . With those Fock matrices, the counterpart of the Hartree-Fock equations, the Pople-Nesbet equations are obtained:

$$\begin{aligned}F^\alpha C^\alpha &= S C^\alpha \epsilon^\alpha \\ F^\beta C^\beta &= S C^\beta \epsilon^\beta.\end{aligned}\tag{4.47}$$

It must be noted that those two equations are not independent of each other, there is a mixing given in (4.46), because  $F^\alpha$  and  $F^\beta$  depend on both sets of coefficients  $C^\alpha$  and  $C^\beta$ . This mixing is exactly the Coulomb interaction between antiparallel

spins. Without this interaction, the Pople-Nesbet equations would be equivalent to two sets of Roothan equations. Therefore, those two equations must be diagonalized simultaneously, and in order to form new Fock matrices, both sets of actual coefficients  $C^\alpha$  and  $C^\beta$  are needed. Additionally, it is worth to mention that the orthogonalization procedure stays the same, like in the RHF case. The matrix  $X = U_S^{-1/2}$  can be used to transform the Pople-Nesbet equations to an orthogonalized basis. Unrestricted solutions obtained in this way will be equal to RHF solutions, if  $N_\alpha = N_\beta$ . For this reasons, the UHF model will usually be used only for spin-polarized systems. However, it turns out that there is a second unrestricted solution, if the calculation is started with a distinct set of coefficients  $C^\alpha$  and  $C^\beta$ . These solutions will be useful for the description of dissociation effects in closed-shell molecules and they will be discussed in more details below.

### 4.5.2 Restricted Open-Shell Hartree-Fock Model - ROHF

In the restricted open-shell Hartree-Fock method, a set of restricted orbitals is used as it was the case in RHF model. To be able to describe spin-polarization effects, electrons are divided in two shells: doubly occupied shell  $D$  with occupation  $f_D = 2$  and singly occupied shell  $S$  with occupation  $f_S = 1$ . The expression for the total energy of the system is then given by

$$E = 2 \left\{ \sum_{i \in D} h_{ii} + \frac{1}{2} \sum_{i,j \in D} [2(ii|jj) - (ij|ji)] \right\} + \sum_{k \in S} h_{kk} + \frac{1}{2} \sum_{k,l \in S} [(kk|ll) - (kl|lk)] \\ + \sum_{i \in D} \sum_{k \in S} [2(ii|kk) - (ik|ki)], \quad (4.48)$$

where indices  $i$  and  $j$  denote orbitals from the doubly occupied shell  $D$  and indices  $k$  and  $l$  correspond to orbitals from singly occupied shell  $S$ . Using variational calculus (see A), two Fock matrices can be defined (one matrix per shell)

$$F_D = h + J(2R^D + R^S) - \frac{1}{2}K(2R^D + R^S) \\ F_S = h + K(2R^D + R^S) - K(R^D + R^S). \quad (4.49)$$

In the previous expression, the Hartree-Fock density matrix  $R$  is introduced in order to keep the notation as simple as possible. The density matrix of a shell is simply defined as

$$R_{ij}^{\text{Shell}} = \sum_{k \in \text{Shell}} C_{ik}^* C_{jk} \equiv (C^{\text{Shell}} C^{\text{Shell} \dagger})_{ij}, \quad (4.50)$$

where the summation is done over orbitals that belong to the corresponding shell and the notation  $C^{\text{Shell}}$  stands for expansion coefficients of orbitals in a given shell. Once the density matrix is introduced, the notation for the Coulomb-matrix  $J$  and

the exchange matrix  $K$  can be rewritten as

$$\begin{aligned} J(R) &= \sum_{i,j=1}^N R_{ij}(ii|jj) \\ K(R) &= \sum_{i,j=1}^N R_{ij}(ij|ji). \end{aligned} \quad (4.51)$$

Once the notation used for Fock matrices is introduced, it can be proceeded to the corresponding Hartree-Fock equations, which are obviously more complicated than in the UHF or RHF case:

$$\begin{aligned} F_T C^T - \sum_{U=1}^2 C^U \varepsilon &= 0 \\ C^{T\dagger} (f_T F_T - f_U F_U) C^U &= 0, \end{aligned} \quad (4.52)$$

where indices  $T$  and  $U$  run over shells  $S$  and  $D$ . To solve the previous equation simultaneously, the single effective Fock matrix  $\bar{F}$  is defined:

$$\begin{aligned} \bar{F} &= R^Z d_Z R^Z + R^D d_D R^D + R_S d_S R^S + a_1 R^Z F_D R^D \\ &+ a_2 R^Z F_S R^S + a_3 R^D (2F_D - F_S) R^S. \end{aligned} \quad (4.53)$$

The index  $Z$  stands for the additional empty shell that corresponds to unoccupied orbitals and matrices  $d_Z, d_D$  and  $d_S$  are arbitrarily chosen Hermitian matrices. The coefficients  $a_1, a_2$  and  $a_3$  are also arbitrarily chosen parameters. Because of those degrees of freedoms, the eigenvalues in ROHF method are not unique, but the expansion set of coefficients  $C$  is invariant under the choice of those degrees of freedom as long as the iterative procedure converges. The obvious choice of matrices is  $d_D = F_D$ ,  $d_S = F_S$  and  $d_Z = 2F_D - F_S$  and they will be used for the implementation. It is worth to mention that the orthogonalization procedure in ROHF method slightly differs from the RHF method. Because the effective Fock matrix is of the form  $\bar{F} \propto RFR$ , the transformation from the non-orthogonal to the orthogonal basis is given by the matrix  $X = U_S^{1/2}$ . For more details about restricted open-shell Hartree-Fock method and its derivation, see [1].

## 4.6 Extrapolation of the Hartree-Fock Hamiltonian via Density Functional Theory

Beyond Hartree-Fock methods described in this work should be connected with VASP. Because VASP is based on DFT and all beyond Hartree-Fock methods require the Hartree-Fock ground state, one has to be able to export the Hartree-Fock Hamiltonian from VASP. The brief discussion of the density functional theory can be found in appendix B. To obtain the Hartree-Fock Hamiltonian via DFT, hybrid potential must be used. In this way, the exact non-local Hartree-Fock exchange can be included. Therefore, the local exchange-functional has to be replaced by non-local exchange, which is defined as

$$E_x[n] = -\frac{e^2}{2} \sum_{i\mathbf{k}} \sum_{j\mathbf{q}} f_{i\mathbf{k}} f_{j\mathbf{q}} \int \int d^3r d^3r' \frac{\psi_{i\mathbf{k}}^*(\mathbf{r}) \psi_{j\mathbf{q}}^*(\mathbf{r}') \psi_{i\mathbf{k}}(\mathbf{r}') \psi_{j\mathbf{q}}(\mathbf{r})}{|\mathbf{r} - \mathbf{r}'|}, \quad (4.54)$$

where the summation is done over the set of Bloch-states  $\{\psi_{i\mathbf{k}}\}$  and the corresponding set of occupation numbers  $\{f_{i\mathbf{k}}\}$ . The indices  $i, j$  run over all bands and sums over  $\mathbf{k}$  and  $\mathbf{q}$  run over all  $\mathbf{k}$ -points used to sample the first Brillouin zone. The corresponding exchange potential is given by

$$V_x(\mathbf{r}, \mathbf{r}') = -\frac{e^2}{2} \sum_{i\mathbf{k}} f_{i\mathbf{k}} \frac{\psi_{i\mathbf{k}}^*(\mathbf{r}')\psi_{i\mathbf{k}}(\mathbf{r})}{|\mathbf{r} - \mathbf{r}'|}. \quad (4.55)$$

Using the Bloch decomposition of Bloch states

$$\psi_{i\mathbf{k}}(\mathbf{r}) = \frac{1}{\Omega} \sum_{\mathbf{G}} C_{i\mathbf{q}}(\mathbf{G}) e^{i(\mathbf{q}+\mathbf{G})\cdot\mathbf{r}} \quad (4.56)$$

the exchange potential can be written as

$$V_x(\mathbf{r}, \mathbf{r}') = \sum_{\mathbf{k}} \sum_{\mathbf{G}\mathbf{G}'} e^{i(\mathbf{k}+\mathbf{G})\cdot\mathbf{r}} V_{\mathbf{k}}(\mathbf{G}, \mathbf{G}') e^{i(\mathbf{k}+\mathbf{G}')\cdot\mathbf{r}'}, \quad (4.57)$$

where

$$V_{\mathbf{k}}(\mathbf{G}, \mathbf{G}') = -\frac{4\pi e^2}{\Omega} \sum_{i\mathbf{q}} f_{i\mathbf{q}} \sum_{\mathbf{G}''} \frac{C_{i\mathbf{q}}^*(\mathbf{G}' - \mathbf{G}'') C_{i\mathbf{q}}(\mathbf{G}' - \mathbf{G}'')}{|\mathbf{k} - \mathbf{q} + \mathbf{G}''|^2} \quad (4.58)$$

is the Fourier representation of exchange potential. In this way, the non-local exchange potential is calculated in VASP. The standard Hartree-Fock type calculation in VASP has the following input file:

```

1  ISTART = 1
2  LHFCALC = .TRUE.
3  AEXX = 1.0
4  NBANDS = number of occupied bands
5  ALGO = All ; TIME = 0.4
6  PRECFOCK = Fast

```

Listing 4.1: The INCAR file of the standard Hartree-Fock type calculation for insulators and semiconductors.

The flag LHFCALC includes hybrid potential and the flag AEXX replaces the local exchange-correlation functional by the non-local exchange defined in (4.54). The derivation of non-local exchange potential in Fourier representation and the standard input file are taken from [27]. Once the Hartree-Fock calculation is performed in VASP, a set of localized orbitals can be obtained by Wannier extrapolation of Bloch states (see section 3.6). Based on that set of the localized Wannier orbitals, one- and two-electron integrals can be calculated.

## 4.7 Examples of Hartree-Fock Calculation

### Total Energy Convergence

In this section, the first results obtained using the developed code will be presented. In the restricted Hartree-Fock calculations, the most common observable that can be obtained is the total energy of the system (4.30). Although the absolute energy value

does not have a significant meaning for the physics of the system, the convergence of the energies due to the choice of the basis set can be considered (table 4.1). From these results, it is obvious that one is very near to the Hartree-Fock limit with large basis sets as cc-pVTZ or aug-cc-pVTZ. For small systems (like the He atom or the H<sub>2</sub> molecule), the Hartree-Fock limit is already approached with pp-cVTZ basis set, but reasonably, for heavier atoms and less symmetric systems, larger basis sets are needed.

Table 4.1: The restricted Hartree-Fock energies obtained at the equilibrium geometry of the system for different basis sets with numerical accuracy of  $10^{-4}$  a.u. (Hartree).

$\frac{\text{Basis Set}}{\text{System}}$	STO-3G	6-31G++	cc-pVDZ	aug-cc-pVDZ	cc-pVTZ	aug-cc-pVTZ	HF Limit [3]
He	-2.808	-2.855	-2.855	-2.856	-2.866	-2.866	-2.866
H <sub>2</sub>	-1.116	-1.131	-1.129	-1.129	-1.133	-1.133	-1.134
BeH <sub>2</sub>	-15.560	-15.767	-15.767	-15.769	-15.772	-15.772	-15.773
H <sub>2</sub> O	-74.963	-76.023	-76.027	-76.041	-76.057	-76.061	-76.065
FH	-98.571	-100.010	-100.019	-100.034	-100.058	-100.061	-100.071
N <sub>2</sub>	-107.496	-108.942	-108.954	-108.961	-108.984	-108.985	-108.997

## Ionization Potential

In the section 4.2, it was mentioned that the energy affinities can not be even qualitatively described via the Hartree-Fock method, because the unoccupied manifold is very inaccurate in the Hartree-Fock theory. However, the ionization potential, equal to the negative value of the orbital energy  $\varepsilon_i$  (Koopman’s theorem) gives a reasonable approximation to the exact one. In this section, one considers the first ionization potential of two dimer molecules: H<sub>2</sub> and N<sub>2</sub>. Corresponding results are listed in table 4.2. As it can be seen, the results for the molecule H<sub>2</sub> agree reasonably well with experimental values. The reason why the result for H<sub>2</sub> is surprisingly good is mostly accidental. Namely, the correlation effects are missing in H<sub>2</sub> (Hartree-Fock completely neglects all correlation effects) and the energy of the ionized H<sub>2</sub><sup>+</sup> is lowered due to relaxation effects, but the correlation energy is 0, because it is a one-electron system. These two contributions cancel each other. In the case of the N<sub>2</sub> molecule, the results agree reasonably with experimental values, too. However, there is a problem that results become worse with larger basis sets. This error lies in the fact that the Hartree-Fock theory is only an approximation and it does not describe the molecular picture of the orbitals in a correct way, and therefore, the ionization potential values fail completely.

Table 4.2: The Ionization potentials of H<sub>2</sub> and N<sub>2</sub> calculated via Koopman’s theorem within a Hartree-Fock theory.

$\frac{\text{Basis Set}}{\text{System}}$	STO-3G	6-31G++	cc-pVDZ	aug-cc-pVDZ	cc-pVTZ	aug-cc-pVTZ	Experiment [3]
H <sub>2</sub>	0.578	0.595	0.592	0.593	0.594	0.594	0.584
N <sub>2</sub>	0.539	0.611	0.608	0.616	0.612	0.615	0.510

## Equilibrium Geometries

At this moment, it is appropriate to present equilibrium experimental geometries of all molecules that will be used in this thesis (table 4.3).

Table 4.3: Experimental geometries of molecules considered in this thesis.

Molecule	Bond length (a.u.)	Bond angle (°)
H <sub>2</sub>	1.40	
N <sub>2</sub>	2.07	
FH	1.73	
BeH <sub>2</sub>	2.52	
H <sub>2</sub> O	1.81	104.52

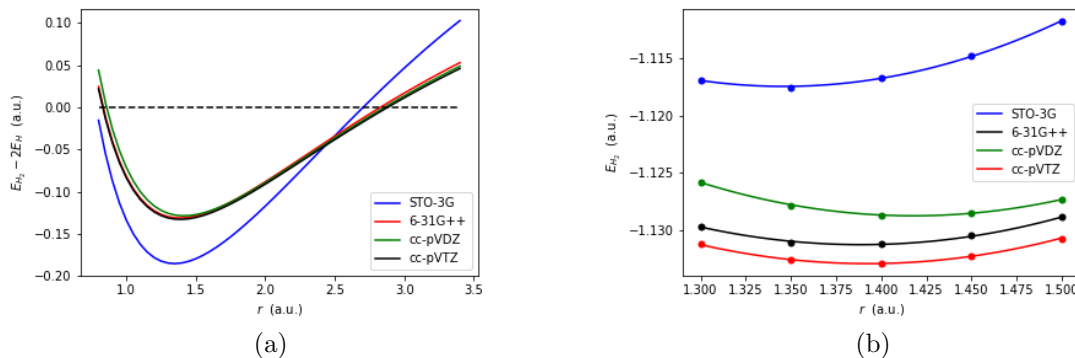
As it was already mentioned, the absolute values of the total energies do not give any physical meaning, but they can be useful for the geometry optimization of some systems. Sometimes, this task can be very difficult, because of many degrees of freedom that can vary in the configurational space. Therefore, one will make a restriction to the systems where only one degree of freedom is varied. For example, in dimers, only the bond length will be varied. In some non-linear systems, like the water molecule, the bond angle will be kept constant, while the bond length O-H will be equal for both H atoms for symmetry reasons. After these considerations, one is left with only one degree of freedom that can be varied - the O-H bond length. The main goal for this section is to see where are the limits of the Hartree-Fock approximation.

One finds that the H<sub>2</sub> dimer is already an interesting example to present the main trends. In figure 4.3-a, the dissociation energy curve of the H<sub>2</sub> molecule is plotted for different basis sets. In this case, there is no need to plot potential curves for augmented correlation consistent basis sets, because they do not improve the situation in comparison with their standard counterparts (see total energy values in table 4.1). Observing these potential curves, it is obvious that the Hartree-Fock theory fails to describe the correct dissociation behaviour in the H<sub>2</sub> molecule. At large distances, the interaction between two H atoms is very weak and they can be considered as two non-interacting H atoms and the dissociation energy should be zero. However, the plot shows that all basis sets end with positive values for the dissociation energy. The reason for that lies in the approximation, as restricted closed-shell orbitals are used to describe states in the H<sub>2</sub> molecule. Therefore, one is not able to describe the half-filled states in the H atom that appear for large internuclear distances. The situation goes especially wrong for the minimal basis set (STO-3G). On the other side, energies near to the optimal geometry are in much better agreement with experimental values. All basis sets are able to provide a qualitatively good estimation of the bond length. In figure 4.3-b total energies near to the equilibrium bond length are plotted (dots) and the optimal bond length is determined from a quadratic fit (corresponding solid lines). The equilibrium bond lengths for each basis set can be found in table 4.4. At the aug-cc-pVTZ level, the relative error of the estimated bond length is already within 1%, in comparison to the experimental ones (table 4.3).

To summarize, the restricted closed-shell Hartree-Fock theory gives very good total energies of systems at configurations near to the equilibrium state. For stretched configurations, RHF theory fails completely and it is not able to predict even the

Table 4.4: The optimal distance between two H atoms in  $H_2$  molecule for different basis sets in RHF.

STO-3G	6-31G++	cc-pVDZ	aug-cc-pVDZ	cc-pVTZ	aug-cc-pVTZ	Experiment [3]
1.346(4)	1.388(3)	1.417(4)	1.418(5)	1.392(3)	1.392(3)	1.40

Figure 4.3: (a) The dissociation energies of  $H_2$  molecule for different basis sets at the level of the restricted closed-shell Hartree-Fock theory; (b) The total energies of the  $H_2$  molecule near to the equilibrium geometry and quadratic fit of simulation data.

correct qualitative behaviour of systems. Via Koopman's theorem, the ionization potential can be qualitatively estimated, but electron affinities in RHF are completely wrong.

## UHF Method as a Solution of the Dissociation Problem

In this section the open-shell calculation will be applied in order to recover the correct dissociation behavior of the  $H_2$  molecule. In the RHF model, the problem arose on stretched configurations, where the dissociation energy was positive. As it was explained in the previous section, the RHF model tries to describe one closed-shell orbital with the same spatial distribution for both electrons. This description must fail because the system behaves as two individual hydrogen atoms at large bond lengths. Unrestricted Hartree-Fock theory is capable of retrieving this second unrestricted solution of two individual atoms. It is worth to mention that two unrestricted solutions exist at all bond lengths, but for small bond lengths the restricted closed-shell solution is favorable, while at large internuclear distances the unrestricted solution of two individual atoms is favorable. In the end, it must be noted that in order to obtain unrestricted solutions for the two individual atoms, the initial guess for the expansion coefficients for spin up  $C^\alpha$  must differ from the coefficients for spin down  $C^\beta$ . If the coefficients are equal for both spin channels and the number of electrons in the system is even, the Pople-Nesbet equations will be equivalent to the Roothaan equations. The dissociation energy in  $H_2$  molecule in RHF and UHF theory using the cc-pVTZ basis set is shown in the figure 4.4. As explained, the UHF dissociation energy tends to 0 at large internuclear distances so that the dissociation of the  $H_2$  molecule is described correctly.

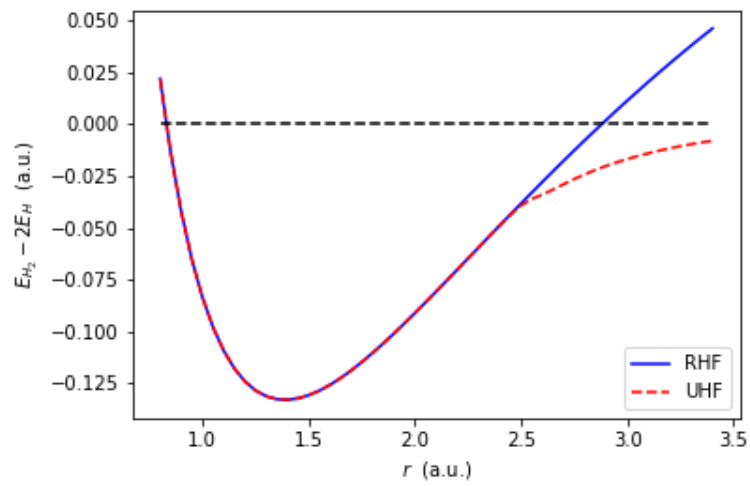


Figure 4.4: Dissociation energies in RHF and UHF theory at cc-pVTZ level.

# Chapter 5

## Møller-Plesset Perturbation Theory

Probably the simplest method to go beyond the Hartree-Fock theory and to include a certain portion of the correlation energy is the many-body perturbation theory (MBPT), also known as Rayleigh-Schrödinger perturbation theory (RSPT). In the first section 5.1 of this chapter, general aspects of the Rayleigh-Schrödinger perturbation theory will be discussed. As it will be seen, it is applicable to all quantum-mechanical systems, where the exact Hamiltonian  $\hat{H}$  is approximated by a simpler one  $\hat{H}_0$ , as it was the case in mean field HF description (see chapter 2). The remaining part of the Hamiltonian is hopefully very small and it is called the perturbation  $\hat{V}$ . The corrections are usually given in terms of the matrix elements of the operator  $\hat{V}$  and all terms that involve the product of  $n$  such matrix elements make the so-called  $n$ -th order perturbation energy. If the choice of the approximate Hamiltonian is the Hartree-Fock Hamiltonian, then the perturbation theory is called Møller-Plesset perturbation theory - MPPT. The MPPT will be discussed in section 5.2, and the main focus will be the second order perturbation energy (MP2). The size-extensivity of perturbation energies is shown in section 5.3. At the end of the chapter, results obtained using the Hartree-Fock approach will be improved with MP2 theory and presented in section 5.4.

## 5.1 Rayleigh-Schrödinger Perturbation Theory

The consistent derivation of RSPT is given in the paper [28] by Per-Olov Lödwin. A good introduction to the perturbation theory can be found in the book by Szabo and Ostlund [3]. In this section, the main results needed for the understanding of the perturbation theory will be presented. As already mentioned, the exact Hamiltonian of the system  $\hat{H}$  is approximated by  $\hat{H}_0$ . Therefore, the Hamiltonian is partitioned as

$$\hat{H} = \hat{H}_0 + \hat{V}, \quad (5.1)$$

where  $\hat{V}$  is called the perturbation term. The goal of the perturbation theory is to solve the eigenvalue problem

$$\hat{H} |\Phi_i\rangle = \varepsilon_i |\Phi_i\rangle, \quad (5.2)$$

where the set of states  $\{|\Phi_i\rangle\}$  are exact eigenstates of the Hamiltonian  $\hat{H}$  with corresponding eigenvalues  $\varepsilon_i$ . Unfortunately, one is able to solve the Schrödinger equation exactly only for approximated Hamiltonians  $\hat{H}_0$ , and to obtain an approximated set of eigenstates  $|i\rangle$  with corresponding eigenvalues  $E_i^{(0)}$

$$\hat{H}_0 |i\rangle = E_i^{(0)} |i\rangle. \quad (5.3)$$

In order to find the procedure, where the eigenstates can be improved systematically, the scaling parameter  $\lambda$  is introduced, so that the Hamiltonian is rewritten as

$$\hat{H} = \hat{H}_0 + \lambda \hat{V}. \quad (5.4)$$

According to this scaling parameter, the exact eigenvalues and exact eigenstates could be expanded as

$$\begin{aligned} \varepsilon_i &= E_i^{(0)} + \lambda E_i^{(1)} + \lambda^2 E_i^{(2)} + \dots \\ |\Phi_i\rangle &= |i\rangle + \lambda |\Psi_i^{(1)}\rangle + \lambda^2 |\Psi_i^{(2)}\rangle + \dots, \end{aligned} \quad (5.5)$$

where the terms  $E_i^{(n)}$  are the  $n$ -th order perturbation energies and  $|\Psi_i^{(n)}\rangle$  are the  $n$ -th order corrections of the corresponding eigenstate. The set of approximated states is orthonormal and by choosing the so-called intermediate normalization  $\langle \Phi_i | i \rangle = 1$ , one obtains the following relation:

$$\langle i | \Psi_i^{(n)} \rangle = 0, \quad \text{for } n \geq 1. \quad (5.6)$$

The corrections of the eigenstates can be further expanded in a set of approximated eigenstates  $\{|i\rangle\}$  as

$$|\Psi_i^{(n)}\rangle = \sum_j c_{ij}^{(n)} |j\rangle, \quad (5.7)$$

where  $n \geq 1$  represents the order of the perturbation and the indices  $i$  and  $j$  run over the number of states. The coefficients  $c_{ij}^{(n)}$  are simply given by

$$c_{ij}^{(n)} = \langle j | \Psi_i^{(n)} \rangle. \quad (5.8)$$

The 0th order perturbation energy values are simply the eigenvalues  $E_i^{(0)}$  of the Hamiltonian  $\hat{H}_0$  and all higher-order energy corrections can be obtained by

$$E_i^{(n)} = \langle i | \hat{V} | \Psi_i^{(n)} \rangle. \quad (5.9)$$

At the end of the section, the first three order perturbation energy values will be given in terms of the matrix elements of  $\hat{V}$  and the eigenvalues  $E_i^{(0)}$ :

$$\begin{aligned} E_i^{(1)} &= \langle i | \hat{V} | i \rangle ; \\ E_i^{(2)} &= \sum_{j \neq i} \frac{\langle i | \hat{V} | j \rangle \langle j | \hat{V} | i \rangle}{E_i^{(0)} - E_j^{(0)}} = \sum_{j \neq i} \frac{|\langle i | \hat{V} | j \rangle|^2}{E_i^{(0)} - E_j^{(0)}} ; \\ E_i^{(3)} &= \sum_{j, k \neq i} \frac{\langle i | \hat{V} | j \rangle \langle j | \hat{V} | k \rangle \langle k | \hat{V} | i \rangle}{(E_i^{(0)} - E_j^{(0)})(E_i^{(0)} - E_k^{(0)})} - E_i^{(1)} \sum_{j \neq i} \frac{|\langle i | \hat{V} | j \rangle|^2}{(E_i^{(0)} - E_j^{(0)})^2}. \end{aligned} \quad (5.10)$$

## 5.2 Møller-Plesset Perturbation Theory

If the results of the previous section are applied on the Hartree-Fock Hamiltonian

$$\hat{H}_0 = \sum_i f(i) = \sum_i \left( \hat{h}(i) + v^{\text{HF}}(i) \right), \quad (5.11)$$

one arrives at Møller-Plesset perturbation theory. Comparing the Hartree-Fock Hamiltonian with the exact many-body Hamiltonian (2.6), the perturbation is given by

$$\hat{V} = \hat{\mathcal{O}}_2 - \sum_i \hat{v}^{\text{HF}}(i) = \sum_{i < j} r_{ij}^{-1} - \sum_{ij} \left( \hat{J}_j(i) - \hat{K}_j(i) \right). \quad (5.12)$$

As already mentioned, the 0th order energy term is simply the eigenvalue of the Hartree-Fock Hamiltonian or the sum of Fock eigenvalues:

$$E_0^{(0)} = \langle \Psi_0 | \hat{H}_0 | \Psi_0 \rangle = \sum_i \varepsilon_i = \sum_i \langle i | \hat{h} | i \rangle + \sum_{ij} \langle ij | ij \rangle. \quad (5.13)$$

Applying the equation (5.10), the first order energy term in Møller-Plesset perturbation theory is given by

$$E_0^{(1)} = \langle \Psi_0 | \hat{\mathcal{O}}_2 | \Psi_0 \rangle - \sum_i \langle \Psi_0 | \hat{v}^{\text{HF}} | \Psi_0 \rangle. \quad (5.14)$$

Using Slater-Condon rule 2.38 and the definition of the averaged Hartree-Fock potential the first order energy is finally given by the following relation:

$$\begin{aligned} E_0^{(1)} &= \frac{1}{2} \sum_{ij} \langle ij | ij \rangle - \sum_{ij} \langle ij | ij \rangle \\ &= -\frac{1}{2} \sum_{ij} \langle ij | ij \rangle. \end{aligned} \quad (5.15)$$

After these considerations, adding the first two energy terms (equations 5.13, 5.15) one obtains the Hartree-Fock ground state energy

$$E_0^{\text{HF}} = E_0^{(0)} + E_0^{(1)} = \sum_i \langle i | \hat{h} | i \rangle - \frac{1}{2} \sum_{ij} \langle ij || ij \rangle, \quad (5.16)$$

that is exactly the energy of the Hartree-Fock determinant given by Slater-Condon rules (equations 2.37, 2.38). From these considerations, the first improvement of the Hartree-Fock energy is given by the second-order energy term, the so-called MP2 energy. Recall the equation for the general second-order perturbation energy (5.10). Because one is interested in the perturbation of the ground state energy, the state  $|i\rangle$  is given by Hartree-Fock determinant  $|\Psi_0\rangle$ . The choice of states  $|j\rangle$  should be carefully determined. Triple and higher excitations do not mix with a Hartree-Fock determinant, because of two-electron nature of the many-body Hamiltonian. Therefore, they can be immediately discarded. As shown in the section 4.2, single excitations  $|\Psi_i^r\rangle$  do not mix with a Hartree-Fock determinant (Brillouin theorem) and they will not be considered, either. In the end, only double excitations  $|\Psi_{ij}^{rs}\rangle$  will appear in the MP2 energy as states, over which the summation needs to be done. To be able to sum over all double excitations exactly once, the sum should be restricted to  $i < j$  and  $r < s$ . Since the double excitations are also eigenstates of the Hartree-Fock Hamiltonian

$$\hat{H}_0 |\Psi_{ij}^{rs}\rangle = (E_0^{(0)} - \varepsilon_i - \varepsilon_j + \varepsilon_r + \varepsilon_s) |\Psi_{ij}^{rs}\rangle, \quad (5.17)$$

the general expression for the second-order energy can be rewritten as

$$E_0^{(2)} = \sum_{i < j} \sum_{r < s} \frac{\|\langle ij || rs \rangle\|^2}{\varepsilon_i + \varepsilon_j - \varepsilon_r - \varepsilon_s}, \quad (5.18)$$

where indices  $i$  and  $j$  run over occupied orbitals and indices  $r$  and  $s$  over unoccupied ones. The equation can be further adjusted for the evaluation over restricted spin orbitals (2.39):

$$E_0^{(2)} = 8 \sum_{i < j} \sum_{r < s} \frac{\langle ij | rs \rangle \langle rs | ij \rangle}{\varepsilon_i + \varepsilon_j - \varepsilon_r - \varepsilon_s} - 4 \sum_{i < j} \sum_{r < s} \frac{\langle ij | rs \rangle \langle sr | ij \rangle}{\varepsilon_i + \varepsilon_j - \varepsilon_r - \varepsilon_s}. \quad (5.19)$$

In a similar way, higher order energy terms can be expressed. In this work, only MP2 energy will be considered, because it is the cheapest one for the calculation, but simultaneously the MP2 energy recovers in average 70-90 % of the total correlation energy. Such a dominance of MP2 energy is expected, because it was seen that the MP2 energy contains only contributions due to double excitations, which monitoring the correlation energy.

### 5.3 Size-Extensivity of MP Energies

From its perturbative nature, it is clear that MP energies are not variational, i.e. the MP energy is not the lowest energy that can be obtained from the actual set of orbitals

that approximate the electronic wave function. To get a better insight, the first two MP energy terms should be considered. Although the set of Hartree-Fock orbitals is improved by the first-order corrections  $|\Psi_i^{(1)}\rangle$ , the sum of these first two energy terms is exactly the Hartree-Fock energy that was obtained by the optimization of Hartree-Fock orbitals only. On the other side, the MP energies are size-extensive at each order of approximation. Consider a system of  $N$  independent non-interacting particles. If the method is size-extensive, then the total energy of the system is given simply as the sum of all particle energies. In this section, it will be explicitly shown, that MP0, MP1 and MP2 energies are size-extensive. It is a very demanding task to prove the size-extensivity at an arbitrary level of the perturbation. A simple way to do it, is to use Feynman diagrams to represent the perturbation theory, where the size-extensivity is the direct consequence of the famous linked-cluster theorem. However, the diagrammatic representation is out of scope of this work. For more details, it is recommended to consider [3, 7]. Let us return now to our first three Møller-Plesset energies. Consider the two non-interacting systems A and B with corresponding Hamiltonian operators  $\hat{H}_A$  and  $\hat{H}_B$  and let us assume that the Hamiltonian of the whole system is simply the sum of these two Hamiltonians  $\hat{H}_{AB} = \hat{H}_A + \hat{H}_B$ . In a similar way, the unperturbed Hamiltonians and perturbations are defined as  $\hat{H}_{0,AB} = \hat{H}_{0,A} + \hat{H}_{0,B}$  and  $\hat{V}_{AB} = \hat{V}_A + \hat{V}_B$ . Because the Hamiltonians are additively separable, the ground state wave function must be multiplicatively separable, so that  $|0_{AB}^{(0)}\rangle = |0_A^{(0)}0_B^{(0)}\rangle$ . From this knowledge, the zero-order energy is given by

$$\begin{aligned} E_{0,AB}^{(0)} &= \langle 0_{AB}^{(0)} | \hat{H}_{0,AB} | 0_{AB}^{(0)} \rangle = \langle 0_A^{(0)} | \hat{H}_{0,A} | 0_A^{(0)} \rangle \langle 0_B^{(0)} | 0_B^{(0)} \rangle + \langle 0_A^{(0)} | 0_A^{(0)} \rangle \langle 0_B^{(0)} | \hat{H}_{0,B} | 0_B^{(0)} \rangle \\ E_{0,AB}^{(0)} &= E_{0,A}^{(0)} + E_{0,B}^{(0)}, \end{aligned} \quad (5.20)$$

where it is explicitly shown, that the energy is size-extensive. The same process is applied for the first order perturbation energy:

$$\begin{aligned} E_{0,AB}^{(1)} &= \langle 0_{AB}^{(0)} | \hat{V}_{0,AB} | 0_{AB}^{(0)} \rangle = \langle 0_A^{(0)} | \hat{V}_{0,A} | 0_A^{(0)} \rangle \langle 0_B^{(0)} | 0_B^{(0)} \rangle + \langle 0_A^{(0)} | 0_A^{(0)} \rangle \langle 0_B^{(0)} | \hat{V}_{0,B} | 0_B^{(0)} \rangle \\ E_{0,AB}^{(1)} &= E_{0,A}^{(1)} + E_{0,B}^{(1)}. \end{aligned} \quad (5.21)$$

To prove the same for the MP2 energy, the first-order MP wave function is needed. If the exact Schrödinger equation is truncated at first-order (equations 5.2, 5.5)

$$\left( \hat{H}_0 + \hat{V} \right) (|0^{(0)}\rangle + |0^{(1)}\rangle) = \left( E_0^{(0)} + E_0^{(1)} \right) (|0^{(0)}\rangle + |0^{(1)}\rangle) \quad (5.22)$$

the following closed-form relation for the first-order wave function is obtained:

$$|0^{(1)}\rangle = - \left( \hat{H}_0 - E_0^{(0)} \right)^{-1} \left( \hat{V} - E_0^{(1)} \right) |0^{(0)}\rangle. \quad (5.23)$$

By introducing operators  $\hat{K} = \hat{H}_0 - E_0^{(0)}$  and  $\hat{L} = \hat{V} - E_0^{(1)}$ , the first-order wave function for the composed system can be written as

$$|0_{AB}^{(1)}\rangle = - \left( \hat{K}_A + \hat{K}_B \right)^{-1} \left( \hat{L}_A + \hat{L}_B \right) |0_{AB}^{(0)}\rangle. \quad (5.24)$$

The last equation can be seen as a sum of two terms and therefore, let us consider one term and use operator identity

$$\left( \hat{K}_A + \hat{K}_B \right)^{-1} = \hat{K}_A^{-1} - \left( \hat{K}_A + \hat{K}_B \right)^{-1} \hat{K}_B \hat{K}_A^{-1} \quad (5.25)$$

to obtain

$$\begin{aligned} -\left(\hat{K}_A + \hat{K}_B\right)^{-1} \hat{L}_A |0_{AB}^{(0)}\rangle &= -\hat{K}_A^{-1} \hat{L}_A |0_A^{(0)} 0_B^{(0)}\rangle + \left(\hat{K}_A + \hat{K}_B\right)^{-1} \hat{K}_B \hat{K}_A^{-1} \hat{L}_A |0_A^{(0)} 0_B^{(0)}\rangle \\ &= -\hat{K}_A^{-1} \hat{L}_A |0_A^{(0)} 0_B^{(0)}\rangle = |0_A^{(1)} 0_B^{(0)}\rangle, \end{aligned} \quad (5.26)$$

where one has used that  $\hat{K}_B$  commutes with  $\hat{K}_A^{-1} \hat{L}_A$  and  $\hat{K}_B |0_B^{(0)}\rangle = 0$  were used. Considering both terms from (5.24) the outcome is

$$|0_{AB}^{(1)}\rangle = |0_A^{(1)} 0_B^{(0)}\rangle + |0_A^{(0)} 0_B^{(1)}\rangle. \quad (5.27)$$

With this result the MP2 energy can be written as

$$\begin{aligned} E_{0,AB}^{(2)} &= \langle 0_{AB}^{(0)} | \hat{V}_{AB} | 0_{AB}^{(1)} \rangle = \langle 0_A^{(0)} | \hat{V}_A | 0_A^{(1)} \rangle \langle 0_B^{(0)} | 0_B^{(0)} \rangle + \langle 0_A^{(0)} | 0_A^{(0)} \rangle \langle 0_B^{(0)} | \hat{V}_B | 0_B^{(1)} \rangle \\ &= E_{0,A}^{(2)} + E_{0,B}^{(2)}, \end{aligned} \quad (5.28)$$

where the size-extensivity of the MP2 energy is proven. For more details about size-extensivity of various electronic structure methods, see Helgaker [9].

## 5.4 Examples of MP2 Calculations

In the subsequent result sections, results from section 4.7 will be appropriately updated and discussed. At the MP2 level, as it was already mentioned, only the total energy is improved, but the wave function remains of the same quality as in RHF theory. Therefore, let us consider total energies in MP2 theory.

### Total Energies

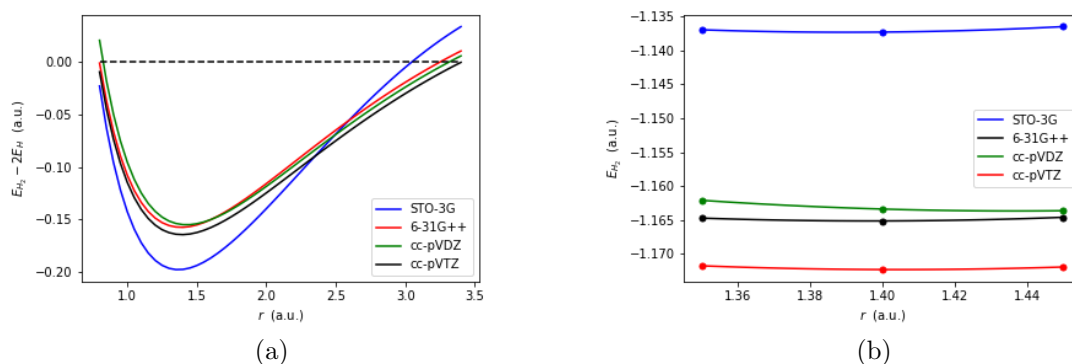
Results for molecules considered in table 4.1 can be found in table 5.1. From those results, it is obvious that larger basis sets are needed to retrieve significant correlation contributions. The minimal basis set does not suffice for correlation consistent calculations and therefore, it will not be used for other correlation consistent calculations. On the other hand, one can notice that the correlation contributions become surprisingly large for systems like H<sub>2</sub>O or the nitrogen molecule N<sub>2</sub>. In the case of the last one, the correlation energy of  $-0.409$  Hartrees is obtained, i.e.  $-11.137$  eV on the MP2 level. In the cases of the He atom and the H<sub>2</sub> molecule, where the exact results are known [3, 21], the MP2 energy retrieves more than 99% of the total correlation energy (at aug-cc-pVTZ level). Clearly, for larger systems the MP2 will become worse and the larger discrepancies between exact results and MP2 values are expected.

### Equilibrium Geometries

In this section, the potential energy curve of the H<sub>2</sub> molecule will be examined again. Let us first see how the situation changes near the optimal geometry. The bond length was already well estimated on the level of Hartree-Fock theory. Here,

Table 5.1: MP2 total energies at the equilibrium geometries of the considered molecules for different basis sets.

Basis Set System	STO-3G	6-31G++	cc-pVDZ	aug-cc-pVDZ	cc-pVTZ	aug-cc-pVTZ	Exact
He	-2.808	-2.881	-2.881	-2.883	-2.894	-2.895	-2.903 [21]
H <sub>2</sub>	-1.130	-1.158	-1.155	-1.156	-1.165	-1.165	-1.175 [3]
BeH <sub>2</sub>	-15.583	-15.817	-15.819	-15.823	-15.840	-15.848	
H <sub>2</sub> O	-74.998	-76.219	-76.231	-76.263	-76.332	-76.344	-76.435 [3]
FH	-98.588	-100.194	-100.223	-100.258	-100.343	-100.355	
N <sub>2</sub>	-107.650	-109.251	-109.265	-109.283	-109.383	-109.394	

Figure 5.1: (a) The energy potential curve of molecule H<sub>2</sub> for different basis sets at MP2 level; (b) The MP2 total energies of H<sub>2</sub> molecule near to the equilibrium geometry and quadratic fit of simulation data.

improvements are expected, because MP2 is quite accurate at the equilibrium geometry. The estimated bond lengths for various basis sets can be found in table 5.2. At the aug-cc-pVTZ level, the optimal bond length differs only by 0.2% from the experimental one (a relative error of 1% was obtained for the RHF theory).

Table 5.2: The estimated bond length in the H<sub>2</sub> molecule at the MP2 level for different basis sets.

STO-3G	6-31G++	cc-pVDZ	aug-cc-pVDZ	cc-pVTZ	aug-cc-pVTZ	Experiment [3]
1.370(5)	1.391(6)	1.429(4)	1.430(4)	1.398(3)	1.398(3)	1.40

The quadratic fit of the simulation data is depicted in figure 5.1-b. In 5.1-a, the whole potential curves for various basis sets are plotted. Comparing these curves with the previous ones (figure 4.3-a), a clear improvement of the dissociation problem can be noticed. However, the problem is still not solved. Although the intersection with  $x$ -axis has shifted to the right, the dissociation energy still becomes positive for large bond lengths.

# Chapter 6

## Direct Full Configuration Interaction Method - FCI

In this chapter, the major subject of this thesis is discussed. It is the famous configuration interaction method, which optimizes the  $N$ -electron wave function within a Slater space. With configuration interaction, it is theoretically possible to obtain the exact correlation energy  $E_{\text{corr}}$ , that is defined as the difference between the exact non-relativistic electronic Hamiltonian eigenvalue (2.7) and the Hartree-Fock energy, obtained in the limit of the complete basis set

$$E_{\text{corr}} = \mathcal{E}_0 - E_0^{\text{HF}}. \quad (6.1)$$

Because of the importance of this term, the correlation energy will be discussed here in more details. As it was seen in chapter 2, certain approximations are applied to be able to solve the non-relativistic Schrödinger equation within the Born-Oppenheimer approximation (see section 2.2). All small effects that can not be treated exactly are called correlation effects. Although the Hartree-Fock method and similar simple methods give about 99% of the ground state energy in most cases, the rest is sometimes needed in order to obtain some properties of the system correctly (excited states, dipole moments, dissociation of molecules, relative energies between phases, atomization energies and others). The correlation energy can be divided into two parts - static correlation energy and dynamic correlation energy. Static correlation energy comes from the degeneracy of the bonding and anti-bonding configuration. In such systems, these configurations have to be treated together. Especially, the description of molecule dissociation requires more configurations to describe the ground state properly, because the bonding and anti-bonding states become nearly degenerated at non-equilibrium distances. For these reasons, the single-determinant methods fails. The simplest method to solve this problem is to include the most important configurations for the ground state calculation, i.e. the so-called multi-configurational self-consistent field or MCSCF. The dynamic correlation effects arise from the fact that the exact electron-electron Coulomb repulsion is approximated by the movement of the electron in the potential of other electrons. The dynamic correlation of electrons due to instantaneous Coulomb repulsion can be resolved by inclusion of many Slater determinants. The method that includes all possible Slater determinants is referred to as full configuration interaction FCI. Although the FCI approach provides a way to systematically retain

correlation energy, this method scales exponentially with the number of electrons  $N$  and, in all realistic cases, except the modest ones, one is limited to a small fraction of the Slater space that can be included in the calculations. In this chapter, deterministic and exact procedures to obtain the CI energy via iterative diagonalization procedures will be considered, while the next chapter gives an insight into stochastic Quantum Monte-Carlo methods, which are able to sample the most important part of the Slater space in an efficient way. The chapter starts with general aspects of configuration interaction theory (section 6.1). In the section 6.2, the discussion about size-extensivity of the full configuration interaction method is given, followed by the section where the first concrete CI implementation is discussed. To be able to perform a CI calculation with a meaningful number of Slater determinants, efficient methods for the storage of Slater determinants (section 6.4) and an efficient method for the matrix-diagonalization are needed (section 6.5).

## 6.1 Introduction to CI

So far, the Hartree-Fock theory and Møller-Plesset Perturbation theory were discussed. All these methods are single-determinant methods. In other words, the  $N$ -electron wave function is approximated by only one Slater determinant - the Hartree-Fock determinant. In the Hartree-Fock theory, one finds the set of  $2P$  optimal spin orbitals and constructs a Slater determinant from them. In a configuration interaction method, this set of optimized spin orbitals will remain unchanged and they will be used for the construction of other Slater determinants. Consider the  $N$  electrons and  $2P$  spin orbitals, then the number of Slater determinants that can be constructed is

$$N_{\text{det}} = \binom{2P}{N}. \quad (6.2)$$

Assuming the fact that electrons have either spin up ( $\alpha$ ) or spin down ( $\beta$ ) and that the spin of the electron can not be changed, the number of possible Slater determinants is restricted to

$$N_{\text{det}} = \binom{P}{N_\alpha} \cdot \binom{P}{N_\beta}, \quad (6.3)$$

where  $N_\alpha$  and  $N_\beta$  are the number of spin up and spin down electrons, respectively. If all Slater determinants are included in the CI expansion, one refers to the full configuration interaction or FCI method. The FCI wave function can be written in the intermediate normalized state as

$$|\Phi^{\text{FCI}}\rangle = |\Psi_0\rangle + \sum_{ir} c_i^r |\Psi_i^r\rangle + \sum_{\substack{i<j \\ r<s}} c_{ij}^{rs} |\Psi_{ij}^{rs}\rangle + \sum_{\substack{i<j<k \\ r<s<t}} c_{ijk}^{rst} |\Psi_{ijk}^{rst}\rangle + \dots \quad (6.4)$$

where  $|\Psi_0\rangle$  is reference Hartree-Fock determinant,  $|\Psi_i^r\rangle$  denotes single excitations,  $|\Psi_{ij}^{rs}\rangle$  denotes doubly excited determinants and so on. The FCI procedure reflects in the calculation of optimal coefficients that minimize the total energy. This procedure corresponds to the variational problem (see appendix A), i.e. to the diagonalization of the corresponding Hamiltonian. The so-called CI matrix (Hamiltonian matrix within

a Slater space) has a strong block form (figure 6.1), because all Hamiltonian matrix elements  $\langle \Psi_1 | \hat{H} | \Psi_2 \rangle$ , where two Slater determinants differ by more than two spin orbitals, are equal to zero. All non-zero Hamiltonian matrix elements are obtained via Slater-Condon rules (equations 2.37, 2.38). The lowest eigenvalue of the CI matrix gives the upper bound of the ground state energy

$$E_{\text{corr}}^{\text{CI}} = E_0^{\text{CI}} - E_0^{\text{HF}}, \quad (6.5)$$

where  $E_{\text{corr}}^{\text{CI}}$  is called basis set correlation energy. The first element of this matrix  $\langle \Psi_0 | \hat{H} | \Psi_0 \rangle$ , i.e. the Hartree-Fock energy is the most negative value in the matrix. The second important fact to notice is that the single excitations  $|\Psi_i^r\rangle$  do not mix with the Hartree-Fock determinant, because of the Brillouin theorem (section 4.2). However, the single excitations still have a small effect on the ground state, because they mix indirectly via double and triple excitations. After these considerations, it is expected that double excitations play a dominant role in the CI ground state (after the Hartree-Fock determinant, of course), because they are the only ones that mix with the reference state directly. The FCI procedure is very attractive for physicists, because the FCI energy is both variational and size-extensive and it also produces the exact correlation within a basis set. The size-extensivity of the FCI wave function will be derived in the section 6.2. From the relation (6.3), it can be concluded that the Slater space grows exponentially with number of electrons, i.e. the number of spin orbitals. Therefore, the FCI procedure is possible only for the smallest systems and for larger systems the CI wave function usually needs to be truncated. The simplest way to truncate the CI wave function is to include all excitations of Hartree-Fock determinant up to the  $k$ -th order, because one expects the following behavior: the higher the level of excitation, the smaller its effect on the ground state is. CAS - complete active space and RAS - restricted active space are also very popular expansion methods, but they will not be discussed in detail here, because the FCI procedure is of main interest for this work. On the other hand, the CAS method will be shortly discussed in the next chapter, because it is needed for an efficient sampling of the Slater space in stochastic CI methods.

## 6.2 Size-Extensivity of the CI Wave Function

As it was shown for Møller-Plesset perturbation theory, one wants to show that the the full configuration interaction is also size-extensive. In this section, the size-extensivity of the wave function will be shown in general for the linear variational problem, discussed in appendix A. Let us introduce an optimized wave function for two subsystems:

$$\begin{aligned} |0_A\rangle &= \sum_i C_{iA} |i_A\rangle \\ |0_B\rangle &= \sum_i C_{iB} |i_B\rangle, \end{aligned} \quad (6.6)$$

	$ \Psi_0\rangle$	$ S\rangle$	$ D\rangle$	$ T\rangle$	$ Q\rangle$	
$\langle \Psi_0  $	$E_0^{\text{HF}}$	$\langle \Psi_0   \hat{H}   S \rangle = 0$	$\langle \Psi_0   \hat{H}   D \rangle$	0	0	
$\langle S  $		$\langle S   \hat{H}   S \rangle$	$\langle S   \hat{H}   D \rangle$	$\langle S   \hat{H}   T \rangle$	0	
$\langle D  $			$\langle D   \hat{H}   D \rangle$	$\langle D   \hat{H}   T \rangle$	$\langle D   \hat{H}   Q \rangle$	$ S\rangle \equiv  \Psi_i^r\rangle$ $ D\rangle \equiv  \Psi_{ij}^{rs}\rangle$ $ T\rangle \equiv  \Psi_{ijk}^{rst}\rangle$ $ Q\rangle \equiv  \Psi_{ijkl}^{rstu}\rangle$
$\langle T  $				$\langle T   \hat{H}   T \rangle$	$\langle T   \hat{H}   Q \rangle$	
$\langle Q  $					$\langle Q   \hat{H}   Q \rangle$	

Figure 6.1: The strong sparse form of the CI matrix: red color denotes the matrix elements that disappear because of Brillouin theorem, while the intensity of grey areas shows the importance of the corresponding matrix elements on the ground state. Note, only the upper triangular part of the CI matrix is shown, because the matrix is Hermitian.

so that the ground state energy of each subsystem can be expressed as

$$E_A = \frac{\langle 0_A | \hat{H}_A | 0_A \rangle}{\langle 0_A | 0_A \rangle}$$

$$E_B = \frac{\langle 0_B | \hat{H}_B | 0_B \rangle}{\langle 0_B | 0_B \rangle},$$
(6.7)

where  $H_A$  and  $H_B$  are Hamiltonian operators of subsystems  $A$  and  $B$ , respectively. For the supersystem  $AB$ , the optimized wave function is a linear combination of direct product states

$$|0_{AB}\rangle = \sum_{ij} C_{i_A, j_B} |i_A j_B\rangle = |0_A 0_B\rangle \equiv |0_A\rangle |0_B\rangle,$$
(6.8)

and equivalent as for subsystems, the total energy of a supersystem is given by

$$E_{AB} = \frac{\langle 0_{AB} | \hat{H}_{AB} | 0_{AB} \rangle}{\langle 0_{AB} | 0_{AB} \rangle}.$$
(6.9)

Using the fact that the Hamiltonian of the composed system is simply the sum of subsystem's Hamiltonians  $\hat{H}_{AB} = \hat{H}_A + \hat{H}_B$  and the fact that two subsystems do not

interact, one obtains

$$\begin{aligned}
E_{AB} &= \frac{\langle 0_{AB} | \hat{H}_A + \hat{H}_B | 0_{AB} \rangle}{\langle 0_{AB} | 0_{AB} \rangle} = \frac{\langle 0_A | \hat{H}_A | 0_A \rangle \langle 0_B | 0_B \rangle}{\langle 0_A | 0_A \rangle \langle 0_B | 0_B \rangle} + \frac{\langle 0_A | 0_A \rangle \langle 0_B | \hat{H}_B | 0_B \rangle}{\langle 0_A | 0_A \rangle \langle 0_B | 0_B \rangle} \\
&= \frac{\langle 0_A | \hat{H}_A | 0_A \rangle}{\langle 0_A | 0_A \rangle} + \frac{\langle 0_B | \hat{H}_B | 0_B \rangle}{\langle 0_B | 0_B \rangle} \\
&= E_A + E_B,
\end{aligned} \tag{6.10}$$

which proves the size-extensivity of linear variational problem. As the configuration interaction method and the Hartree-Fock approximation are based on the linear variational problem, the size-extensivity holds for CI and Hartree-Fock approximations, too. Note that there is an additional condition for the size-extensivity. If the system  $A$  is expanded in the space of size  $\mathcal{S}_A$  and the system  $B$  in space of size  $\mathcal{S}_B$ , then the supersystem must be expanded over the whole product space  $\mathcal{S}_A \otimes \mathcal{S}_B$ . The important consequence of this condition is that the truncated CI wave function is not size-extensive anymore. To make it clearer, consider the CI expansion of fragments  $A, B$ , where only single and double excitations are included - CISD. To be size-extensive, the expansion of the composed wave function also has to contain triples and quadruples that arise as composition of singles/doubles from two fragments  $A$  and  $B$ . Therefore, the size-extensivity holds only for the full configuration interaction FCI, where all possible configurations are included. In the end, note that the FCI correlation energy defined by (6.5) is also size extensive, because both FCI and Hartree-Fock energies are size-extensive.

### 6.3 Determinant-Based Direct CI Method

The first implementations of CI appeared together with Hartree-Fock calculations, but they were able to include only very few Slater determinants or configurational state functions CSFs. Because Slater determinants in general are not eigenfunctions of the spin operator  $\hat{S}^2$ , appropriate linear combinations are constructed in such a way that they satisfy this condition. Such functions are called configurational state functions, i.e CSFs. In terms of CSFs, the size of the CI matrix is smaller than in terms of Slater determinants, and they ensure correct physical properties of the ground state wave function, which is not the case with Slater determinants. Therefore, in the first implementations of configuration interaction, CSFs were used more often than Slater determinants. In these first implementations, the CI matrix was explicitly calculated and stored on a disc or a magnetic tape and at each iteration of the CI procedure, all matrix elements had to be loaded. The new epoch, which has enabled CI calculations on drastically larger systems was introduced by Roos and Siegbahn [29]. In this method the CI matrix is not calculated explicitly anymore, but the evaluation of the contraction

$$\sigma = HC, \tag{6.11}$$

where  $C$  is a CI vector (the coefficients of the CI expansion from equation (6.4)), is done at each iteration of CI procedure on the fly. In this process, some iterative diagonalization procedure is used to find the converged CI vector that approximates the ground state. Iterative diagonalization procedures are very important in CI

calculations, and they will be discussed later in section 6.5. After these considerations, the main task in the CI procedure is the efficient evaluation of the matrix multiplication (6.11). For this purpose, the concept of alpha (beta) strings was introduced by Handy [30]. An alpha (beta) string is simply the ordered product of creation operators with the  $\alpha$  spin ( $\beta$  spin). Consider the Slater determinant

$$|I\rangle = |\chi_{1\alpha}\chi_{2\alpha}\chi_{3\alpha}\chi_{1\beta}\chi_{4\beta}\chi_{5\beta}\rangle \quad (6.12)$$

then the alpha and beta strings are

$$\begin{aligned} I_\alpha &= \chi_{1\alpha}\chi_{2\alpha}\chi_{3\alpha} = a_{1\alpha}^\dagger a_{2\alpha}^\dagger a_{3\alpha}^\dagger \\ I_\beta &= \chi_{1\beta}\chi_{4\beta}\chi_{5\beta} = a_{1\beta}^\dagger a_{4\beta}^\dagger a_{5\beta}^\dagger, \end{aligned} \quad (6.13)$$

so that the Slater determinant can be rewritten as

$$|I\rangle = |I_\alpha I_\beta\rangle \equiv |I_\alpha\rangle |I_\beta\rangle. \quad (6.14)$$

The number of alpha strings  $N_{\text{str}}^\alpha$ , and beta strings  $N_{\text{str}}^\beta$ , respectively are given in equation (6.3) by the first and the second factor, respectively. The first task in an CI implementation is the construction of all alpha (beta) strings by distributing  $N_\alpha$  ( $N_\beta$ ) electrons among  $P$  spin orbitals. Because each Slater determinant can be constructed by combining one alpha and one beta string, the natural choice for the representation of the CI vector is a matrix of dimensions  $N_{\text{str}}^\alpha \times N_{\text{str}}^\beta$ , where the row index points to the alpha string and the column index points to the beta string. Therefore, the names CI vector and CI matrix will be used interchangeably. Recall now the many-body Hamiltonian in second quantization, derived in the section 2.7

$$\hat{H} = \sum_{ij}^P (i|\hat{h}|j)\hat{E}_{ij} + \frac{1}{2} \sum_{ijkl}^P (ij|kl) \left[ \hat{E}_{ij}\hat{E}_{kl} - \delta_{jk}\hat{E}_{il} \right] \quad (6.15)$$

and insert it into (6.11) to obtain

$$\sigma_{I_\alpha I_\beta} = \sum_{J_\alpha, J_\beta} \langle I_\beta I_\alpha | \sum_{ij} (i|\hat{h}|j)\hat{E}_{ij} + \frac{1}{2} \sum_{ijkl} (ij|kl) (\hat{E}_{ij}\hat{E}_{kl} - \delta_{jk}\hat{E}_{il}) | J_\alpha J_\beta \rangle C_{J_\alpha J_\beta}. \quad (6.16)$$

The first direct and efficient implementation of the latter equation was done by Olsen [31] and this implementation is appropriate for full CI calculations. The equation (6.16) can be further simplified. In the first step, the Hamiltonian can be rewritten in such a way that the two-electron Hamiltonian part with the single excitation operator  $\hat{E}_{il}$  can be added to the one-electron part of the Hamiltonian

$$\begin{aligned} \hat{H} &= \sum_{ij} (i|\hat{h}|j)\hat{E}_{ij} + \frac{1}{2} \sum_{ijkl} (ij|kl) \left[ \hat{E}_{ij}\hat{E}_{kl} - \delta_{jk}\hat{E}_{il} \right] \\ &= \sum_{ij} (i|\hat{h}|j)\hat{E}_{ij} - \frac{1}{2} \sum_{ijl} (ij|jl)\hat{E}_{il} + \frac{1}{2} \sum_{ijkl} (ij|kl)\hat{E}_{ij}\hat{E}_{kl} \\ &= \sum_{ij} \left[ (i|\hat{h}|j) - \frac{1}{2} \sum_k (ik|kj) \right] \hat{E}_{ij} + \frac{1}{2} \sum_{ijkl} (ij|kl)\hat{E}_{ij}\hat{E}_{kl} \\ &= \sum_{ij} \tilde{h}_{ij}\hat{E}_{ij} + \frac{1}{2} \sum_{ijkl} (ij|kl)\hat{E}_{ij}\hat{E}_{kl}, \end{aligned} \quad (6.17)$$

where the modified one-electron integrals  $\tilde{h}_{ij}$  are defined as

$$\tilde{h}_{ij} = (i|\hat{h}|j) - \frac{1}{2} \sum_k (ik|kj). \quad (6.18)$$

This transformation of the one-electron integrals should be performed before the actual full CI calculations start. In this moment, it is appropriate to note that one- and two-electron integrals used in CI programs are the molecular integrals over canonical spin orbitals and they substantially differ from the molecular integrals over Gaussian basis functions that were discussed in chapter 3. Therefore, after the SCF calculation is performed and HF spin orbitals are obtained, the transformation of molecular integrals over Gaussian functions to integrals over Hartree-Fock orbitals must be performed. Because this task is often computationally more demanding than the entire Hartree-Fock calculation, it will be discussed separately in appendix C. The next simplification noticed first by Handy and Knowles [32,33] reflects in the following fact: differ two alpha strings  $I_\alpha$  and  $J_\alpha$  by two spin orbitals, then the contribution to the sigma vector is independent of the beta strings. Recall the definition of the total excitation operator (2.50) and inserting it into (6.16), the sigma vector can be split into three terms

$$\sigma_{I_\alpha I_\beta} \equiv \sigma(I_\alpha, I_\beta) = \sigma_1(I_\alpha, I_\beta) + \sigma_2(I_\alpha, I_\beta) + \sigma_3(I_\alpha, I_\beta), \quad (6.19)$$

where  $\sigma_1$  depends only on the alpha strings,  $\sigma_2$  on the beta strings only and the third term  $\sigma_3$ , computationally the most demanding one, depends on both - alpha and beta strings. In the  $\sigma_1$  part, all excitation operators belong to alpha electrons, so that the beta strings  $I_\beta$  and  $J_\beta$  have to be identical  $I_\beta = J_\beta$ . Therefore, the term  $\sigma_1$  is given by

$$\sigma_1(I_\alpha, I_\beta) = \sum_{J_\alpha} \langle I_\alpha | \sum_{ij} \tilde{h}_{ij} \hat{E}_{ij}^\alpha + \frac{1}{2} \sum_{ijkl} (ij|kl) \left( \hat{E}_{ij}^\alpha \hat{E}_{kl}^\alpha \right) | J_\alpha \rangle C(J_\alpha I_\beta). \quad (6.20)$$

In a similar way, the analogous expression containing only beta excitations is given by

$$\sigma_2(I_\alpha, I_\beta) = \sum_{J_\beta} \langle I_\beta | \sum_{ij} \tilde{h}_{ij} \hat{E}_{ij}^\beta + \frac{1}{2} \sum_{ijkl} (ij|kl) \left( \hat{E}_{ij}^\beta \hat{E}_{kl}^\beta \right) | J_\beta \rangle C(I_\alpha J_\beta). \quad (6.21)$$

The last term, containing alpha and beta excitations simultaneously, is given by the following relation

$$\sigma_3(I_\alpha, I_\beta) = \sum_{J_\alpha J_\beta} \sum_{ijkl} \langle I_\alpha | \hat{E}_{ij}^\alpha | J_\alpha \rangle \langle I_\beta | \hat{E}_{kl}^\beta | J_\beta \rangle (ij|kl) C(J_\alpha J_\beta). \quad (6.22)$$

Further simplifications are due to spin symmetry and they are very important for the minimization of the computational time for the FCI algorithm. For this purpose, the spin projection  $M_S$  should be considered. This value is given via

$$M_S = \frac{1}{2}(N_\alpha - N_\beta). \quad (6.23)$$

If  $M_S = 0$  (number of electrons with spin up equal to the number of electrons with spin down), terms  $\sigma_1$  and  $\sigma_2$  are connected via the following relation

$$\sigma_2(I_\alpha, I_\beta) = (-1)^S \sigma_1(I_\beta, I_\alpha), \quad (6.24)$$

where  $S$  is the total spin number. The relation was implemented for the first time by Olsen and coworkers [31]. For singlet states ( $S = 0$ ), the CI matrix  $C(I_\alpha, I_\beta)$  is symmetric. The symmetry can also be applied for  $\sigma_3$ , where the  $ijkl$ -th component of  $\sigma_3$  is directly connected with  $klij$ -th component of  $\sigma_3$  by

$$\sigma_3^{ijkl}(I_\alpha, I_\beta) = (-1)^S \sigma_3^{klij}(I_\beta, I_\alpha). \quad (6.25)$$

This equation introduces the restriction  $(ij) \geq (kl)$ . To exploit this restriction in an efficient way, the term  $\sigma_3$  (6.22) is rewritten as

$$\sigma_3(I_\alpha, I_\beta) = \sum_{(ij) \geq (kl)} \sigma_3^{ijkl}(I_\alpha, I_\beta) + \sum_{(ij) < (kl)} (-1)^S \sigma_3^{klij}(I_\beta, I_\alpha). \quad (6.26)$$

Defining

$$\tilde{\sigma}_3(I_\alpha, I_\beta) = \sum_{(ij) \geq (kl)} \sigma_3^{ijkl}(I_\alpha, I_\beta) \cdot (1 + \delta_{(ij), (kl)})^{-1}, \quad (6.27)$$

the term  $\sigma_3$  is finally given by

$$\sigma_3(I_\alpha, I_\beta) = \tilde{\sigma}_3(I_\alpha, I_\beta) + (-1)^S \tilde{\sigma}_3(I_\beta, I_\alpha). \quad (6.28)$$

Note that the second pair of parentheses in (6.27) prevents the double counting of terms with  $i = k$  and  $j = l$ . Summarized, for systems with  $M_S = 0$ , the term  $\sigma_2$  is obtained by the cost of matrix transpose of  $\sigma_1$  and the calculation of  $\sigma_3$  is replaced by the calculation of  $\tilde{\sigma}_3$  (6.27). The whole sigma step is therefore given by the following relation:

$$\sigma(I_\alpha, I_\beta) = \sigma_1(I_\alpha, I_\beta) + \tilde{\sigma}_3(I_\alpha, I_\beta) + (-1)^S [\sigma_1(I_\beta, I_\alpha) + \tilde{\sigma}_3(I_\beta, I_\alpha)]. \quad (6.29)$$

Let us have a closer look at the formal implementation methods for the latter relation. From a historical point of view, two slightly different methods have been developed: the string driven approach and the integral driven approach [34]. In the string driven approach, one loops over all alpha (beta) strings and obtains all allowed excitations by applying excitation operator  $\hat{E}_{ij}^\alpha$ . Once the excitation operator is applied

$$\hat{E}_{ij}^\alpha |I_\alpha\rangle = \Gamma_{ij}(I_\alpha) |I'_\alpha\rangle, \quad (6.30)$$

the new string is obtained and the phase factor  $\Gamma_{ij}(I_\alpha) = \pm 1$  must be calculated, too. This phase factor arises from the antisymmetrical nature of the wave function (see section 2.7). Recall the definition of the factor  $\Gamma_i$  (2.43) and rewrite the factor  $\Gamma_{ij}$  simply as

$$\Gamma_{ij}(I_\alpha) = \Gamma_i \Gamma_j = (-1)^{\sum_{k=1}^{i-1} n_k + \sum_{l=1}^{j-1} n_l} = (-1)^{p_i + p_j} = (-1)^{p_j - p_i}, \quad (6.31)$$

where  $p_j - p_i$  denotes the number of electrons in orbitals between the orbital  $i + 1$  and the orbital  $j - 1$ . The simplest algorithm for the calculation of the term  $\sigma_1$  is given in listing 6.1.

```

1 DO loop over  $|I_\alpha\rangle$ 
2   DO loop over  $k, l$ 
3      $|J_\alpha\rangle = \Gamma_{kl}(I_\alpha) \cdot \hat{E}_{kl}^\alpha |I_\alpha\rangle$ 
4     !add one-electron contributions
5     DO loop over  $|I_\beta\rangle$ 
6        $\sigma_1(I_\alpha, I_\beta) += \Gamma_{kl}(I_\alpha) \cdot \tilde{h}_{kl} C(J_\alpha, I_\beta)$ 
7     END loop  $|I_\beta\rangle$ 
8
9     DO loop over  $j, i$ 
10       $|K_\alpha\rangle = \Gamma_{ij}(J_\alpha) \cdot \hat{E}_{ij}^\alpha |J_\alpha\rangle$ 
11      !add two-electron contributions
12      DO loop over  $|I_\beta\rangle$ 
13         $\sigma_1(I_\alpha, I_\beta) += \frac{1}{2} \Gamma_{ij}(J_\alpha) \Gamma_{kl}(I_\alpha) \cdot (ij|kl) C(K_\alpha, I_\beta)$ 
14      END loop  $|I_\beta\rangle$ 
15    END loop  $i, j$ 
16  END loop  $l, k$ 
17 END loop  $|I_\alpha\rangle$ 

```

Listing 6.1: The simple algorithm for the evaluation of  $\sigma_1$ .

In modern computational architectures, because of the non-uniform memory access, temporal and spatial locality of data should be used in order to implement an efficient algorithm. Because of these considerations, the latter listing could be straightforwardly vectorized. The vectorized algorithm is represented in listing 6.2. The two algorithms will be compared in section 6.6. Returning now to the implementation of  $\sigma_3$ , where excitations over both spins are presented. This implementation is computationally more demanding than the algorithm described in listings 6.1 and 6.2. The simplest version of a string driven algorithm is presented in listing 6.3.

```

1 DO loop over  $|I_\alpha\rangle$ 
2    $F(\cdot) = 0.0$ 
3   DO loop over  $k, l$ 
4      $|J_\alpha\rangle = \Gamma_{kl}(I_\alpha) \cdot \hat{E}_{kl}^\alpha |I_\alpha\rangle$ 
5     !add one-electron contributions
6      $F(J_\alpha) += \Gamma_{kl}(I_\alpha) \cdot \tilde{h}_{kl}$ 
7
8     DO loop over  $j, i$ 
9        $|K_\alpha\rangle = \Gamma_{ij}(J_\alpha) \cdot \hat{E}_{ij}^\alpha |J_\alpha\rangle$ 
10      !add two-electron contributions
11       $F(K_\alpha) += \frac{1}{2} \Gamma_{ij}(J_\alpha) \Gamma_{kl}(I_\alpha) \cdot (ij|kl)$ 
12    END loop  $i, j$ 
13  END loop  $l, k$ 
14   $\sigma_1(I_\alpha, \cdot) += \sum_{J_\alpha} C(J_\alpha, \cdot) \cdot F(J_\alpha)$ 
15 END loop  $|I_\alpha\rangle$ 

```

Listing 6.2: The vectorized algorithm for the evaluation of  $\sigma_1$ .

```

1 DO loop over  $|I_\alpha\rangle$ 
2   DO loop over  $l, k$ 
3      $|J_\alpha\rangle = \Gamma_{kl}(I_\alpha) \cdot \hat{E}_{kl}^\alpha |I_\alpha\rangle$ 
4     DO loop over  $|I_\beta\rangle$ 
5       DO loop over  $j, i$ 
6          $|J_\beta\rangle = \Gamma_{ij}(I_\beta) \cdot \hat{E}_{ij}^\beta |I_\beta\rangle$ 
7          $\sigma(I_\alpha, I_\beta) += \Gamma_{ij}(I_\beta) \Gamma_{kl}(I_\alpha) \cdot (ij|kl) C(J_\alpha, J_\beta)$ 

```

```

8   END loop  $i, j$ 
9   END loop  $|I_\beta\rangle$ 
10  END loop  $k, l$ 
11 END loop  $|I_\alpha\rangle$ 

```

Listing 6.3: The pure string driven algorithm for the evaluation of  $\sigma_3$ .

The vectorization of the algorithm for the calculation of  $\sigma_3$  is not so simple as for the  $\sigma_1$ . To be able to vectorize the  $\sigma_3$  term, the string driven and integral driven approaches must be combined. In the integral driven approach, one loops over orbital indices  $i$  and  $j$ , and forms a sublist  $\mathcal{M}$  of strings that do not disappear under the action of the excitation operator  $\hat{E}_{ij}$  and the sublist of new strings  $\mathcal{N}$ , created as  $\mathcal{N} = \hat{E}_{ij}\mathcal{M}$ . Additionally, the array of phase factors  $\Gamma_{ij}(\mathcal{M})$  has to be calculated. This combined vectorized algorithm is shown in listing 6.4.

```

1  !integral driven part
2  DO loop over  $l, k$ 
3    set up  $\mathcal{M}$ ,  $\mathcal{N}$  and  $\Gamma_{ij}(\mathcal{M})$  by
4    DO loop over  $|I_\alpha\rangle$ 
5       $|\mathcal{N}(I_\alpha)\rangle = \Gamma_{kl}(\mathcal{M}(I_\alpha)) \cdot \hat{E}_{kl}^\alpha |\mathcal{M}(I_\alpha)\rangle$ 
6       $C'(I_\alpha, :) = C(\mathcal{N}(I_\alpha), :) \cdot \Gamma_{kl}(\mathcal{M}(I_\alpha))$ 
7    END loop over  $|I_\alpha\rangle$ 
8
9    !string driven part
10   DO loop over  $|I_\beta\rangle$ 
11      $F(:, I_\beta) = 0.0$ 
12     DO loop over  $j, i$ 
13        $|J_\beta\rangle = \Gamma_{ij}(I_\beta) \cdot \hat{E}_{ij}^\beta |I_\beta\rangle$ 
14        $F(J_\beta) += \Gamma_{ij}(I_\beta) \cdot (ij|kl)$ 
15     END loop  $i, j$ 
16
17      $V = C'F$ 
18      $\sigma(:, I_\beta) += V$ 
19   END loop  $|I_\beta\rangle$ 
20 END loop  $k, l$ 

```

Listing 6.4: The vectorized string-integral driven algorithm for the implementation of  $\sigma_3$ .

## 6.4 Graphical Representation of Slater Determinants

The essential part of each CI implementation is the computer implementation of Slater determinants and fast addressing scheme for them. Each Slater determinant is decomposed into two strings as mentioned in (6.14). Each string is represented by a 4-byte or 8-byte integer depending on the number of orbitals, where the bitwise representation of an integer represents the occupation of a specific orbital in the given string. The  $i$ -th bit of an integer tells whether  $i$ -th orbital of a string is occupied or not. Consider a system with 5 spin-up electrons in 7 orbitals, then the integer 31 will represent the following string:

$$|31\rangle \equiv 1 \cdot 2^0 + 1 \cdot 2^1 + 1 \cdot 2^2 + 1 \cdot 2^3 + 1 \cdot 2^4 + 0 \cdot 2^5 + 0 \cdot 2^6 \equiv |1111100\rangle = a_1^\dagger a_2^\dagger a_3^\dagger a_4^\dagger a_5^\dagger |0\rangle. \quad (6.32)$$

In this way, each string is represented by an integer smaller than  $2^P$ , where  $P$  represents the total number of spatial orbitals. It has to be noted that this bit representation of a string is not unique. Consider the following case

$$\begin{aligned} a_1^\dagger a_2^\dagger a_3^\dagger a_4^\dagger a_5^\dagger |0\rangle &= |1111100\rangle \equiv |31\rangle \\ a_2^\dagger a_1^\dagger a_3^\dagger a_4^\dagger a_5^\dagger |0\rangle &= |1111100\rangle \equiv |31\rangle. \end{aligned} \quad (6.33)$$

It is clear that these two strings differ by a minus sign because of the anticommutation relation (2.47), but they have an identical bit representation. Therefore, in order to avoid ambiguity, a fixed ordering of the creation operators in a string must be established. The normal ordering will be used. In the normal ordering, the creation operator with a larger orbital index within a string comes to the right side and beta string comes to the right side of alpha string, as it is in the case (6.14). Because the bit representation does not fulfill operator algebra, one needs to take care of the minus sign each time one string is perturbed. In the case of excitations, the phase factor is calculated via (6.31), as it was explained in the last section. The last thing to note is the fact that if one manipulates strings via electron excitations only (operator  $\hat{E}_{ij}$  (2.48)), one needs to take care of the minus sign only within a string and not within the whole Slater determinant. In other words, one can write

$$\hat{E}_{ij}^\alpha \hat{E}_{kl}^\beta |I_\alpha I_\beta\rangle = (-1)^{2N_\alpha} \hat{E}_{ij}^\alpha |I_\alpha\rangle \hat{E}_{kl}^\beta |I_\beta\rangle = \Gamma_{ij}(I_\alpha) \Gamma_{kl}(I_\beta) |J_\alpha J_\beta\rangle, \quad (6.34)$$

where  $N_\alpha$  is the number of electrons with spin  $\alpha$  and the action of operator  $\hat{E}_{kl}^\beta$  does not change the sign of a determinant crossing the alpha string  $|I_\alpha\rangle$ . Summarized, each Slater determinant is represented by two integers and two indices are needed to access a specific determinant. In order to obtain an efficient addressing scheme for Slater determinants, a graph representation of the alpha (beta) strings will be introduced [9, 10, 36]. Separately for each spin, one graph representing all possible strings will be constructed. Because the graphs are constructed in an identical way for both spins, spin indices will be discarded in the rest of this section. The Graph  $\mathcal{G}(P : N)$  consisting of vertices and vertical and diagonal arcs has the head at  $(e = 0, o = 0)$  and the tail of a graph is given by a vertex  $(e = N, o = P)$ . Each walk in a graph, starting from a head and ending in a tail, represents one string. To specify the occupation of a string, one defines that each diagonal arc starting in a vertex  $(e, o)$  and ending in  $(e + 1, o + 1)$  indicates that orbital  $o + 1$  is occupied and each vertical arc starting in  $(e, o)$  and ending in  $(e, o + 1)$  represents an unoccupied orbital  $o + 1$ . Consider again a system of 5 electrons in 7 orbitals, which requires a graph  $\mathcal{G}(7 : 5)$  depicted in figure 6.2. The blue walk in a graph, denoted by  $|31\rangle$  is a state in (6.32). In a similar way, the red walk denoted by  $|115\rangle$  corresponds to a string  $|1100111\rangle$ . In order to determine a unique address for each Slater determinant, the weights are assigned to each vertex and each arc. The vertex weights are defined by the following recursion:

$$\begin{aligned} W(e = 0, o = 0) &= 1 \\ W(e, o) &= W(e, o - 1) + W(e - 1, o - 1). \end{aligned} \quad (6.35)$$

In a graph (figure 6.2) all vertex weights are shown. From Vertex weights, arc weights can be defined, too. They are given by the following rules:

$$\begin{aligned} Y^0(e, o) &= 0 \\ Y^1(e, o) &= W(e + 1, o + 1) - W(e, o) = W(e + 1, o), \end{aligned} \quad (6.36)$$

where  $Y^0(e, o)$  is a weight of a vertical arc starting at  $(e, o)$  and  $Y^1(e, o)$  is a weight of diagonal arc starting at vertex  $(e, o)$ . Each walk from head to tail can be represented as a union of vertical and diagonal arcs and the address  $I$  of a given string is simply the sum of all arc weights contained in that string. The relation for the calculation of a string address can be written as

$$I = 1 + \sum_{i=1}^P Y^{e_i - e_{i-1}}(e_i, i), \quad (6.37)$$

where  $e_i - e_{i-1}$  denotes whether the actual orbital is occupied or not, i.e. whether the actual arc is diagonal or vertical. Considering a string (6.32), it is visible that the address of that particular string is 1. It makes sense, because the string  $|31\rangle$  represents the lowest-lying state. By calculating the address for the string represented by the blue line, the address 16 is obtained in a similar fashion. For a string  $|124\rangle \equiv |0011111\rangle = a_3^\dagger a_4^\dagger a_5^\dagger a_5^\dagger a_6^\dagger a_7^\dagger |0\rangle$ , the address 21 is obtained, and it is equal to the total number of strings  $\binom{7}{5}$ . Similarly, one can list all strings and prove that their addresses are all integers in the range 1 – 21. The last step that remains to be done, is the explicit construction of all strings, i.e. the construction of an array of integers, where a bit representation of each integer corresponds to one string. Additionally, this array has to be sorted with respect to the addressing scheme, as explained above. There are also methods to adapt graphs to be able to use advantages of symmetry point group or to adapt graphs for RAS CI calculation, but they will be out of scope of this work. For more details, see [36].

## 6.5 Iterative Diagonalization Procedures - Davidson Method

To be able to perform CI calculations for big systems ( $10^6$  Slater determinants or more), an efficient iterative diagonalization procedure is needed. LAPACK related diagonalization routines based on Givens rotations and Householder transformations can be used for matrices of maximal dimension  $10^4 - 10^5$ . Therefore, one needs an alternative iterative methods to do that. In section 6.3, the method for the contraction  $\sigma = HC$  was introduced to avoid the explicit construction and storage of the full CI matrix. The next step is to provide a good diagonalization method, which can retrieve a specific eigenvalue and corresponding eigenstate from CI vectors only. Because all these methods have iterative nature, a good initial state must be provided. In configuration interaction related methods, the obvious choice is simply the Hartree-Fock determinant (2.20), because the Hartree-Fock determinant usually dominates the exact ground state. The Hartree-Fock determinant could be a bad choice in systems with strong static correlation that causes multi-configurational ground state, but such systems are beyond the scope of this thesis. The simplest iterative procedure satisfying these conditions is the steepest descent method, in which a residual vector is calculated as

$$r = (H - E\mathbb{1})C, \quad (6.38)$$

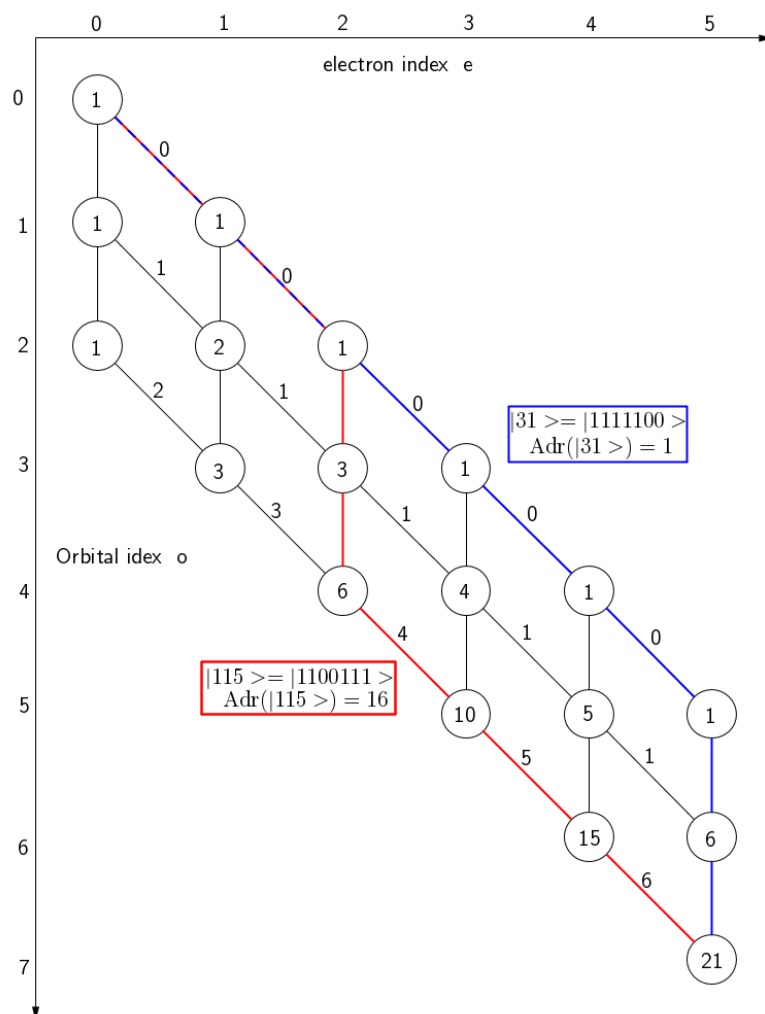


Figure 6.2: Graphical representation of Slater determinants. Each walk in a graph corresponds to one string. For example, the red line represents the string  $|115\rangle = |1100111\rangle$  and has an address 16. Each walk represents uniquely one string and the associated address is also unique. Note, weights of all vertical arcs are equal to 0 and therefore, they are not denoted explicitly in a graph.

where  $E$  is the approximate eigenvalue  $E = \langle C | \hat{H} | C \rangle / \langle C | C \rangle$ . The old eigenvector is then updated according to

$$C_i += \frac{r_i}{E - H_{ii}}. \quad (6.39)$$

Although this method is rather simple and requires the storage of only two vectors of the dimension of the CI matrix (trial vector and residual vector), it is unstable and requires a large number of iterations to achieve reasonable convergence. Therefore, a more robust schemes would be greatly appreciated. The requirement that only contractions of the form  $HC$  are used for the determination of the eigenstate could be an instantaneous reminder of Krylov subspace related methods [37]. In the spirit of Lanczos algorithm, E.R. Davidson has developed a robust algorithm able to compute the lowest eigenvalue and corresponding eigenstate of a system. Liu had improved the method to be able to calculate a few of the lowest eigenvalues and corresponding eigenvectors simultaneously. A good overview of original papers and further implementations and applications can be

found in [38–41]. The Davidson algorithm will be explained in more detail, because of its wide application in electronic structure methods. The complete algorithm is represented in listing 6.5.

```

1 Define starting vector  $u^1 = C_{\text{trial}}$ 
2  $U_0 = []$ 
3  $\Sigma_0 = []$ 
4
5 DO  $i=1, \text{NMAX}$ 
6    $\sigma^i = Hu^i$ 
7    $U_i = [U_{i-1}, u^i]$ 
8    $\Sigma_i = [\Sigma_{i-1}, \sigma^i]$ 
9
10  DO  $j=1, i$ 
11     $\bar{H}(j, i) = \langle u^j | \sigma^i \rangle = \langle u^j | \hat{H} | u^i \rangle$ 
12     $\bar{H}(i, j) = \bar{H}(j, i)$ 
13  ENDDO
14
15   $(\theta, s) = \text{DIAG}(\bar{H})$ 
16   $C = U_i s$ 
17   $r = (H - \theta \mathbf{1})C = (\Sigma_i - \theta U_i)s$ 
18   $r = (D_H - \theta \mathbf{1})^{-1}r$ 
19   $r = r - U_j U_j^\dagger r$ 
20  IF ( $\|r\| < \text{eps}$ ) EXIT
21   $u^{j+1} = r/\|r\|$ 
22 ENDDO

```

Listing 6.5: Davidson algorithm.

The algorithm starts with choosing the trial eigenvector  $u^1$  - simply the coefficient 1 on the Hartree-Fock determinant and 0 otherwise. In the spirit of Krylov subspace methods, the contraction  $\sigma^i = Hu^i$  is generated and both vectors are stored in matrices  $U$  and  $\Sigma$ , which become larger by one column in each iteration. Then, the Hamilton matrix  $\bar{H}$  in a defined subspace  $U$  is calculated and its lowest eigenvalue  $\theta$  and the corresponding eigenvector  $s$  are calculated (step 15 in listing 6.5). Because the matrix  $\bar{H}$  is very small, the diagonalization is done via LAPACK routines for symmetric matrices. The new approximated CI solution is given in step 16. From this approximated solution the residual vector is calculated in the same way as in the steepest descent algorithm (the matrix  $D_H$  is the diagonal part of the Hamilton matrix  $H$ ). Before the residual vector is added to the Krylov subspace, it needs to be Gram-Schmidt orthogonalized with respect to the entire current Krylov subspace (step 19). If the norm of the new subspace vector is smaller than some threshold value, the procedure is converged and the ground state eigenvalue is approximated by  $\theta$  and the corresponding eigenstate is simply given by  $Us$ . The Davidson method is much more robust compared to the steepest-descent algorithm. Although the cost of one iteration is approximately equal for both methods, the number of iterations to achieve convergence decreases significantly in the Davidson algorithm, especially for larger systems. However, the price must be paid in the form of higher memory consumption. For an efficient implementation of the Davidson algorithm, the matrices  $U_i$  and  $\Sigma_i$  must be stored in memory. If the subspace in step 17 of the algorithm is not stored, then it must be recomputed as contraction  $HC$  and that means two contractions of the form  $HC$  per iteration. This situation is undesirable

for large FCI problems. The generalization of the Davidson algorithm for simultaneous computation of a few lowest-lying eigenvalues is straightforward. In the so-called Davidson-Liu algorithm, in order to compute  $N$  eigenstates,  $N$  initial trial vectors are needed. In each iteration, the subspace is expanded by  $N$  vectors, and  $N$  residual vectors are calculated. Each residual vector with the norm larger than some threshold value is accepted and Gram-Schmidt orthogonalized with respect to the entire subspace  $U$ . For more details of this version of the algorithm, see [40, 41]. In the Davidson-Liu algorithm, the subspace grows very fast and it can not fit into main memory anymore. In this case, the deflation of space can help. The deflation represents the extraction of the  $N$  optimal eigenstates from the current Krylov subspace and in the next step the size of the Krylov subspace is again  $N$ . Generally deflation does not show good performance and it should be avoided, if possible. Therefore, it was not implemented in this thesis.

## 6.6 Examples of CI Calculations

With a full configuration interaction method, we are able to calculate the total energies of systems with exact correlation energies within a given basis set. One hopes, the dissociation problem that remained unsolved will be described exactly within the FCI theory.

### Total Energies

Although the correlation energies that will be presented in this section are "exact", one is restricted to modest systems and basis sets, because of the exponential scaling. In the cases of the He atom or molecule  $H_2$ , the FCI calculation will be possible for all available basis sets, because the corresponding Slater space is still very small (about  $5 \cdot 10^3$  Slater determinants for aug-cc-pVQZ basis set). On the other hand, for the  $BeH_2$  molecule, it is possible to calculate FCI wave function on the 6-31G++ level and cc-pVDZ level (about  $4 \cdot 10^6$  Slater determinants). As soon as the cc-pVTZ level is reached, the dimension of the corresponding Slater space is  $10^9$  and this is not possible for standard CI calculations. The results obtained for those systems are given in table 6.1. Although all FCI results are available for the minimal basis set, they will not be presented here, because it was already mentioned in section 5.4 that they are not useful for the accurate calculation of physical properties.

Table 6.1: FCI correlation energies obtained at equilibrium geometries for different basis sets.

Basis Set System	6-31G++	cc-pVDZ	aug-cc-pVDZ	cc-pVTZ	aug-cc-pVTZ	aug-cc-pVQZ	Exact
He	-2.887	-2.888	-2.890	-2.900	-2.901	-2.903	-2.903 [21]
$H_2$	-1.165	-1.163	-1.165	-1.172	-1.173	-1.175	-1.175 [3]
$BeH_2$	-15.831	-15.836					

### Equilibrium Geometry

In this section, the full configuration interaction method will be used to describe the dissociation of the  $H_2$  molecule. Let us start again with results near to the equilibrium

Table 6.2: The estimated bond length of H<sub>2</sub> molecule at the FCI level for different basis sets.

STO-3G	6-31G++	cc-pVDZ	aug-cc-pVDZ	cc-pVTZ	aug-cc-pVTZ	Experiment [3]
1.390(3)	1.397(4)	1.437(4)	1.438(5)	1.403(3)	1.403(3)	1.40

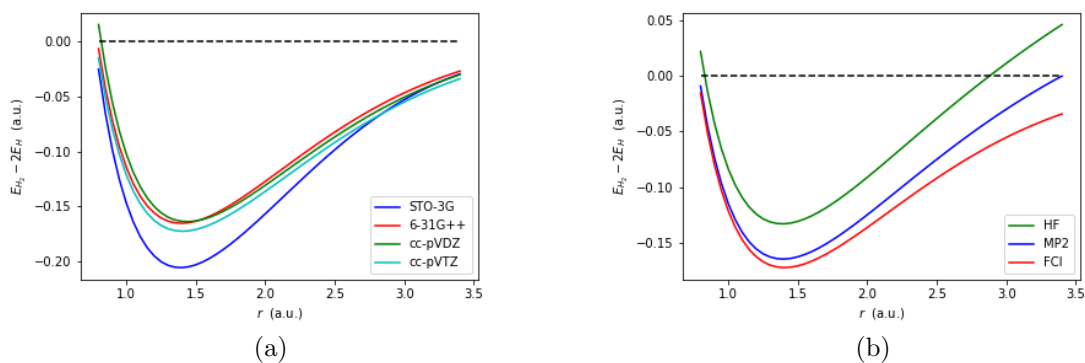


Figure 6.3: (a) The dissociation energy curve of the H<sub>2</sub> molecule for different basis sets at FCI level; (b) the dissociation curve of the H<sub>2</sub> molecule for all three calculation methods with cc-pVTZ basis set.

bond length. Nothing interesting can be obtained, since very accurate results were already obtained in the MP2 approximation. The optimal bond lengths for various basis sets are given in table 6.2. Significant improvements in comparison with MP2 are not obtained, but the bond length predictions were already very good on the MP2 level. Let us now turn to the interesting part. In figure 6.3-a, the potential energy curve of the H<sub>2</sub> molecule is depicted. It is clear that the dissociation energy converges to zero at large distances and it does not become positive anymore. Such a behaviour does not depend on the quality of the basis set, because already at the STO-3G level, the qualitative description of dissociation in the H<sub>2</sub> molecule is correct. For more quantitative results (especially for larger systems), larger basis sets have to be used. All three methods (RHF, MP2 and FCI) are shown together in figure 6.3-b, where one can notice that all three potential energy curves are quite similar (i.e. parallel) near to the equilibrium bond length, but at stretched configurations only full configuration interaction is capable of describing the situation correctly.

## Ground State and the First Excited State of H<sub>2</sub> Molecule

This section presents an application of excited CI states and the application of the Davidson-Liu algorithm described in section 6.5. The electronic structure of the ground state and the first excited state are shown in 6.4. The ground state is clearly a singlet wave function ( $S = 0$ ) and the first excited state is a triplet state ( $S = 1$ ). To be able to obtain triplet states, the FCI calculation must be extended to different  $S_z$  sectors and the 2 lowest eigenstates must be obtained simultaneously. The ground state is already shown in the previous section in figure 6.3. In the ground state, both electrons occupy the bonding symmetric  $\sigma$  orbital and for this reason an antisymmetric spin function must be expected in order to fulfill the Pauli exclusion principle - an antisymmetric wave function. This situation is fulfilled when both electrons have

antiparallel spins - singlet spin state ( $S = 0, M_S = 0$ ). It is clear that the ground state is a bonding state with bond length  $R = 1.403(3)$  at the cc-pVTZ level. The first excited state corresponds to one electron in the bonding symmetric  $\sigma$  state, and one electron in the anti-bonding antisymmetric state  $\sigma^*$ . To obtain an antisymmetric two-electron wave function, the spin function must be symmetric, because the spatial part is already antisymmetric. Therefore, the spins must be parallel and the excited state is a triplet state ( $S = 1, M_S = 1$ ). The triplet state is a non-bonding state and the energy of the state in dependence of the bond length is depicted in figure 6.5. It must also be clear that the described molecular picture is only an approximation of the exact FCI states, but as expected, the single Slater determinants described in figure 6.4 have a dominant role in the corresponding FCI states.

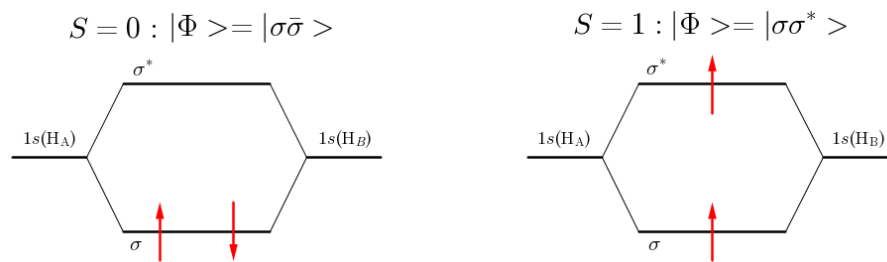


Figure 6.4: Electronic structure of two lowest lying states in the  $H_2$  molecule - singlet spin state on the left and the triplet state on the right side.

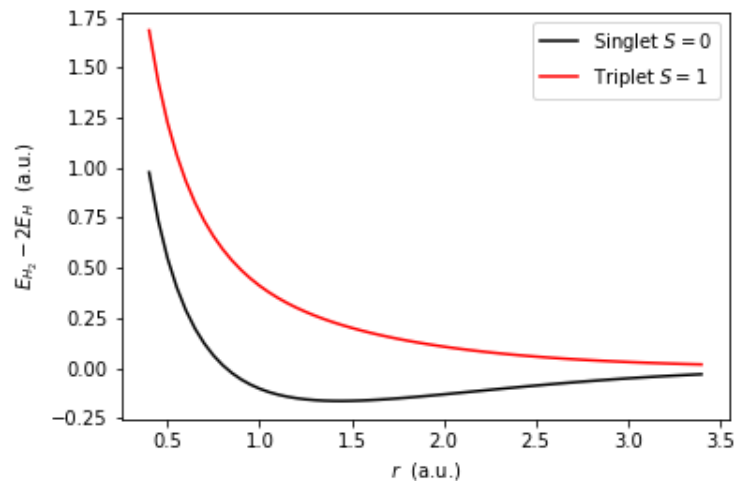


Figure 6.5: Two lowest-lying energy states of the  $H_2$  molecule at various bond lengths.

## Correlation Energy in fcc Helium

The first application of the developed code in solids will be presented in this section. Helium in an fcc lattice will be considered. The goal is to show that the correlation

energy in fcc Helium is approximately additive. In other words, the correlation energy per site does not depend on the size of the system. For this purpose, a supercell of 8 He atoms will be used. The DFT ground state is calculated in VASP for that supercell. Thereafter, the Hartree-Fock ground state (see section 4.6) is calculated and a set of localized Wannier orbitals is obtained as it was explained in section 3.6. A slight complications arises because only the occupied manifold is accurately described in the Hartree-Fock calculation. To resolve this issue, the RPA density matrix and the RPA natural orbitals are used to obtain a more accurate set of unoccupied orbitals which are correlation consistent. On the set of occupied HF orbitals and the RPA natural orbitals, one- and two-electron integrals are calculated in VASP. Once the integrals have been obtained, CI calculation can be performed.

The described procedure is performed on He clusters of different size. At the beginning, only one He atom is considered. Thereafter, two neighboring atoms are correlated together. This procedure is repeated, until a maximum cluster size of 4 atoms (out of 8) is achieved. For each cluster size, the corresponding set of integrals are calculated and the CI calculations are performed. Maximal cluster size is chosen to be 4. Each helium site is described with five orbitals: one doubly occupied  $1s$  orbital and 4 unoccupied orbitals in the second shell (one  $2s$  and three  $2p$  orbitals). The correlation energy per site is listed in the table 6.3. From these results, it can be concluded that the correlation energy does not depend significantly on the cluster size, i.e. the entire correlation contributions come from the correlation between electrons on one site. However, there is a small inter-atom contribution, which is Van der Waals like. Therefore, the correlation energy per site increases slightly with cluster size.

Table 6.3: Correlation energy per site and corresponding Slater space sizes of He clusters of different size.

Cluster size	1	2	3	4
$E_{\text{corr}}^{\text{FCI}}$ (eV)	-0.860	-0.861	-0.862	-0.863
$\mathcal{S}$	25	2025	$2 \cdot 10^5$	$24 \cdot 10^6$

# Chapter 7

## Full Configuration Interaction Quantum Monte Carlo - FCIQMC

### 7.1 Algorithm Description

In the last section, the deterministic CI method was explained, where the solution of the many-body problem is obtained by an iterative diagonalization procedure. The main issues with those methods are the memory requirements needed to store the CI vectors and also the CPU time for the evaluation of the contractions  $HC$ , where the vector  $C$  has a dimension of the underlying Slater space. With those methods, one is able to manipulate Slater spaces of a maximal dimension  $10^9 - 10^{10}$ . To be able to work on larger Slater spaces, approximations must be introduced - complete active space CI (CAS CI), restricted active space CI (RAS CI), truncated CI and other related methods. However, when those approximations are applied, all the unique properties of the FCI method deteriorate and they are often not much better than coupled cluster methods. Therefore, in this chapter the deterministic CI method with explicit iterative diagonalization is discarded and more recent stochastic algorithms are introduced. In the group of A. Alavi, the stochastic method based on the long-time integration of the imaginary-time Schrödinger equation in a discrete Slater space was recently introduced. This method borrows basic concepts from diffusion quantum Monte Carlo (DMC) [42] and Green's function Monte Carlo methods (GFMC) [43]. The origins of the algorithm can be found in [44, 45], and various extensions and applications have appeared, too [46–54]. As it was mentioned in (6.4), the FCI wave function is simply a linear combination of all Slater determinants

$$|\Phi\rangle = \sum_i C_i |\Psi_i\rangle, \quad (7.1)$$

where  $C_i$  is a weight of the corresponding determinant  $|\Psi_i\rangle$  in the exact wave function. From the time-independent Schrödinger equation, one obtains the matrix eigenvalue problem that the coefficients  $C_i$  satisfy

$$\sum_j H_{ij} C_j = \sum_j \langle \Psi_i | \hat{H} | \Psi_j \rangle C_j = E_0^{\text{FCI}} C_i, \quad (7.2)$$

where  $\langle \Psi_i | \hat{H} | \Psi_j \rangle$  are the CI matrix elements defined via Slater-Condon rules (2.37, 2.38). Introducing the imaginary time  $\tau = it$ , the time-dependent Schrödinger

equation (2.1) becomes

$$\frac{\partial \Phi}{\partial \tau} = -\hat{H}\Phi. \quad (7.3)$$

From a formal solution, and with a given starting wave function  $\Psi(\tau = 0) = \Psi_0$ , the exact wave function in the limit of long time is given by

$$\Phi = \lim_{\tau \rightarrow \infty} e^{-\tau(\hat{H} - E_0^{\text{FCI}})} \Psi_0. \quad (7.4)$$

In most cases, the Hartree-Fock determinant  $\Psi_0$  will be used as the starting point. The main problem of the FCIQMC method is to find a method to integrate equation (7.3) in a Slater space and to obtain (7.4). For this reason, the following modified Hamiltonian matrix  $\bar{H}$  with matrix elements is defined:

$$\bar{H}_{ij} = H_{ij} - E_{\text{HF}}\delta_{ij} = \langle \Psi_i | \hat{H} | \Psi_j \rangle - E_{\text{HF}}\delta_{ij}, \quad (7.5)$$

where  $E_{\text{HF}}$  is Hartree-Fock energy. In this way, the spectrum of the Hamiltonian matrix is shifted and the lowest eigenvalue of the matrix  $\bar{H}$  corresponds to the correlation energy  $E_{\text{corr}}^{\text{FCI}}$ . Inserting (7.1) into (7.3), the following set of coupled first-order differential equations for the coefficients  $C_i$  is obtained:

$$-\frac{dC_i}{d\tau} = \sum_j H_{ij}C_j - EC_i, \quad (7.6)$$

where  $E$  is an arbitrary energy shift introduced to control the time evolution of the coefficients  $C_i$ . It can be immediately seen that having coefficients satisfying the eigenvalue equation  $\sum_j H_{ij}C_j = EC_i$  leads to the stationary solution  $dC_i/d\tau = 0$  if  $E = E_0^{\text{FCI}}$ . Inserting  $\bar{H}$  (7.5) in the place of  $H$  in the previous equation leads to

$$-\frac{dC_i}{d\tau} = \sum_j (\bar{H}_{ij} - S\delta_{ij})C_j = (\bar{H}_{ii} - S)C_i + \sum_{j \neq i} \bar{H}_{ij}C_j, \quad (7.7)$$

with a new energy shift  $S = E - E_{\text{HF}}$ . As the coefficients  $C_i$  approach the stationary solution, the shift  $S$  becomes the eigenvalue of  $\bar{H}$ , i.e. the correlation energy  $E_{\text{corr}}^{\text{FCI}}$ . The last equation is the essence of the quantum Monte Carlo full configuration interaction method. The next step is to provide efficient and smart numerical algorithm for sampling of (7.7). As it was seen in the previous chapter, the need to store all CI coefficients in main memory was a limiting factor in the direct CI method. Therefore, one wants to be able to store only the most important contributions to the FCI solution, but in such a way that the developed algorithm finds that part of Slater space by itself. For this purpose, a population of walkers is introduced. The walker  $\omega$  is located on a specific Slater determinant  $|\Psi\rangle$  and holds a sign  $s_\omega = \pm 1$ . The coefficient  $C_i$  is said to be proportional to the signed sum of walkers  $N_i$  on that particular determinant  $|\Psi_i\rangle$

$$C_i \propto N_i = \sum_\omega s_\omega \delta_{i,i_\omega}, \quad (7.8)$$

where  $i_\omega$  is the index of the Slater determinant corresponding to the walker  $\omega$ . Because of  $s_\omega$ ,  $N_i$  can be both positive or negative, but the total number of walkers  $N_w$  must

be positive and it can be written simply as the sum of the absolute values of all signed sums on each determinant

$$N_w = \sum_i |N_i|. \quad (7.9)$$

Having the population defined, rules for the evolution of the population are needed. The equation (7.7) can be adopted for the walker population and for the time evolution and Euler's forward method can be used for time integration of the differential equation (7.7).

$$N_i(\tau + \delta\tau) = [1 - \delta\tau(\bar{H}_{ii} - S)] N_i(\tau) - \delta\tau \left[ \sum_{j \neq i} \bar{H}_{ij} N_j(\tau) \right], \quad (7.10)$$

The time evolution can be divided into three independent steps: spawning step (reflects the last term on the right hand side of the previous equation), diagonal death/cloning step (middle term on the right hand side in the previous equation) and the annihilation step. All three steps are performed at each time step  $\tau$  of a simulation and in the order in which they are explained below.

### 1. The Spawning Step

For each existing walker  $\omega$  on a determinant  $|\Psi_{i_\omega}\rangle$ , the coupled determinant (either single or double excitation)  $|\Psi_j\rangle$  is chosen with a normalized probability  $p_{\text{gen}}(j|i_\omega)$ . One attempts to spawn a new walker on that determinant with a normalized signed probability

$$p_s(j|i_\omega) = -\frac{\delta\tau |\bar{H}_{i_\omega j}|}{p_{\text{gen}}(j|i_\omega)}. \quad (7.11)$$

If  $p_s$  is larger than a random number from a uniform distribution, the spawning is successful. If  $p_s > 1$ , then  $\lfloor p_s \rfloor$  walkers are spawned with a probability 1 and one additional walker with probability  $p_s - \lfloor p_s \rfloor$ . The sign of the new spawned walker is determined in the following way: if  $\bar{H}_{i_\omega j} < 0$ , then the sign of the new spawned walker is the same as the sign of its parent, and opposite to the parent sign if  $\bar{H}_{i_\omega j} > 0$ . It should be noted that the total number of newly spawned walkers should be much smaller than the actual number of parent walkers.

### 2. The Diagonal Death/Cloning Step

In each time step, for each determinant the probability

$$p_d(i_\omega) = \delta\tau C_{i_\omega} (\bar{H}_{i_\omega i_\omega} - S) \quad (7.12)$$

is computed. If  $p_d > 0$ , then  $\lfloor p_d \rfloor$  walkers die immediately and one additional walker dies with probability  $p_d - \lfloor p_d \rfloor$ , and otherwise  $\lfloor |p_d| \rfloor$  walkers are cloned and one additional walker is cloned with probability  $|p_d| - \lfloor |p_d| \rfloor$ . Death/Cloning is an immediate process and such walkers are removed/added in the simulation immediately. From the fact that all diagonal elements of a matrix  $\bar{H}$  are positive and from the fact that  $S$  tends to be negative (approaches the correlation energy that is always negative), the computed probability  $p_d$  is always positive, i.e. only death events can happen. Only if  $S > 0$  and for determinants  $|\Psi_i\rangle$ , where  $\bar{H}_{ii} < S$  the cloning events are allowed. Therefore, the cloning is very rare and it happens only for positive values of the energy shift  $S$ . The cloning can be used for fast growth of the walker population.

### 3. The Annihilation Step

After the spawning and death/cloning steps, all walkers (parent walkers, newly spawned walkers and eventually cloned walkers) are merged together in one list. If two walkers of opposite sign are found to be on the same determinant, they will be annihilated, i.e. they will be removed from the simulation. The way how to do all these steps in memory efficient manner will be discussed later in section 7.6. The additional annihilation step does not have the origin in (7.10), but it is needed to partially overcome the problems related to the Fermion sign problem [55]. The Fermion sign problem will be discussed later in the chapter, because that is one of the best-known unsolved problems in many-body quantum physics.

The flowchart of the entire FCIQMC procedure is presented in the figure 7.1. This version corresponds to the original version of code [44]. Significant performance improvements are obtained using the initiator method extension - called initiator quantum Monte Carlo configuration interaction method iFCIQMC [45], which will be discussed in section 7.5. A semi-stochastic approach [46] was also developed, in which an important part of Slater space is treated in a deterministic fashion with iterative-like diagonalization procedures and the rest of the space is treated as explained above. However, this approach did not become widely adopted as the initiator approach and therefore, it will not be discussed in more details in this thesis. Although the FCIQMC method is designed for the calculation of ground states only, there are extensions based on the stochastic sampling of reduced one-particle and two-particle density matrices, that allow computations of the excited energy states [47–49].

## 7.2 Simulation Modes and Energy Estimators

Two simulation modes in the FCIQMC method are possible. The first one is the constant  $S$  mode and each simulation starts in this mode. The shift is fixed on some value - for example 0 should be a reasonable choice and the simulation starts with only one walker - usually on the Hartree-Fock determinant. During this period, the spawning events dominate death events and an exponential growth of the walker population is obtained. If even faster initial growth of the walker population is desired, positive values for the energy shift can be adopted. For positive values of  $S$ , cloning events occur on determinants  $|\Psi_i\rangle$ , where  $S > \bar{H}_{ii}$ . However, if this is not needed, positive values for the energy shift  $S$  should be avoided. After some time, one should notice that the rate of deaths and annihilations becomes equal to the rate of spawning steps and the total number of walkers stabilizes on some system specific value  $\mathcal{N}$ . The parameter  $\gamma = \mathcal{N}/N_{\text{FCI}}$ , where  $N_{\text{FCI}}$  is the size of the full Slater space (6.3), can be defined and it is an indicator of how many walkers are needed to sample the exact wave function. Small values of the factor  $\gamma$  are greatly desired, because in those cases the FCIQMC method shows significant advantage in comparison to the direct FCI method. For  $\gamma$  values near to unity, the whole Slater space is populated and the advantage of the FCIQMC algorithm disappears. It turns out that the parameter  $\gamma$

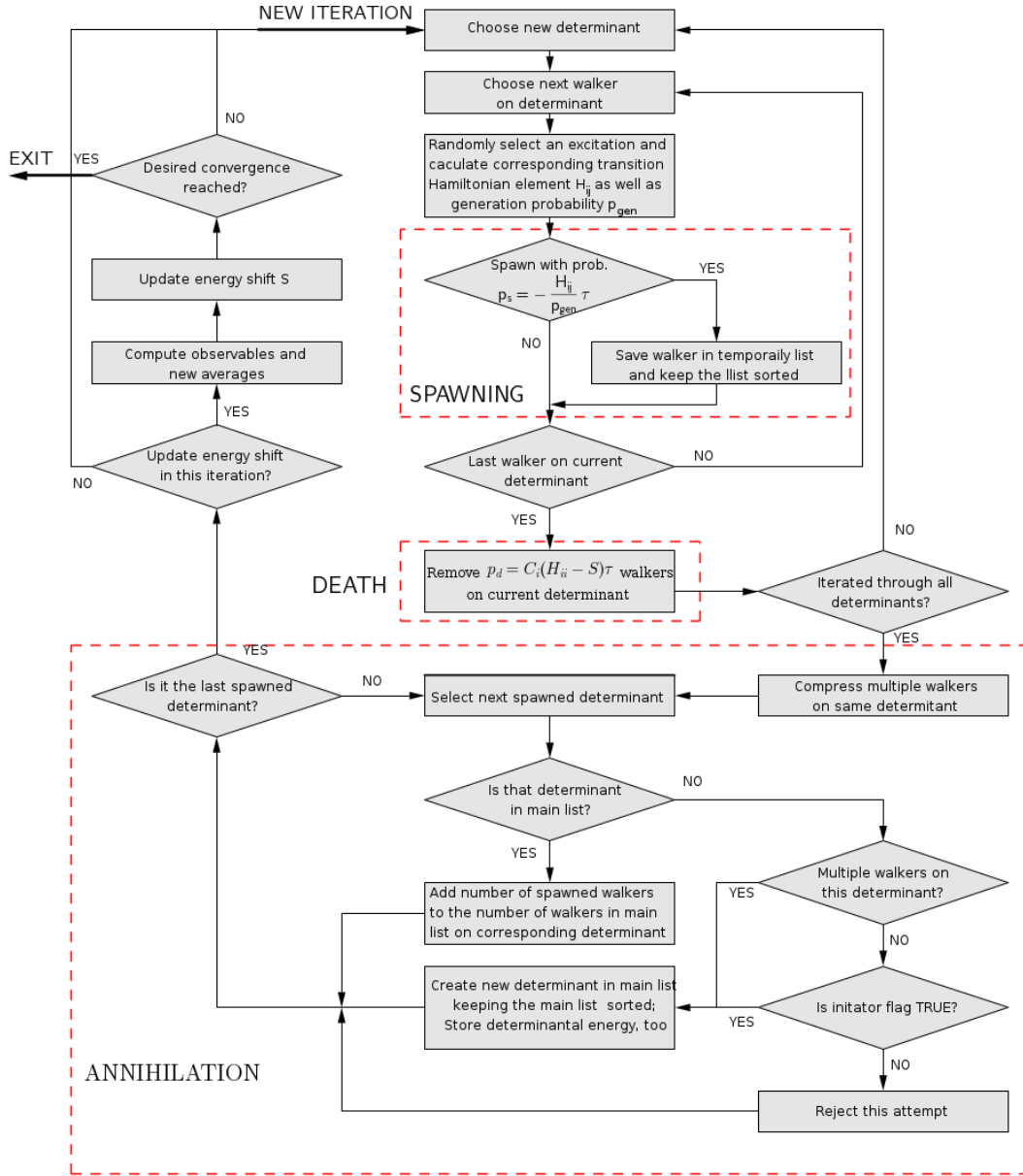


Figure 7.1: The flowchart of the FCIQMC algorithm. Spawning, death and annihilation steps are shown separately.

is system dependent and it will be discussed in more detail in the results section 7.9. Once the plateau in the number of walkers is reached, the simulation mode can be switched to the constant  $N$  mode. In this mode, the number of walkers should be kept constant and the energy shift  $S$  is allowed to vary by the following rule

$$S(\tau) = S(\tau - T\delta\tau) - \frac{\xi}{T\delta\tau} \ln \frac{N_w(\tau)}{N_w(\tau - T\delta\tau)}, \quad (7.13)$$

where  $\xi$  is a damping parameter, which is introduced to avoid large fluctuations in  $S$ . The damping factor has typical values of  $\xi \in [0.05, 0.5]$ . The integer value  $T$  in the previous equation indicates after how many time steps the energy shift  $S$  is updated. The usual value of this parameter is  $T \in [1, 10]$ . Note, if the current

number of walkers  $N_w(\tau)$  decreases in comparison to  $N_w(\tau - T\delta\tau)$ , the energy shift  $S(\tau)$  will increase compared to the old value  $S(\tau - T\delta\tau)$ . Increased energy shift values will cause a decrease of the overall death probability and one expects a growth of the number of walkers. If the number of walkers increases the shift will become more negative and the overall death probability will increase, causing again a stabilization of the total number of walkers  $N_w$ .

Clearly, the total energy of a system is the most important observable, obtainable in the FCIQMC simulation. Therefore, one needs to develop clever methods for the calculation of the total energy. As it was already mentioned in the last section, the energy shift  $S$  should stabilize on the value of the correlation energy for the exact coefficients  $C_i$ . Knowing the Hartree-Fock energy, the total energy can be computed, too. The correlation energy is obtained by the averaged  $S$  value during the constant  $N_w$  simulation mode. After each  $T$  steps, a new  $S$  value is added to the average. Our analysis procedure to obtain averages in the FCIQMC simulation will be discussed in the section 7.8 of this chapter. Although the energy shift provides a good measure of the total energy, one would highly appreciate other energy estimator that will converge to approximately the same value as the energy shift. In the spirit of statistical quantum mechanics, the energy expectation value of the exact ground state (7.1) could be written as

$$\frac{\langle \Phi | \hat{H} e^{-\tau \hat{H}} | \Phi \rangle}{\langle \Phi | e^{-\tau \hat{H}} | \Phi \rangle} = \frac{E e^{-\tau E} \langle \Phi | \Phi \rangle}{e^{-\tau E} \langle \Phi | \Phi \rangle} = E^{\text{FCI}}. \quad (7.14)$$

It is easy to see that the same energy value is obtained, if the energy is projected out onto the Hartree-Fock wave function instead of the exact FCI wave function:

$$\frac{\langle \Psi_0 | \hat{H} e^{-\tau \hat{H}} | \Phi \rangle}{\langle \Psi_0 | e^{-\tau \hat{H}} | \Phi \rangle} = \frac{E e^{-\tau E} \langle \Psi_0 | \Phi \rangle}{e^{-\tau E} \langle \Psi_0 | \Phi \rangle} = E^{\text{FCI}}. \quad (7.15)$$

Inserting (7.1) in the previous equation, the following energy expression is obtained for the current approximate solution  $|\Phi(\tau)\rangle$

$$E(\tau) = \frac{\langle \Psi_0 | \hat{H} e^{-\tau \hat{H}} | \Phi(\tau) \rangle}{\langle \Psi_0 | e^{-\tau \hat{H}} | \Phi(\tau) \rangle} = \frac{\langle \Psi_0 | \hat{H} | \Phi(\tau) \rangle}{\langle \Psi_0 | \Phi(\tau) \rangle} = \frac{\sum_i C_i(\tau) \langle \Psi_0 | \hat{H} | \Psi_i \rangle}{\sum_j C_j(\tau) \langle \Psi_0 | \Psi_j \rangle} = \sum_i \langle \Psi_0 | \hat{H} | \Psi_i \rangle \frac{C_i(\tau)}{C_0(\tau)}. \quad (7.16)$$

In order to adopt the obtained expression for the FCIQMC algorithm, equation (7.8) is used further to replace the coefficients  $C_i(\tau)$ . It can also be noted that the coupling matrix elements  $\langle \Psi_0 | \hat{H} | \Psi_i \rangle$  are non-zero only if the determinant  $|\Psi_i\rangle$  is equal to the reference state  $|\Psi_0\rangle$  or single or double excitations. The final version of the second energy estimator is therefore given by

$$E(\tau) = E_{\text{HF}} + \sum_{i \in \{S, D\}} \langle \Psi_0 | \hat{H} | \Psi_i \rangle \frac{N_i(\tau)}{N_0(\tau)} = E_{\text{HF}} + \sum_{i \in \{S, D\}} \bar{H}_{0i} \frac{N_i(\tau)}{N_0(\tau)}. \quad (7.17)$$

It is clear that if  $|\Phi(\tau)\rangle$  approaches the exact FCI wave function  $|\Phi\rangle$ , then  $E(\tau)$  approaches the exact FCI energy  $E^{\text{FCI}}$ . The two energy estimators  $S$  and  $E(\tau)$  are independent of each other, especially for large Slater spaces. This independence arises from the fact that  $E(\tau)$  is completely determined by a very small part of the

Slater space coupled to the Hartree-Fock determinant  $|\Psi_0\rangle$  and the energy shift  $S$  is a property of the total number of walkers and of the distribution of walkers over the whole Slater space.

### 7.3 Stability Criteria

In this section, the errors due to the imaginary time steps  $\delta\tau$  will be discussed. From the Euler-forward method that is used for the discretization of the Schrödinger equation, the equation (7.10) can be recast in vector notation as

$$N(\tau + \delta\tau) = (\mathbb{1} - \delta\tau(\bar{H} - S\mathbb{1})) N(\tau), \quad (7.18)$$

where the amplification matrix  $G$  can be read off immediately

$$G = \mathbb{1} - \delta\tau(\bar{H} - S\mathbb{1}). \quad (7.19)$$

To ensure the stability of the numerical algorithm, the spectrum of the amplification matrix must have absolute values smaller than 1. This condition is simply given by

$$-1 \leq \lambda_G = 1 - \delta\tau(\lambda_{\bar{H}} - S) \leq 1, \quad (7.20)$$

where  $\lambda_A$  denotes the eigenvalue of corresponding matrix  $A$ . Taking into account that the minimal eigenvalue of the matrix  $\bar{H}$  is  $E_{\text{corr}}^{\text{FCI}}$  and let the largest eigenvalue be  $\bar{E}_{\text{max}}$ , the previous condition can be rewritten in a simpler form

$$\delta\tau \leq \frac{2}{\bar{E}_{\text{max}} - E_{\text{corr}}^{\text{FCI}}} \quad (7.21)$$

Because the true eigenvalues are not known, in the first approximation  $E_{\text{corr}}^{\text{FCI}}$  can be replaced by  $S$  or the energy estimator  $E(\tau)$  and the best approximation of  $\bar{E}_{\text{max}}$  would be the largest diagonal value of  $\bar{H}$ .

The obtained restriction on the time step is a direct consequence of applying a simple integration method for the initial value problem. There is also the second restriction, arising from the algorithmic rules explained in 7.1. Namely, if the spawning probability (7.11) is much larger than 1, multiple walkers are spawned on certain determinants with a probability of 100% and that could lead to inefficient sampling of the Slater space. Therefore, the time step should be chosen in such a way that  $p_s$  is near unity most of the time. Reported values of  $\delta\tau$  lie in the range of  $[10^{-4} - 10^{-3}]$ a.u. [44]. Of course, for larger Slater spaces, smaller time steps must be used in order to converge to the exact ground state. It will become obvious in section 7.9 that the value of the correlation energy is not influenced by the value of the time step, as long as they are in the above mentioned range. More details will be provided in the result section.

### 7.4 Sampling Rules

As it was mentioned in the description of the algorithm, to be able to calculate spawning probability between two connected Slater determinants, the generation

probability of the excited state  $|\Psi_j\rangle$  from the reference state  $|\Psi_i\rangle$  is needed. Assuming at the beginning that one starts with  $|\Psi_i\rangle$  and ends with the singly excited state  $|\Psi_j\rangle = \hat{a}_q^\dagger \hat{a}_p |\Psi_i\rangle$ , where it is clear that both operators have to belong to the same spin, the generation probability can be written in the form

$$p_{\text{gen}}^\sigma(j|i) = p_1 p_{\text{gen}}^\sigma(q|p) p_{\text{gen}}(p), \quad (7.22)$$

where  $p_1$  reflects the ratio between the number of single and double excitation. In most cases, the number of single excitations is quite small in comparison to the number of double excitations and  $p_1$  should be a small number near to 0 and then the probability to draw a double excitation is simply  $p_2 = 1 - p_1$ . Probabilities  $p_1$  and  $p_2$  could also be chosen in an approximate way, and it will suffice, as long as the sum of these two probabilities is 1. It is found that the FCIQMC algorithm converges for a wide range of chosen  $p_1$ , but with longer simulation time needed for larger  $p_1$ . The probability  $p_{\text{gen}}(p)$  is simply the reciprocal value of the total number of electrons

$$p_{\text{gen}}(p) = \binom{N_e}{1}^{-1} = \frac{1}{N_e}, \quad (7.23)$$

but the conditional probability  $p_{\text{gen}}^\sigma(q|p)$  is already restricted to certain orbitals by the choice of  $p$ . The spin of the orbital  $q$  must be equal to the spin of the orbital  $p$  and if the point group symmetry of the underlying system is exploited, then the irreducible representation of both orbitals must be equal, i.e  $\Gamma_q = \Gamma_p$ . The conditional probability  $p_{\text{gen}}(q|p)$  is then simply given as the reciprocal value of the number of available orbitals with predetermined spin  $\sigma$  and irreducible representation  $\Gamma_p$ . If the point group symmetry is not exploited, the generation probability simplifies to

$$p_{\text{gen}}^\sigma(j|i) = p_1 \cdot \binom{N_e}{1}^{-1} \binom{P - N_\sigma}{1}^{-1}, \quad (7.24)$$

where  $N_\sigma$  is the number of electrons with particular spin  $\sigma$ .

Let us now turn to the double excitations. From the reference state  $|\Psi_i\rangle$  one can create doubly excited states  $|\Psi_j\rangle = \hat{a}_r^\dagger \hat{a}_s^\dagger \hat{a}_q \hat{a}_p |\Psi_i\rangle$ . The generic expression for the generation probability of double excitations is given by

$$p_{\text{gen}}^{\sigma\sigma'}(j|i) = p_2 p_{\text{gen}}^{\sigma\sigma'}(r, s|p, q) p_{\text{gen}}(p, q), \quad (7.25)$$

where  $p_{\text{gen}}(p, q)$  is the probability to draw two orbitals  $p$  and  $q$  and it is given by

$$p_{\text{gen}}(p, q) = \binom{N_e}{2}^{-1}. \quad (7.26)$$

The remaining part can be calculated from the following relation:

$$p_{\text{gen}}(r, s|p, q) = p_{\text{gen}}(r|s, p, q) p_{\text{gen}}(s|p, q) + p_{\text{gen}}(s|r, p, q) p_{\text{gen}}(r|p, q), \quad (7.27)$$

which is adopted for the exploitation of point group symmetry. In this relation, the order in which orbitals  $r$  and  $s$  are drawn is important. The first term gives the probability that  $s$  is drawn before  $r$  and vice versa. The probability  $p_{\text{gen}}(r|p, q)$  is simply the reciprocal number of the available orbitals with the spin equal to one of the

orbitals  $p$  or  $q$ . The spin of the last orbital  $r$  that has to be drawn is already determined and the irreducible representation of the orbital  $r$  is given by  $\Gamma_r = \Gamma_s \otimes \Gamma_q \otimes \Gamma_p$ . The conditional probability  $p_{\text{gen}}(r|s, p, q)$  is then given by the reciprocal value of the number of orbitals with predetermined spin and irreducible representation  $\Gamma_r$ . In case when symmetry information is used, the summands from the last equation are in general not equal, but if the point group symmetry is not exploited, the generation probability simplifies to

$$p_{\text{gen}}^{\sigma\sigma'}(j|i) = p_2 \cdot \binom{N_e}{2}^{-1} \left[ \delta_{\sigma\sigma'} \binom{P - N_\sigma}{2}^{-1} + (1 - \delta_{\sigma\sigma'}) \binom{P - N_\sigma}{1}^{-1} \binom{P - N_{\sigma'}}{1}^{-1} \right], \quad (7.28)$$

where two different terms arise because of two spin possibilities - same and opposite spins. The probabilities chosen in this way have to be normalized, i.e.

$$\sum_i p_{\text{gen},i} \cdot N_i = 1, \quad (7.29)$$

where the number  $N_i$  denotes the total number of possible excitations with corresponding probabilities  $p_{\text{gen},i}$ .

## 7.5 Initiator Quantum Monte Carlo Configuration Interaction - iFCIQMC

In the initiator approach, one tries to find a method which will be able to reduce the required number of walkers but to keep the accuracy of the simulation unchanged. The so-called initiator approach was a simple and successful extension of the original method that was able to achieve this goal. In the initiator method, only certain determinants are able to spawn walkers on the still unpopulated determinants and they are called initiators. That means that all non-initiator determinants are only able to spawn walkers on already populated determinants. Effectively, this extension of the code restricts the Slater space to the space of initiators and their single and double excitations. In this sense, the initiator approach is the approximation of the FCIQMC method, equivalent to the CAS and RAS extensions of the deterministic counterparts with iterative diagonalization procedures. The advantage of the initiator method is that the initiator space is allowed to grow dynamically. At the beginning of the simulation, initiators are the only determinants for which one knows in advance that they will have large amplitudes  $C_i$  in the final wave function. In most cases, the starting initiator space is chosen as CAS space  $(n, m)$ . In the CAS method, the Hilbert space is partitioned into three groups:

- **Frozen Core:** consisting of  $N_e - n$  electrons doubly occupied in  $\frac{N_e - n}{2}$  lowest lying orbitals, assumed to be strongly bound and exhibits little fluctuations.
- **Active Space:** Additional  $n$  electrons distributed over the next  $m$  orbitals.
- **Virtual Space:** The remaining  $P - m$  unoccupied orbitals.

The dynamic of the initiator space is achieved with an additional rule, which states that each non-initiator determinant becomes an initiator, if the number of walkers on this determinant exceeds a predetermined number  $n_a$ . In this way, the initiator approach is fully defined with parameters  $(n, m)_{n_a}$ . In the case  $(n, m)_{n_a \rightarrow 0}$  all determinants will become initiators and the initiator FCIQMC will approach the exact FCIQMC method. The interesting situation is also  $(n, m)_{n_a \rightarrow \infty}$ , where the initiator space will remain constant during the whole simulation and only initiators and their excitations would be populated with walkers. To summarize, all rules of the initiator approach are listed below:

- Initial initiator space: CAS space  $(n, m)$  with  $n$  electrons distributed over  $m$  orbitals.
- Spawning rule: Initiator determinants are able to spawn walkers on all determinants as it was the case in the original FCIQMC algorithm. Non-initiators can spawn walkers on other determinants, only if those determinants are already populated.
- Spawning rule - extension: If two non-initiators try to spawn walkers of the same sign on the same unpopulated determinant, this spawning event will be accepted, because this is assumed to be a sign coherent event.
- Initiator space enlargement: Each non-initiator determinant will become initiator, if the number of walkers exceeds predefined number  $n_a$ .

## 7.6 Technical Details of FCIQMC Algorithm

All newly developed algorithms must be implemented in such a way that modern computer architectures are exploited in an efficient manner. The two most important properties are efficient memory usage and high parallelization of the algorithm. As it was already discussed in the previous chapter, the Slater space for all but the most modest systems is enormous, and therefore, all CI simulations can easily run out of memory. If the algorithm is performed in such a way that one  $M$ -byte integer is reserved for each Slater determinant, this is highly undesirable because the memory requirements in this case are  $N_{\text{det}} \cdot M$  bytes. In the case of the H<sub>2</sub>O molecule ( $N_e = 10$ ) in the cc-pVDZ basis set, the total memory required to store all information about walkers would be 6.74 Gb of RAM memory. Although this can be achieved with today's computers, the situation changes for the cc-pVTZ basis set, where 58 orbitals are used to describe a water molecule, where the total memory requirements amount to 76.4 Tb of RAM and this number exceeds the RAM memory capacity of most today's computer architectures. Therefore, the algorithm must be implemented in a way that variables are initialized only for the determinants where walkers are already populated. Here, the system defined parameter  $\gamma$  introduced in section 7.2 plays a significant role, because memory requirements are reduced by a factor  $\gamma$ . The initiator method is important exactly for these reasons, because it contributes to the reduction of the  $\gamma$  parameter.

The second property that becomes progressively important with modern computer architectures is the parallelization of the numerical algorithms. The FCIQMC

algorithm is very suitable for the parallelization with MPI and OpenMP, like all Monte Carlo algorithms. The two algorithmic steps described in 7.1 can be realized independently from other walkers, i.e. the parallelization can be done without communication overhead. The third step of the algorithm, walker list merging and the annihilation, is the only part that must be done with communication overhead. To summarize, the most efficient way to perform FCIQMC is to use dynamical variables and to use 2-byte integers for the initial initiator space and 1-byte integers for other populated determinants. In this way, the most efficient memory usage is achieved. To be able to have efficient parallelization, all cores should have fast access to all two-electron integrals ( $pqrs$ ), but at the same time the replication of integrals on all cores is undesirable. The walker list is on the other hand distributed among cores and the cores communicate with each other in the annihilation step.

## 7.7 Fermion Sign Problem in FCIQMC

The Fermion sign problem arises from Pauli exclusion principle and causes exponential growth of statistical errors in Monte Carlo sampling methods. In a quantum system with Hamiltonian operator  $\hat{H}$ , the expectation value of some observable  $\hat{O}$  is then given by

$$\langle \hat{O} \rangle = \frac{1}{Z} \text{Tr}[\hat{O} \exp(-\beta \hat{H})] ; \quad Z = \text{Tr}[\exp(-\beta \hat{H})]. \quad (7.30)$$

where  $Z$  is the partition function. In order to evaluate the last expression, the Taylor expansion of the exponential function is needed to obtain

$$Z = \sum_{n=0}^{\infty} \sum_{i_1 \dots i_n} \frac{(-\beta)^n}{n!} \langle i_1 | \hat{H} | i_2 \rangle \dots \langle i_n | \hat{H} | i_1 \rangle = \sum_j p(j). \quad (7.31)$$

Analogously, the expression for the expectation value of an observable becomes

$$\langle \hat{O} \rangle = \frac{1}{Z} \sum_j p(j) \hat{O}(j) = \frac{\sum_j p(j) \hat{O}(j)}{\sum_j p(j)}, \quad (7.32)$$

where  $j$  stands for one configuration of the system ( $i_1, i_2 \dots i_n$ ) and the corresponding sum run over all configurations, where  $M$  is the number of configurations. If two configurations  $j_1 = (i_1 \dots i_p \dots i_q \dots i_n)$  and  $j_2 = (i_1 \dots i_q \dots i_p \dots i_n)$  interchange particles  $i_p$  and  $i_q$ , the corresponding weights  $p(j_1)$  and  $p(j_2)$  differ by sign. Therefore, the standard Monte Carlo methods can not be applied. The alternative way to treat this expectation is to introduce a sign for the configuration  $s(j) = \text{sign}[p(j)]$  and, thus, one obtains

$$\langle \hat{O} \rangle = \frac{\sum_j \hat{O}(j) s(j) |p(j)|}{\sum_j s(j) |p(j)|} = \frac{\langle \hat{O} s \rangle'}{\langle s \rangle'}, \quad (7.33)$$

where  $'$  stands for the expectation value with respect to weights  $|p(j)|$ , i.e. with respect to the partition function  $Z' = \sum_j |p(j)|$ . Note that the ratio between two partition functions can be written in terms of the free energy difference as  $Z/Z' = \exp(-\beta N \Delta f)$ . However, at the same time, applying the relation (7.33), one finds

that  $\langle s \rangle = \sum_j s(j)|p(j)| / \sum_j |p(j)| = Z/Z'$ . The relative error of the sign variable  $s$  is at the end

$$\frac{\Delta s}{\langle s \rangle} = \frac{\sqrt{\frac{\langle s^2 \rangle - \langle s \rangle^2}{M}}}{\langle s \rangle} = \frac{\sqrt{1 - \langle s \rangle^2}}{\sqrt{M} \langle s \rangle} \propto \frac{1}{\sqrt{M} \langle s \rangle} = \frac{e^{\beta N \Delta f}}{\sqrt{M}}. \quad (7.34)$$

The last expression exactly expresses the Fermion sign problem, where one notes that the relative error of the expectation value grows exponentially with the number of particles and with temperature. Let us now turn to the manifestation of the Fermion sign problem in the FCIQMC algorithm. From the equation for the evolution of the walker population (7.10,7.18), the transition matrix can be defined and divided into positive and negative parts as

$$T_{ij} = -(\bar{H}_{ij} - S\delta_{ij}) = T_{ij}^+ - T_{ij}^-, \quad (7.35)$$

with  $T_{ij}^+ = \max(T_{ij}, 0)$  and  $T_{ij}^- = |\min(T_{ij}, 0)|$ . After that, the change of walker distribution in one timestep  $\delta\tau$  can be recast in two parts

$$\begin{aligned} \Delta N_i^+ &= \delta\tau \sum_j (T_{ij}^+ N_j^+ + T_{ij}^- N_j^-), \\ \Delta N_i^- &= \delta\tau \sum_j (T_{ij}^- N_j^+ + T_{ij}^+ N_j^-). \end{aligned} \quad (7.36)$$

Adding and subtracting the latter equations, the following result can be obtained:

$$\begin{aligned} \Delta(N_i^+ + N_i^-) &= \delta\tau \sum_j (T_{ij}^+ + T_{ij}^-)(N_j^+ + N_j^-), \\ \Delta(N_i^+ - N_i^-) &= \delta\tau \sum_j (T_{ij}^+ - T_{ij}^-)(N_j^+ - N_j^-). \end{aligned} \quad (7.37)$$

Through this last transformation, a set of two independent linear differential equations is obtained for the two variables  $N^+$  and  $N^-$ . The stationary solutions of these equations are simply the lowest lying eigenvalues of the corresponding projection operators

$$\begin{aligned} P^+ &= \mathbb{1} + (T^+ + T^-), \\ P^- &= \mathbb{1} + (T^+ - T^-) = \mathbb{1} - (\bar{H} - S\mathbb{1}). \end{aligned} \quad (7.38)$$

Note that the eigenvalue of the projector  $P^-$  is exactly the same as the amplification matrix of the FCIQMC algorithm (7.19), and therefore, the eigenstate of the operator  $P^-$  is exactly the desired solution of the FCIQMC problem. For this reason, the algorithm should follow the evolution of the variable  $N^+ - N^-$ , which is achieved by introducing the annihilation step in the algorithm, where walkers with opposite sign on the same determinant are removed from the simulation (see section 7.1). The Fermionic sign problem arises from the fact that  $\lambda^+ \geq \lambda^-$  (lowest lying eigenvalues of projectors  $P^+$  and  $P^-$  respectively). This is proven by Spencer [56], where more details about this derivation and Fermion sign problem in FCIQMC can be found. Thus, if the annihilation is not performed, the population of  $N^+ + N^-$  will become

exponentially larger than  $N^+ - N^-$  and the latter variable will be totally lost in the statistical noise of the former one. To summarize, the Fermionic problem in the FCIQMC method arises as a consequence of the relation  $\lambda^+ \geq \lambda^-$ , where the desired solution corresponds to  $\lambda^-$  (walker growth of  $N^+ \pm N^-$  is proportional to  $\lambda^\pm$ ). Systems with a larger gap between  $\lambda^+$  and  $\lambda^-$  become progressively more difficult to be simulated using the FCIQMC algorithm, because a larger number of walkers is needed to be able to perform annihilation.

## 7.8 Statistical Error Analysis in FCIQMC Algorithm

As in all Monte Carlo simulations, the expectation values of the observables and their statistical errors are very important. In the FCIQMC algorithm, one is interested in obtaining precise statistical errors of the energy shift  $S$  and of the projected energy  $E(\tau)$  (see section 7.2). Assume, in general, that some function  $f$  is evaluated for each random variable  $x_i$  ( $f(x_i) \equiv f_i$ ), which is drawn from the distribution  $\rho(x)$ . Then, the estimator of the mean value of  $f$  is given by

$$\bar{f} = \frac{1}{N} \sum_{i=1}^N f_i \quad (7.39)$$

If the ergodicity is assumed, then

$$\lim_{n \rightarrow \infty} \bar{f} = \langle f \rangle, \quad \text{where } \langle f \rangle = \int dx \rho(x) f(x) \quad (7.40)$$

the estimator (7.39) becomes a true ensemble average in the limit of large sampling data. For finite numbers  $n$ , there is some statistical error of  $\bar{f}$  denoted as  $\sigma$ , which is estimated as the standard deviation of  $\bar{f}$

$$\sigma = \sqrt{\langle \bar{f}^2 \rangle - \langle \bar{f} \rangle^2}. \quad (7.41)$$

Combining equations (7.39) and (7.41) and introducing the correlation function

$$\gamma_{ij} \equiv \gamma_{|i-j|} = \gamma_t = \langle f_i f_j \rangle - \langle f_i \rangle \langle f_j \rangle, \quad (7.42)$$

one arrives to the following expression for the statistical error of  $\bar{f}$ :

$$\sigma^2 = \frac{\gamma_0}{N} + \frac{2}{N^2} \sum_{t=1}^{N-1} (N-t) \gamma_t \quad (7.43)$$

For uncorrelated data sets  $\gamma_t = 0, \forall t \neq 0$ , the previous expression simplifies to  $\sigma = \sqrt{\gamma_0/N}$ , but in FCIQMC method, the data sets are strongly correlated and the correlation function can not be neglected. In these situations, one performs either the Flyvbjerg-Petersen error analysis [57, 58] or the block averaging [58, 59]. Both methods will be explained below, especially because the statistical error of  $S$  is most easily calculated by Flyvbjerg-Petersen analysis, while the block averaging is far more

suitable for the error analysis of the projection approximation  $E(\tau)$ . In the Flyvbjerg-Petersen analysis, one starts with a set of values  $\{S_1, S_2 \dots S_N\}$ . This set of data is then transformed according to the following linear transformation

$$\begin{aligned} S_i^{(m)} &= \frac{1}{2}(S_{2i-1}^{(m-1)} + S_{2i}^{(m-1)}); \\ N^{(m)} &= \frac{1}{2}N^{(m-1)} = \frac{1}{2^m}N. \end{aligned} \quad (7.44)$$

What is special about the last equations is the fact the mean value and the variance are invariant under this transformation ( $\bar{S}^{(m)} = \bar{S}^{(m-1)}$ ,  $\sigma_{\bar{S}}^{(m)} = \sigma_{\bar{S}}^{(m-1)}$ ). In this way, the data set is halved in each iteration and therefore, the correlation between data becomes smaller and the estimator of variance  $\gamma_0^{(m)}/N^{(m)}$  becomes larger in each iteration and converges to some value. This value is then taken as an estimator for the statistical error of the energy shift and the result from the simulations is then  $S = \bar{S} \pm \sigma_{\bar{S}}$ , with

$$\begin{aligned} \bar{S} &= \frac{1}{N} \sum_{i=1}^N S_i \quad \text{and} \\ \sigma_{\bar{S}} &= \frac{\gamma_0^{(m)}}{\sqrt{N^{(m)}}} = \frac{\gamma_0^{(m)}}{\sqrt{N/2^m}}. \end{aligned} \quad (7.45)$$

In the case of the projection energy (7.17), the situation is more complicated. This problem arises, because the projected energy depends on two random variables  $H_\tau$  and  $w_\tau$  :

$$E(\tau) \equiv E_\tau = \frac{\sum_{i \in \{S, D\}} H_{0i} N_i^{(\tau)}}{N_0^{(\tau)}} \equiv \frac{H^{(\tau)}}{w_\tau}. \quad (7.46)$$

Therefore, the mean value of the projected energy is given by the following expression

$$\bar{E}_\tau = \frac{\bar{H}}{\bar{w}} = \frac{\frac{1}{N} \sum_i H_i}{\frac{1}{N} \sum_i w_i} = \frac{\sum_i H_i}{\sum_i w_i}, \quad (7.47)$$

where  $N = \tau/\delta\tau$ . Therefore, the Flyvbjerg-Petersen analysis can not be applied in its original form as it was presented above. The second method is used instead. The set of  $N$  data points  $\{H_1, H_1 \dots H_N\}$  is divided in chunks of size  $b$ , so that  $n = N/b$ . After the data has been divided in blocks, the mean value can be computed for each block

$$\bar{H}_i = \frac{1}{b} \sum_{j=(i-1)b+1}^{ib} H_j, \quad i = 1, 2 \dots n, \quad (7.48)$$

and similarly  $\bar{w}_i$  can be calculated. Then, the mean value of the energy can be rewritten as

$$\bar{E}_\tau = \frac{1}{n} \sum_i \frac{\bar{H}_i}{\bar{w}_i} + \delta_b, \quad (7.49)$$

where the error  $\delta_b$  is small and decreases further with increasing blocksize  $b$  and therefore, when the fluctuations of  $\delta_b$  become smaller than the fluctuations of  $\bar{E}_\tau$ , the set of data  $\{\bar{H}_1/\bar{w}_1 \dots \bar{H}_n/\bar{w}_n\}$  can be treated as single stochastic variable. The

error estimator can be found as the standard deviation of the above mentioned set of data. It should be noted that the error of the projection energy in this case increases with blocksize  $b$ , and the final value is taken from the blocksize where the standard deviation stabilizes.

## 7.9 Calculations with FCIQMC Method

The goal of this section is not a repetition of the results obtained in the previous chapter using the direct FCI method, but rather the systematic investigation of the FCIQMC code. For this purpose, the  $\text{BeH}_2$  molecule at cc-pVTZ level will be considered.

First, the convergence of the FCIQMC procedure due to the timestep  $\delta\tau$  will be considered. Corresponding results are shown in table 7.1. It is obvious that the CPU time depends strongly on the value of timestep. Too small values must be avoided, because the time evolution is slow. The optimal value of the timestep is found to be  $\delta\tau = 0.01$ , where the convergence is obtained in less than 1h. For too large values of  $\delta\tau$ , the sampling becomes incorrect leading to the wrong total energies. For timesteps chosen in this series of calculations, total energies converge to the correct value which was already obtained with direct CI in the section 6.6.

Table 7.1: Results of FCIQMC method obtained for various timesteps  $\delta\tau$ . The values  $\gamma = 0.05$  and  $p_1 = 0.1$  were used.

$\delta\tau$	0.0005	0.001	0.002	0.005	0.01	0.02
$E_{\text{corr}}^{\text{FCI}} (10^{-2}\text{a.u.})$	-6.908	-6.904	-6.907	-6.908	-6.909	-6.909
CPU time (h)	9.5	5.1	2.4	1.4	1.0	2.4
Direct FCI correlation energy $E_{\text{corr}}^{\text{FCI}} = -6.908 \cdot 10^{-2}$ a.u.						

Probably the most important parameter for the FCIQMC procedure, the  $\gamma$  value, will now be considered. This parameter determines the number of walkers needed for obtain the exact FCI ground state. This value is system dependent and small values are highly desirable. The FCIQMC energies of the  $\text{BeH}_2$  molecule in dependence on different  $\gamma$  values are presented in the table 7.2. Note that for  $\gamma = 0.0001$  the procedure did not converge and reasonable results can not be obtained. However, this could be expected, because the total number of walkers in the simulation was roughly 400, and these 400 walkers must be distributed on  $4 \cdot 10^6$  determinants. In this mode, there is also a high probability that the Hartree-Fock determinant remains without walkers and then the total energy can not be obtained from (7.17) anymore. Furthermore, no weight on the Hartree-Fock determinant is totally unreasonable. With increasing  $\gamma$ , the correlation energy becomes more precise, but the CPU time increases at the same time. At  $\gamma = 0.05$ , the correlation energy did not differ significantly from the value obtained with the direct FCI method. 2.4 h were needed to converge on this particular value. Therefore, it can be concluded that  $\gamma = 0.05$  for the  $\text{BeH}_2$  molecule, or in other words,  $2 \cdot 10^5$  walkers were needed to predict the exact FCI ground state. It is worth to mention that,

already at  $\gamma = 0.005$ , the correlation energy differ only by 0.4% from the exact value and the CPU time needed to obtain that result was only 20 minutes.

Table 7.2: FCIQMC results for various  $\gamma$  values. The values  $\delta\tau = 0.002$  and  $p_1 = 0.1$  were used.

$\gamma$	0.0001	0.0005	0.001	0.005	0.01	0.05	0.1	0.5	1.0	2.0
$E_{\text{corr}}^{\text{FCI}} (10^{-2}\text{a.u.})$	-	-6.922	-6.872	-6.933	-6.914	-6.907	-6.907	-6.909	-6.908	-6.908
CPU time (h)	-	0.05	0.10	0.34	0.58	2.4	5.2	9.0	7.1	16.9

Direct FCI correlation energy  $E_{\text{corr}}^{\text{FCI}} = -6.908 \cdot 10^{-2}$  a.u.

Furthermore, the total energy and the CPU time needed for the convergence of the FCIQMC algorithm in dependence of the parameter  $p_1$  will be considered. For this purpose, a series of simulations with different parameters  $p_1$  were executed. The timestep  $\delta\tau = 0.002$  and the parameter  $\gamma = 0.05$  will be used in these calculations. The results are presented in the table 7.3. It is obvious that all calculations converge to the same energy value and it does not depend on the parameter  $p_1$  as long as the condition  $p_1 + p_2 = 1$  is fulfilled. For these calculations, the CPU time does not depend significantly on the parameter  $p_1$ . However, larger values of the parameter  $p_1$  show better statistics. Such a behavior is also mentioned in other publications [58]. To make these time measurements significant, it must be noted that all calculations are executed on a single core (lx-AMD64).

Table 7.3: Total FCI energies and CPU time needed for the convergence of the FCIQMC algorithm for various  $p_1$  values for the example of the BeH<sub>2</sub> molecule at cc-pVTZ level. The simulations are done for  $\gamma = 0.05$  and  $\delta\tau = 0.002$ . Note that the first value of the  $p_1$  parameter is the ratio between the number of single excitations and total number of excitations.

$p_1$	0.0235	0.1	0.3	0.5	0.7	0.9
$E_{\text{corr}}^{\text{FCI}} (10^{-2}\text{a.u.})$	-6.905	-6.907	-6.909	-6.909	-6.907	-6.909
CPU time (h)	2.8	2.4	3.4	3.0	2.6	2.4

Direct FCI correlation energy  $E_{\text{corr}}^{\text{FCI}} = -6.908 \cdot 10^{-2}$  a.u.

In the end, the total energies obtained with FCIQMC on BeH<sub>2</sub> molecule for various basis sets and corresponding Slater space sizes are listed (table 7.4).

Table 7.4: Total FCIQMC energies and corresponding Slater space sizes of BeH<sub>2</sub> for different basis sets.

	6-31G++	cc-pVDZ	aug-cc-pVDZ
$E^{\text{FCI}} (\text{a.u.})$	-15.831	-15.836	-15.840
$\mathcal{S}$	$4 \cdot 10^6$	$4 \cdot 10^6$	$9 \cdot 10^9$

# Chapter 8

## Conclusion

The main goal of this thesis was the implementation of the configuration interaction method, which gives one the ability to calculate exact correlation effects within a given basis set. In order to be able to test FCI calculations on molecular systems, Gaussian basis functions as well as calculation of one- and two-electron integrals were implemented. McMurchie scheme was used for the integral evaluation. After the integrals were obtained, the Hartree-Fock method was implemented as a starting point for FCI calculation. Three different models of the Hartree-Fock theory were implemented: restricted closed-shell Hartree-Fock (RHF), unrestricted open-shell Hartree-Fock (UHF) and restricted open-shell Hartree-Fock ROHF. Based on these ground state calculations, FCI calculations can be performed. First, the direct configuration interaction method with an iterative diagonalization procedure was implemented, which is able to handle systems up to  $10^8$  Slater determinants and to calculate not only the ground state of the system, but the excited states, too. On the other hand, the full configuration quantum Monte Carlo method (FCIQMC) was implemented. It allows calculations on larger systems (up to  $10^{10}$  Slater determinants). The main disadvantageous is that the FCIQMC method does not allow the calculation of excited states. There are density matrix extensions of FCIQMC code that allow the calculations of excited states, too. However, they were not considered in this work. Using the code, it is possible to calculate one- and two-electron FCI density matrices and thereby one is capable of calculating natural orbitals, too. The possibility of density matrix calculations provides an opportunity of applying the code in density matrix embedding theory (DMET). The code could also be applied as impurity solver in dynamical mean field theory (DMFT) or it can be simply used for direct calculations in small molecular or solid systems.

In this work, all implementations were tested on small molecular systems showing the limits of success of the corresponding methods. RHF theory provides reasonable results for total energy of systems, especially at equilibrium geometries. Due to the statical correlation effects on stretched configurations, RHF theory fails totally in the description of the dissociation of molecules. For the simplest systems, UHF solution can solve the problem of dissociation, but it does not provide a systematic solution of the problem. The orbital energy levels obtained on the Hartree-Fock level can be used as a qualitative description. However, for the accurate quantitative results of excitation energies, more accurate methods are needed. Additionally,

Koopman's theorem provides a reasonable prediction of ionization energies, but simultaneously it gives totally incorrect results for electron affinity values. MP2 theory improves the total energy values by retrieving a fraction of the correlation energy, but it does not provide substantially better wave functions. On the other hand, configuration interaction provides exact correlation energies and it can be used to predict correct dissociation effects, as well as better estimation of the ionization potential and the electron affinities. The same results were obtained using FCIQMC method, as with the direct CI method with the additional advantage of the possibility for handling larger systems. Instead of repeating all the results that were obtained using the direct CI method, properties of the FCIQMC method were systematically studied on the example of the BeH<sub>2</sub> molecule.

In the end, there is a lot of work to be done in the future until the code is ready to be implemented in VASP. Further development of the FCIQMC method, as well as parallelization of the code will be greatly appreciated. In order to proceed with investigations on solids, the DMET or DMFT loop should also be implemented. Such implementations will be subject of further work.

# APPENDICES

# Appendix A

## Variational Theorem

The variational problem is one of the most popular theorems in physics. For a given Hamiltonian  $\hat{H}$  and for a set of basis functions  $|\Psi_i\rangle$ , it gives the best possible approximation of a ground state. Denote an energy functional  $E[\Phi]$  that is defined as an expectation value of the corresponding Hamiltonian

$$E[\Phi] = \langle \Phi | \hat{H} | \Phi \rangle. \quad (\text{A.1})$$

To find the best possible approximation for  $\Phi$ , one requires that the variation of the functional disappears:

$$\delta E = \delta \langle \Phi | \hat{H} | \Phi \rangle = \langle \delta \Phi | \hat{H} | \Phi \rangle + \langle \Phi | \hat{H} | \delta \Phi \rangle = 0. \quad (\text{A.2})$$

In a given basis the best linear approximation is

$$|\Phi\rangle = \sum_i c_i |\Psi_i\rangle, \quad (\text{A.3})$$

With an additional constraint, that the wave function is normalized  $\langle \Phi | \Phi \rangle = 1$ , one uses the method of Lagrange multipliers in order to minimize the total energy. The Lagrange function is

$$\begin{aligned} \mathcal{L} &= \langle \Phi | \hat{H} | \Phi \rangle - E(\langle \Phi | \Phi \rangle - 1) \\ &= \sum_{ij} c_i^* c_j \langle \Psi_i | \hat{H} | \Psi_j \rangle - E \left( \sum_{ij} c_i^* c_j \langle \Psi_i | \Psi_j \rangle \right), \end{aligned} \quad (\text{A.4})$$

where  $E$  is the total energy of a system, i.e. the Lagrange multiplier. To find the best coefficients  $c_i$ , the variation of the Lagrange function has to be zero.

$$\delta \mathcal{L} = \sum_{ij} (\delta c_i^* c_j + c_i^* \delta c_j) \langle \Psi_i | \hat{H} | \Psi_j \rangle - E \sum_{ij} (\delta c_i^* c_j + c_i^* \delta c_j) \langle \Psi_i | \Psi_j \rangle = 0. \quad (\text{A.5})$$

Assuming the energy  $E$  is real and the Hamiltonian is a Hermitian operator, collecting terms with  $\delta c_i^*$  with the fact that indices  $i$  and  $j$  are interchangeable, yields to:

$$\sum_i \delta c_i^* \left( \sum_j \langle \Psi_i | \hat{H} | \Psi_j \rangle c_j - E \sum_j \langle \Psi_i | \Psi_j \rangle c_j \right) + \text{c.c.} = 0 \quad (\text{A.6})$$

Defining the Hamiltonian and overlap matrix as usual

$$\langle \Psi_i | \hat{H} | \Psi_j \rangle = H_{ij} , \quad \langle \Psi_i | \Psi_j \rangle = S_{ij}, \quad (\text{A.7})$$

yields a system of linear equations, that can be written as

$$\sum_j H_{ij} c_j = E \sum_j S_{ij} c_j, \quad (\text{A.8})$$

or even simpler in the matrix notation as

$$H\mathbf{c} = E S\mathbf{c}. \quad (\text{A.9})$$

The vector  $\mathbf{c}$  is simply the vector of coefficients  $c_i$ . The previous equation is simply a generalized eigenvalue problem and its lowest eigenvalue is the best approximation and the upper limit of the true Hamiltonian eigenvalue  $\mathcal{E}_0$  in the space spanned by the basis  $|\Psi_i\rangle$ :

$$E = \frac{\langle \Phi | \hat{H} | \Phi \rangle}{\langle \Phi | \Phi \rangle} \geq \mathcal{E}_0. \quad (\text{A.10})$$

In a similar way, higher eigenvalues of the equation (A.9) are upper limits of the corresponding exact eigenvalues of the Hamiltonian. For an orthonormal set of orbitals  $|\Psi_i\rangle$ , the overlap matrix is just  $\delta_{ij}$ , so that the equation (A.9) becomes a simple eigenvalue problem

$$H\mathbf{c} = E\mathbf{c}. \quad (\text{A.11})$$

One additional fact, that should be made clear, is that the variation of  $|\Phi\rangle$  and  $\langle\Phi|$  can be done separately (see equation (A.6)), because of the complex nature of the wave function, but essentially the same informations are obtained from both variations.

# Appendix B

## Density Functional Theory

After Schrödinger proposed his quantum wave mechanics at the beginning of the 20th century, all physicist were concerned to solve this problem for many-body systems of  $N$  electrons. One of the first theories was the Hartree-Fock theory, that solves  $N$  independent one-electron Schrödinger equations and uses a single Slater-determinant to approximate the exact antisymmetric wave function. Although this theory includes exact exchange effects, it is expensive and applicable only to the modest system sizes, such as atoms and molecules. In 1930s, L.H. Thomas and E. Fermi proposed a model to describe the ground state of a system by the electron density only. This was a brilliant idea, because it simplifies the equations from  $3N$  variables of the  $N$ -electron wave function  $|\Psi(\mathbf{r}_1, \mathbf{r}_2, \dots, \mathbf{r}_N)\rangle$  to 3 variables of electron density  $n(\mathbf{r})$ . The so-called Thomas-Fermi model is a very crude approximation, because the electronic density is approximated by a uniform density of  $N$  electrons in the total volume of the system. Therefore, the Thomas-Fermi model provides reasonably good results only for metals, but for the more complex systems this model is completely wrong, because the actual orbital structure of electrons is not included at all. A more accurate method, which is also based on the fact that the ground state can be described only by density, is proposed by W. Kohn and L.J. Sham [60] - density functional theory. DFT is based on two Hohenberg-Kohn theorems (P. Hohenberg, W. Kohn). The first one states:

**Hohenberg-Kohn 1:** In a system of  $N$  interacting particles in an external potential  $V_{\text{ext}}(\mathbf{r})$ , the potential is uniquely defined by the ground state density  $n_0(\mathbf{r})$ .

From this theorem, it can be concluded that all properties of a system can be described only by the density  $n_0(\mathbf{r})$ . The second theorem states:

**Hohenberg-Kohn 2:** There exists a functional  $F[n]$ , depending only on the density  $n(\mathbf{r})$  for each external potential  $V_{\text{ext}}(\mathbf{r})$ . From the variational principle (see appendix A) the minimum of that functional corresponds to the ground state of the system, so that the density, which minimizes the functional  $F[n]$  is exactly the ground state density  $n_0(\mathbf{r})$ .

Although these theorems are very useful, they do not give any practical way to compute the ground state density and other properties of a system. Therefore, the

Kohn-Sham scheme is developed to overcome this problem. In this scheme, one replaces the full interacting system with a fictitious non interacting system of  $N$  electrons in an effective local one-particle potential  $V_{\text{eff}}(\mathbf{r})$ . Therefore, the energy functional can be written as

$$E[n] = T[n] + U[n] + V_{\text{ext}}[n], \quad (\text{B.1})$$

where  $T[n]$  is the kinetic energy functional,  $U[n]$  the electron-electron interaction and  $V_{\text{ext}}[n]$  is the attractive Coulomb potential of the nuclei. A short overview of these terms will be given below.

Let us start with the kinetic energy term. Within DFT, the kinetic energy functional is decomposed into the kinetic energy of  $N$  non-interacting electrons and the remainder that is assigned to correlation effects.

$$\begin{aligned} T[n] &= T_s[n] + T_c[n], \quad \text{where} \\ T_s[n] &= -\frac{1}{2} \sum_{i=1}^N \int d^3r \phi_i^*(\mathbf{r}) \nabla^2 \phi_i(\mathbf{r}). \end{aligned} \quad (\text{B.2})$$

Note that the term  $T_s[n]$  depends implicitly on the electron density, because the one-electron orbitals are functions of the density, i.e.  $\phi_i[n]$ .

The second term is the electron-electron interaction  $U[n]$ . It is approximated by the Hartree term, that has exactly the same form as the Coulomb repulsion in Hartree-Fock theory

$$U[n] \approx U_H[n] = \frac{1}{2} \int \int d^3r d^3r' \frac{n(\mathbf{r})n(\mathbf{r}')}{|\mathbf{r} - \mathbf{r}'|}. \quad (\text{B.3})$$

The external potential is handled in a classical way within a Born-Oppenheimer approximation (see section 2.2), as it is the case in the Hartree-Fock theory. The rest can be described formally by an additional functional, called exchange-correlation energy functional, defined as

$$E_{\text{xc}}[n] = T_c[n] + U[n] - U_H[n]. \quad (\text{B.4})$$

It is clear that this term contains the exchange effects that are completely neglected in the description of  $U[n]$  and the correlation effects. Correlation effects emphasize all the many-body quantum effects that can not be described by these simple approximations. Therefore, the exchange-correlation functional could be split into exchange effects and correlation effects, like

$$E_{\text{xc}}[n] = E_x[n] + E_c[n], \quad (\text{B.5})$$

To finally obtain the famous Kohn-Sham equations, the variational theorem is applied to the energy functional:

$$E[n] = T_s[n] + U_H[n] + V_{\text{ext}}[n] + E_{\text{xc}}[n]. \quad (\text{B.6})$$

Defining corresponding potentials to the energy functionals  $V_I = \frac{\delta E_I}{\delta n(\mathbf{r})}$ , one arrives to:

$$\begin{aligned} \left[ -\frac{1}{2} \nabla^2 + V_H(\mathbf{r}) + V_{\text{ext}}(\mathbf{r}) + V_{\text{xc}}(\mathbf{r}) \right] \phi_i &= \left[ -\frac{1}{2} \nabla^2 + V_{\text{eff}}(\mathbf{r}) \right] \phi_i = \epsilon_i \phi_i \\ \left[ -\frac{1}{2} \nabla^2 + \int d^3r' \frac{n(\mathbf{r}')}{|\mathbf{r} - \mathbf{r}'|} - \sum_A^M \frac{Z_A}{|\mathbf{r} - \mathbf{r}_A|} + V_{\text{xc}}(\mathbf{r}) \right] \phi_i &= \epsilon_i \phi_i. \end{aligned} \quad (\text{B.7})$$

The latter equations are called Kohn-Sham eigenvalue equations with corresponding Kohn-Sham eigenvalues  $\epsilon_i$  and eigenstates  $\phi_i$ . The Kohn-Sham eigenfunctions  $\phi_i$  do not have any specific physical meaning, they are introduced only as a tool to describe the charge density

$$n(\mathbf{r}) = \sum_{i=1}^N |\phi_i(\mathbf{r})|^2. \quad (\text{B.8})$$

The total energy of a system is given by the equation (B.1), or alternatively by the following equation:

$$E = \sum_{i=1}^N \epsilon_i - \frac{1}{2} \int \int d^3r d^3r' \frac{n(\mathbf{r}')}{|\mathbf{r} - \mathbf{r}'|} + E_{\text{xc}}[n] - \int d^3r V_{\text{xc}}[n]n(\mathbf{r}) \quad (\text{B.9})$$

So far, DFT is an exact theory, but the term  $E_{\text{xc}}$  i.e.  $V_{\text{xc}}$  is unknown. Therefore, good approximations are needed for this term. Over a long period of time, different methods for the approximation of exchange-correlation effects were developed. The most important and the widest used methods are discussed below.

## Local-Density Approximation - LDA

In this class of approximations, the exchange-correlation energy depends on the charge density at each point in space

$$E_{\text{xc}}^{\text{LDA}}[n] = \int d^3r n(\mathbf{r})\epsilon_{\text{xc}}(n). \quad (\text{B.10})$$

The leading problem is now to construct the exchange-correlation density  $\epsilon_{\text{xc}}$ . Note that in the LDA schemes

$$V_{\text{xc}}[n] = \epsilon_{\text{xc}}[n] + n(\mathbf{r}) \frac{\partial \epsilon_{\text{xc}}[n(\mathbf{r})]}{\partial n(\mathbf{r})}. \quad (\text{B.11})$$

The exchange and correlation effects are normally treated separately in LDA. The most successful description of the exchange density  $\epsilon_{\text{x}}$  is based on homogeneous electronic gas, like as it is done in Thomas-Fermi theory. The exchange density within this approximation looks like

$$\epsilon_{\text{x}} = -\frac{3e^2}{4} \left(\frac{3}{\pi}\right)^{1/3} \int d^3r n(\mathbf{r})^{1/3}. \quad (\text{B.12})$$

On the other side, there are no simple analytical expressions for correlation effects. The correlation energy density is usually calculated from quantum Monte-Carlo simulations for simple reference systems (jellium) and parametrized as a function of the charge density. The most famous parameterizations are:

- Ceperley-Alder, *Phys. Rev. Lett* **45**, 566 (1980).
- Pedrew-Zunger (PZ81), *Phys. Rev. B* **23**, 5048 (1981).
- Cole-Pedrew (CP). *Phys. Rev. A* **25**, 1265 (1982).
- Pedrew-Wang (PW92), *Phys. Rev. B* **45**, 13244 (1992).

## Generalized Gradient Approximation - GGA

In GGA approximations, one considers not only the charge density at each point in space, but also the change of the density at each point. That can be written as

$$E_{xc}^{GGA}[n] = \int d^3r f(n(\mathbf{r}), \nabla n(\mathbf{r})). \quad (\text{B.13})$$

The most commonly used implementation of GGA is currently the Perdew-Burke-Ernzerhof functional [*Phys. Rev. Lett* **77**, 3865 (1996)].

## Hybrid Functionals

From the fact that pure DFT calculations (within LDA or GGA) underestimate the band gap of materials and that all Hartree-Fock calculations overestimate the band gap, a portion of the exact non-local Hartree-Fock exchange potential is added to DFT calculations with the hope of achieving better band gap estimations. The non-local exchange functional in DFT is given by (4.54). The well-known hybrid functionals are:

- PBE0 [Perdew J.P., Ernzerhof M., *J. Chem. Phys.* **105**(22), 9982 (1996)]
- B3LYP [Becke A.D., *Phys. Rev. A* **38**(6), 3098 (1988) and Lee C., Yang W., Parr R.M. *Phys. Rev. B* **37**(2), 785 (1988)]
- HSE [Jochen H., Scuseria G., Ernzerhof M., *J. Chem. Phys.* **118**(18), 8207 (2003)].

## Plane Wave Implementation of DFT

After the exchange-correlation has been treated in the approximate way with one of the methods described above, one needs a basis set for the translation of equations in algebraical matrix equations. For this purpose, plane waves are often used in periodic DFT calculations. From the Bloch theorem (4.56), it is known that the electron wave function can be represented as a superposition of plane waves for periodic crystal potentials. Therefore, the plane wave method is particularly suitable for solids and periodic structures. Additionally, plane waves offer a complete basis set that treats the entire space equally. Transforming the Kohn-Sham equation into Fourier space, one obtains

$$\sum_{\mathbf{G}'} \left[ \frac{1}{2} |\mathbf{k} + \mathbf{G}|^2 \delta_{\mathbf{G}, \mathbf{G}'} + \tilde{V}_H(\mathbf{G} - \mathbf{G}') + \tilde{V}_{\text{ext}}(\mathbf{G} - \mathbf{G}') + \tilde{V}_{xc}(\mathbf{G} - \mathbf{G}') \right] C_{i, \mathbf{k} + \mathbf{G}'} = \epsilon_i C_{i, \mathbf{k} + \mathbf{G}}, \quad (\text{B.14})$$

where all  $\tilde{V}$  terms represent the corresponding potentials in Fourier space. This equation can be simply solved by diagonalization of the Hamiltonian matrix in Fourier space given in brackets of the previous equation. The exact solution is obtained for the infinite-dimensional set of plane waves. However, one is always restricted to a finite-dimensional set. Relying on the fact that the plane waves with lower kinetic

energy contribute more than plane waves with higher energy, a cutoff energy  $E_{\text{cut}}$  defined by

$$\frac{1}{2}|\mathbf{k} + \mathbf{G}|^2 \leq E_{\text{cut}} \quad (\text{B.15})$$

can be introduced. In this way, the calculational accuracy can be improved by increasing the value of the cutoff energy. The main disadvantage of this method is that the electronic wave function oscillates in regions near the core, because of divergent long-range nature of the Coulomb potential. These oscillations for core electrons can not be accurately described by a reasonable number of plane waves. For this reason, the pseudopotential method is adopted. The pseudopotential replaces the divergent ionic potential within a cutoff radius by a weaker one to avoid the oscillation effects. Outside the cutoff radius, the ionic potential as well as the wave function is unchanged. Only core electrons are affected by the pseudopotential approximation and, therefore, it could be assumed this approximation would not change the accuracy of results because the valence electrons are mostly responsible for the determination of the materials properties. The next and the last approximation discussed here is the evaluation of integrals over the first Brillouin zone. These integrals are very important, because many physical properties are calculated in this way. Because of the fact that the electron wave function does not change too rapidly for small distances in Fourier space, the integrals over the Brillouin zone can be replaced by a summation over a finite number of  $\mathbf{k}$ -points. This approximation is given by

$$\int_{\text{BZ}} d^3k \tilde{f}(\mathbf{k}) \approx \frac{1}{\Omega} \sum_i w_i \tilde{f}(\mathbf{k}_i), \quad (\text{B.16})$$

where the integral of the function  $f(\mathbf{r})$  is desired. The function  $\tilde{f}(\mathbf{k})$  is the corresponding Fourier transformation and  $w_i$  are appropriate weights. The set of  $\mathbf{k}$ -points used in the calculation is homogeneously distributed over the Brillouin zone

$$\mathbf{k} = \sum_{i=1}^3 \frac{n_i}{N_i} \mathbf{b}_i, \quad \text{with } n_i = 0, \dots, N_i - 1. \quad (\text{B.17})$$

The numbers  $N_i$  denote the density of the  $\mathbf{k}$ -mesh for each reciprocal direction. A sufficiently dense  $\mathbf{k}$ -mesh should always be chosen in such a way that the total energy of the system converges to the desired accuracy.

The plane-wave pseudopotential implementation is the most widely used implementation for DFT theory. This method is also implemented in VASP [61].

# Appendix C

## Transformation of Molecular Integrals

In this appendix, the transformation of molecular integrals will be considered. As described in chapter 3, the molecular integrals can be exactly analytically evaluated over Gaussian orbitals. This set of integrals is given by

$$(pq|rs) = (\phi_p\phi_q|\phi_r\phi_s) = \int d^3r d^3r' \phi_p^*(\mathbf{r})\phi_q(\mathbf{r})r_{12}^{-1}\phi_r^*(\mathbf{r}')\phi_s(\mathbf{r}') \quad \text{for } p, q, r, s = 1, 2, \dots, P \quad (\text{C.1})$$

After the Hartree-Fock calculation (chapter 4) has been performed, a set of  $P$  optimal Hartree-Fock orbitals

$$\psi_i = \sum_{p=1}^P C_{pi}\phi_p, \quad \text{for } i = 1, 2, \dots, P \quad (\text{C.2})$$

is obtained. Note,  $\psi_i$  is only the spatial part of the Hartree-Fock orbital. In this appendix, one uses indices  $p, q, r, s$  for Gaussian orbitals and two-electron integrals over Gaussians, while indices  $i, j, k, l$  are used for Hartree-Fock orbitals. Two-electron integrals evaluated over Hartree-Fock orbitals are necessary for the evaluation of Slater-Condon rules (2.37, 2.38) and for all post Hartree-Fock methods (Møller-Plesset perturbation theory, Coupled Cluster approximation, configuration interaction). Similarly as integrals over Gaussians, integrals over Hartree-Fock orbitals are given as

$$(ij|kl) = (\psi_i\psi_j|\psi_k\psi_l) = \int d^3r d^3r' \psi_i^*(\mathbf{r})\psi_j(\mathbf{r})r_{12}^{-1}\psi_k^*(\mathbf{r}')\psi_l(\mathbf{r}') \quad \text{for } i, j, k, l = 1, 2, \dots, P. \quad (\text{C.3})$$

The number of those integrals is equal to  $P^4$ . Including the eight-fold symmetry of the integrals for real orbitals, the number of unique two-electron integrals is equal to  $P^4/8$ . The simplest way to store all those integrals is a four-dimensional array. There are also methods that allow the storage of only  $P^4/8$  unique integrals, but in this case, the implementation of the function to access an integral from four indices is necessary. In this work, one needs fast access of integrals and therefore, all  $P^4$  integrals will be stored in a four-dimensional array. To obtain transformation rules for the integrals,

the equation (C.2) is inserted in the equation (C.3):

$$(ij|kl) = (\psi_i\psi_j|\psi_k\psi_l) = \sum_{p,q,r,s}^P (C_{pi}\phi_p C_{qj}\phi_q|C_{rk}\phi_r C_{sl}\phi_s) = \sum_{p,q,r,s}^P C_{pi}C_{qj}C_{rk}C_{sl}(pq|rs). \quad (\text{C.4})$$

The naive implementation of this transformation would have four loops for the summation (indices  $p, q, r, s$ ) and four DO loops to store all transformed integrals (indices  $i, j, k, l$ ). This results in an algorithm that scales as  $P^8$ . For larger basis sets, this becomes a computationally very demanding task. Therefore, one needs more efficient algorithm that will be presented here. For this purpose, the equation (C.4) is rewritten as

$$(ij|kl) = \sum_p C_{pi} \left( \sum_q C_{qj} \left( \sum_r C_{rk} \left( \sum_s C_{sl}(pq|rs) \right) \right) \right). \quad (\text{C.5})$$

To evaluate the latter equation, each sum is evaluated separately. In this way, one transforms each pair of indices separately. The whole procedure contains four such transformations ( $s \rightarrow l$ ,  $r \rightarrow k$ ,  $q \rightarrow j$  and  $p \rightarrow i$ ). The cost of this algorithm is  $P^5$  and thus much more efficient than the naive algorithm  $P^8$ . The algorithm is sketched in listing C.1. Further speed up of this algorithm could be gained through the parallelization, which is very straightforward in this particular case. However, the parallelization of the code is out of scope of this work.

```

1 DO loop over  $l, s, r, q, p = 1, P$ 
2    $(pq|rl) += C_{sl}(pq|rs)$ 
3 END loop  $p, q, r, s, l$ 
4
5 DO  $k = 1, P$  loop over  $k, l, r, q, p = 1, P$ 
6    $(pq|kl) += C_{rk}(pq|rl)$ 
7 END loop  $p, q, r, l, k$ 
8
9 DO  $j, k, l, q, p = 1, P$ 
10   $(pj|kl) += C_{qj}(pq|kl)$ 
11 END loop  $p, q, l, k, j$ 
12
13 DO  $i, j, k, l, p = 1, P$ 
14   $(ij|kl) += C_{pi}(pj|kl)$ 
15 END loop over  $p, l, k, j, i$ 
    
```

Listing C.1: The efficient algorithm for the transformation of two-electron molecular integrals. The cost of the algorithm is  $P^5$  where  $P$  denotes the number of Gaussian (i.e. Hartree-Fock) orbitals.

# Bibliography

- [1] Cook, D.B. (1998). *Handbook of computational chemistry*. Oxford, England: Oxford University Press.
- [2] Born and Huang (1954). *Dynamical theory of crystal lattices*. Oxford, England: Oxford University Press.
- [3] Szabo and Ostlund (1996). *Modern quantum chemistry*. New York , United States: Dover Publications.
- [4] Slater, J. C. (1929). The theory of complex spectra. *Phys. Rev.* **34**(10), 1293-1322.
- [5] Condon, E. U. (1930). The theory of complex spectra. *Phys. Rev.* **36**(7), 1121-1133
- [6] Lancaster and Blundell (2014). *Quantum field theory for the gifted amateur*. Oxford, England: Oxford university press.
- [7] Mattuck, R. D. (1992). *A guide to Feynman diagrams in the many-body problem* (2nd ed.). New York, United States: Dover publications.
- [8] Shavitt and Bartlett (2009). *Many-body methods in chemistry and physics: MBPT and coupled-cluster theory*. Cambridge, England: Cambridge University Press.
- [9] Helgaker, Jørgensen, Olsen (2000). *Molecular electronic-structure theory*. Chichester, England: John Wiley & Sons.
- [10] Sherill, C. D. (1995). *An introduction to configuration interaction theory*. Retrieved from <http://vergil.chemistry.gatech.edu/notes/ci.pdf>
- [11] Cramer, C. J. (2002). *Essentials of computational chemistry*. Chichester, England: John Wiley & Sons.
- [12] Slater, J. C. (1930). Atomic shielding constants. *Phys. Rev.* **36**(1), 57-64.
- [13] Hogan, Ruiz and Ozdogan (2010). *Molecular Integrals over Slater-type Orbitals. From pioneers to recent progress*. Retrieved from: <http://www.researchgate.net/publication/200710102/>.
- [14] Hehre, Stewart, Pople (1969). Self-consistent molecular-orbital methods. Use of Gaussian expansions of Slater-type atomic orbitals. *J. Chem. Phys.* **51**, 2657-2666.
- [15] Binkley, Pople and Hehre (1980). Self-consistent molecular orbital methods. Split-valence basis sets for first-row elements. *J. Am. Chem. Soc.* **102**, 939-947.

- [16] Hehre, Sitchfield and Pople (1972). Self-consistent Molecular orbital methods. Further extensions of Gaussian-type basis sets for use in molecular orbitas studies of organic molecules. *J. Chem. Phys.* **56**, 2257-2261.
- [17] Dunning, T. H. Jr. (1989). Gaussian basis sets for use in correlated molecular calculations. The atoms boron through neon and hydrogen. *J. Chem. Phys.* **90**, 1007-1023.
- [18] Woon, Dunning (1993). Gaussian basis sets for use in correlated molecular calculations. The atoms aluminum through argon. *J. Chem. Phys.* **98**, 1358-1371.
- [19] Woon, Dunning (1995). Gaussian basis sets for use in correlated molecular calculations. Core-valence basis sets fro boron through neon. *J. Chem. Phys.* **103**, 4572-4585.
- [20] McMurchie and Davidson (1978). One- and two-electron integrals over Cartesian Gaussian functions. *J. Comp. Phys.* **26**, 218-231.
- [21] Thijsen, J. M. (2007). *Computational physics* (2nd ed.). New York, United States: Cambridge University Press
- [22] Boys, S. F. (1950). A general method of calculation for the stationary states of any molecular system. *Proc. Roy. Soc. A* **200**, 542-554.
- [23] Bloch, F. (1928). Über die qunatenmechanik der Elektronen in Krisllgittern (Doctoral dissertation). Retrieved from <https://link-springer-com.uaccess.univie.ac.at/content/pdf/10.1007%2FBF01339455.pdf>
- [24] Wannier, G. H. (1937). The structure of electronic excitation levels in insulating crystals. *Phys. Rev.* **52**, 191-197.
- [25] Vanderbilt and Marzari (1997). Maximally localized generalized Wannier functions for composite energy bands. *Phys. Rev. B* **56**, 12847-12865.
- [26] Souza, Marzari, Vanderbilt (2001). Maximally localized Wannier functions for entangled energy bands. *Phys. Rev. B* **65**, 035109.
- [27] The VASP Manual (2018, August 8). Typical hybrrid functional and Hartree-Fock calculations. Retrieved from [https://cms.mpi.univie.ac.at/vasp/vasp/Typical\\_hybrid\\_functional\\_Hartree\\_Fock\\_calculations.html](https://cms.mpi.univie.ac.at/vasp/vasp/Typical_hybrid_functional_Hartree_Fock_calculations.html)
- [28] Lödwın P. (1951). A note on the quantum-mechanical perturbation theory. *J chem Phys* **19**, 1396-1401.
- [29] Roos and Siegbahn (1981). The complete active space SCF (CASSCF) method in a Newton-Raphson formulation with application to the HNO molecule *Chem. Phys. Lett.* **74**, 2384-2396.
- [30] Knowles and handy (1984). A new determinant-based full configuration interaction program. *J. Chem. Phys.* **111**, 315-321.

- [31] Olsen, Roos, Jørgensen and Jensen (1988). Determinant based configuration interaction algorithms for complete and restricted configuration interaction spaces. *J. Chem. Phys.* **89**,2185.
- [32] Knowles and Handy (1988). A determinant based full configuration interaction. *Comp. Phys. Comm.* **54**(1), 75-83.
- [33] Knowles, P. J. (1989). Very large full configuration interaction calculation. *Chem. Phys. Lett.* **155**(6), 513-517.
- [34] Ansaloni, Bendazzoli, Evangelisti, Rossi (2000). A parallel full-CI algorithm. *Comp. Phys. Comm.* **128**, 496-515.
- [35] Gagliardi, Bendazzoli, Evangelisti (1997). Direct-list algorithm for configuration interaction calculations. *J. Comp. Chem.* **18**(11), 1329-1343.
- [36] Duch W. (1985). Graphical representation of Slater determinants. *J. Phys. A: Math. Gen.* **18**, 3283-3307.
- [37] Saad, Y. (2003). *Iterative methods for sparse linear systems* (2nd ed.). Philadelphia, USA: society for industrial and Applied Mathematics.
- [38] Davidson, E.R. (1975). The iterative calculation of a few lowest eigenvalues and corresponding eigenvectors of large real-symmetric matrices. *J. Comp. Phys.* **17**,87-94.
- [39] Leininger L., Sherrill C.D., Allen W.D., Schaeffer A.H. (2001). Systematic study of selected diagonalization methods for configuration interaction matrices. *J. Comp. Chem.* **22**, 1574-1589.
- [40] Liu , B. (1978). The simultaneous expansion method for the iterative solution of several of the lowest-lying eigenvalues and corresponding eigenvectors of large real-symmetric matrices. *Numerical Algorithms in chemistry: Algebraic methods*; Technical report LBL-8158; Lawrence Berkeley, USA, 49-53.
- [41] Sadkane. M., Sidje R.B. (1999). Implementation of a variable block Davidson method with deflation for solving large sparse eigenproblems. *Numerical Algorithms* **20**, 217-240.
- [42] Metropolis N., Ulam S. (1941). The Monte Carlo method. *J. Am. Stat. Assoc.* **44**, 335.
- [43] Kalos M.H. (1962). Monte Carlo calculations of the ground state of three- and four-body nuclei . *Phys. Rev.* **128**, 1791.
- [44] Booth T. and Alavi, A. (2009). Fermion Monte Carlo without fixed nodes: A game of life, death, and annihilation in Slater determinant space. *J. Chem. Phys.* **131**, 054106.
- [45] Cleland, Booth and Alavi (2010). Communications: Survival of the fittest: Accelerating convergence in full configuration-interaction quantum Monte Carlo. *J. Chem. Phys.* **132**, 041103.

- [46] Petruzielo F.R., Holmes A.A., Changlani H.J., Nightingale M.P., Umrigar C.J. (2012). Semistochastic Projector Monte Carlo Method. *Phys. Rev. Lett* **109**, 230201.
- [47] Blunt N.S., Smart S.D., Booth G.H., Alavi A. (2015). An excited-state approach within full configuration interaction quantum Monte Carlo. *J. Chem. Phys.* **143**, 134117.
- [48] Overy C., Booth G.H., Blunt N.S., Shepherd J.J., Cleland D., Alavi A. (2014). Unbiased reduced density matrices and electronic properties from full configuration interaction quantum Monte Carlo. *J. Chem. Phys.* **141**, 244117.
- [49] Blunt N.S., Booth G.H., Alavi A. (2017). Density matrices in full configuration interaction quantum Monte Carlo: Excited states, transition dipole moments and parallel distribution. *J. Chem. Phys.* **46**, 244105.
- [50] Vigor W.A., Spencer J.S., Bearpark M.J., Thom A.J.W. (2016). Understanding and improving the efficiency of full configuration interaction quantum Monte Carlo. *J. Chem. Phys.* **144**, 094110.
- [51] Booth G.H., Smart S.D., Alavi A. (2014). Linear scaling and parallelizable algorithms for stochastic quantum chemistry. *Mol. Phys.* **112**, 1855.
- [52] Cleland D.M., Booth G.H., Alavi A. (2011). A study of electron affinities using the initiator approach to full configuration interaction quantum Monte Carlo. *J. Chem. Phys.* **134**, 024112.
- [53] Booth G.H., Alavi A. (2010). Approaching chemical accuracy using full configuration-interaction quantum Monte Carlo: A study of ionization potentials. *J. Chem. Phys.* **132**, 174104.
- [54] Booth G.H., Cleland D., Thom A.J.W., Alavi A. (2011). Breaking the carbon dimer: The challenges of multiple bond dissociation with full configuration interaction quantum Monte Carlo methods. *J. Chem. Phys.* **135**, 084104.
- [55] Schmidt K.E., Kalos M.H. (1984). *Applications of the Monte Carlo method in statistical physics*. Heidelberg, Germany: Springer-Verlag
- [56] Spencer J.P., Blunt N.S., Foulkes W.M. (2012). The sign problem and population dynamics in the full configuration interaction quantum Monte Carlo method. *J. Chem. Phys.* **136**, 054110.
- [57] Flyvbjerg H., Petersen H.G. (1989). Error estimates of averages of correlated data. *J. Chem. Phys.* **91**, 461-466.
- [58] Leikanger K.R. (2013). *Full configuration Monte Carlo studies of quantum dots*. Master's thesis, University of Oslo.
- [59] Frenkel D., Smit b. (2002). *Understanding molecular simulations*. San Diego, California, USA: Academic Press.

- [60] Kohn and Sham (1965). Self-consistent equations including exchange and correlation effects. *Phys. Rev.* **140**, 1133-1138.
- [61] Kresse and Furthmüller (1996). Efficient iterative schemes for *ab initio* total-energy calculations using a plane-wave basis set. *Phys. Rev. B* **54**, 11169-11186.